

EURISOL User Group

Report on the first EURISOL User Group Topical Meeting ¹

The formation and structure of r-process nuclei,
between N=50 and 82 (including ⁷⁸Ni and ¹³²Sn
areas)

INFN-Laboratorio Nazionale del Sud, Catania, 9 -11 December 2009.

¹Coordinated by Angela Bonaccorso, INFN, Sez. di Pisa, Italy.

The first EURISOL UG topical meeting by the title: "The formation and structure of r-process nuclei, between N=50 and 82 (including ^{78}Ni and ^{132}Sn areas)" was held at the INFN-Laboratorio Nazionale del Sud, Catania, 9-11 December 2009. The goal of such meetings is to keep updated the Physics case for EURISOL as expressed by the Key Experiments document issued by Task 10 at the end (July 2009) of the EURISOL DS project.

The Catania meeting was related to the key experiment originally presented under the title

The r-process path between the N=50 and N=82 shells

DETAILS ON THE MEETING FORMAT

There were 25 talks at the meeting. The slides can be found at <http://agenda.ct.infn.it/conferenceTimeTable.py?confId=236>.

They were grouped according to the keywords and observables namely:

Generalities on the r-process

**Stéphane Goriely (Institut d'Astronomie et d'Astrophysique - Université Libre de Bruxelles) The r-process: a longstanding mystery with still many nuclear and astrophysics pending questions

**Olivier Sorlin (GANIL) Experimental studies on the r-process at SPIRAL2

**Gabriel Martínez Pinedo (GSI - Darmstadt) The role of nuclear physics in r-process nucleosynthesis

**Rene Reifarth (GSI -Darmstadt) Experiments close to stability contributing to our understanding of the r-process

** Bradley Cheal (The University of Manchester, UK) Optical techniques for r-process nuclei

Mass Measurements and Calculations. β -decay

**Jacek Dobaczewski (University of Warsaw/Jyväskylä) New ideas in the nuclear energy density functional approach

** Ari Jokinen (University of Jyväskylä) Exploring the structure of neutron-rich nuclei by direct mass measurements

**Alexander Herlert (ISOLDE-CERN) Mass measurements on neutron-rich nuclei at ISOLTRAP: Present status and future perspectives

**David Verney (IPN Orsay) Structure of nuclei "North and Northeast of ^{78}Ni ": contribution from beta-decay

**Dimitry Testov (FLNR, JINR) Delayed multiple neutron emission from photo-fission fragments.

Coulomb excitations, dipole strength, pigmy resonance

**Angela Bracco (INFN and University of Milano) The Pygmy Dipole Resonance in the neutron rich nucleus ^{68}Ni

**Kostanze Boretzky (GSI- Darmstadt) Dipole strength in neutron-rich Ni and Sn isotopes

**Thorsten Kroell (Institut fuer Kernphysik, Technische Universitaet Darmstadt) Coulomb excitation of neutron-rich nuclei around ^{132}Sn at REX-ISOLDE

**Jan Diriken (IKS - KU Leuven) Coulomb excitation of ^{73}Ga with MINIBALL at REX-ISOLDE

**Edoardo G. Lanza (INFN Sezione di Catania) On the nature of the Pygmy Resonances

**Gianluca Colò (INFN and University of Milano) Single-particle and collective strength in neutron-rich nuclei using non-relativistic effective forces

Structure around N=82

**Magdalena Gorska (GSI - Darmstadt) Structure of heavy Cd and In isotopes up to N=82

**Angela Gargano (INFN, Sez. di Napoli) Neutron-Rich Nuclei around Closed Shells: Nuclear Forces and Shell Structure

**Gary Simpson (LPSC Grenoble) Current status of gamma-ray spectroscopy data in the ^{132}Sn region

**Steven Pain (University of the West of Scotland, UK) Neutron transfer measurements around the doubly-magic ^{132}Sn

**Calin Ur (INFN-LNL and University of Padova) Study of neutron-rich nuclei with PRISMA-CLARA. Future perspectives with EURISOL

**Maria Colonna (INFN-LNS Catania) Testing the low density behavior of neutron-rich systems

Light nuclei astrophysics

**Marco La Cognata (INFN-LNS) Solving the large discrepancy between inclusive and exclusive measurements of the ${}^8\text{Li} + {}^4\text{He} \rightarrow {}^{11}\text{B} + \text{n}$ reaction cross section at astrophysical energies.

**Silvio Cherubini (University of Catania and INFN-LNS) Nuclear Astrophysics research in Catania

General talks

**Luciano Calabretta (INFN-LNS) Introducing the LNS facilities

**Yorick Blumenfeld (CERN-ISOLDE) The future of EURISOL and open discussion

From the meeting

At the meeting the detailed role of measurements on atomic masses, β -decay lifetimes, continuum effects, neutron capture cross sections was discussed in the contributions by Olivier Sorlin, Stéphane Goriely and Gabriel Martínez Pinedo, while more technical issues on measurements were discussed by Rene Reifarth and Bradley Cheal.

There was then a set of contributions specifically on mass measurements and calculations and β -decay life-times. The most advanced theoretical approaches to calculate nuclear masses using the nuclear energy density functional method were discussed by Jacek Dobaczewski. Experimental mass measurements were instead presented by Ari Jokinen and Alexander Herlert. β -decay and delayed multiple neutron emission were discussed respectively by David Verney and Dimitry Testov.

Ni and Sn isotopes have been studied to understand their collective vs. single particle properties. Experimental talks by Angela Bracco and Kostanze Boretzky on the dipole strength in neutron-rich Ni and Sn isotopes introduced the subject. The theoretical approaches to understand the data and the physics behind them were presented by Edoardo G. Lanza and Gianluca Colò. It appears at the moment that for nuclei far from the stability valley single particle degrees of freedom dominate over collective excitations. Thorsten Kroell and Jan Diriken both presented studies made at REX-ISOLDE on Coulomb excitation of neutron-rich nuclei, in the Sn and Ga regions.

A very important role in understanding the r-process is played by atomic masses and structure around $N=82$. In fact, the influence of the separation energy (S_n) values on the r-abundance peaks at the $N=82$ shell closure is extremely important. Using mass models which give rise to strong shell closures, one obtains a local increase of the S_n values around $N=70$ and a very abrupt drop immediately after $N=82$. They originate from a predicted strong quadrupole deformation around ^{110}Zr and a strong shell closure at $N=82$, respectively. As a result, neutron captures are stalled for a while around $A=110$, $N=70$ and are subsequently directly driven to the closed shell $N=82$. These important questions were discussed from the experimental point of view by Magdalena Gorska, Gary Simpson, Steven Pain and Calin Ur while theoretical shell model calculations were presented by Angela Gargano. Maria Colonna discussed instead the reaction dynamics. The talk by Steven Pain presented some very recent data on a neutron transfer experiment on ^{132}Sn . For long time it was believed that this nucleus could present a strong weakening of the spin-orbit gap and thus it could represent the limit of applicability of traditional mean field approach. However from the experiment analysis rather "normal" spectroscopic factors have been deduced and thus it is concluded that studies of more exotic species have to be done far beyond ^{132}Sn .

Finally Silvio Cherubini and Marco La Cognata presented an experimental technique known as "Trojan Horse" which overcomes the lack of the combination of very low energy neutron beams on exotic nuclei targets, through the use of breakup/transfer experiments from weakly bound nuclei on targets/projectiles of astrophysical interest.

The conclusions of the meeting were that the following items should be addressed in the path for the realization of EURISOL.

1 Mass measurements

The recent achievements pave the way for a study of ground-state properties of the most exotic nuclei, achievable only with the next generation facilities, like EURISOL. Measurement techniques have already been developed beyond the necessary precision for nuclear structure studies. In the forthcoming years and with new facilities the main two issues in terms of atomic mass measurements are:

- 1) What is the gain in production of exotic isotopes in new facilities compared to

the present ones? The present ion trap facilities have demonstrated that required precision can be achieved in few tens of ms. Typical beta decay half-lives of medium mass nuclei are still in the range of 100 ms and moving few neutrons further from the stability will not change the situation drastically. Thus the half-lives are not the limiting factor, but the reach of exotic isotopes is mainly defined by the production yields in the future facilities.

2) Ion manipulation and purification prior to the trap measurements becomes increasingly important in the future. Ion traps have limited capacity for isobaric contaminations and isobaric background tends to increase with the new facilities, like EURISOL. Thus the technical challenge lies in the purification of the sample. This is a general problem which holds for many spectroscopic studies, not only for trap measurements, with future facilities.

All in all, there is still room for precision mass measurement of neutron-rich nuclei in the future facilities, like EURISOL. It is expected that storage ring facilities, like FAIR or RIKEN will provide large sets of new data and most probably they can reach further from the stability. However, there are a couple of issues supporting ion trap techniques at future ISOL facilities: Firstly, the precision obtainable will always be superior compared to storage ring approaches and secondly, storage ring data rely on the precise calibrations from the Penning trap measurements.

2 Perspectives for β -decay studies of stopped fission fragment beams

Beta decay properties of neutron rich nuclei are a very important ingredient in any r-process calculation. More specifically, it is important to know as precisely as possible ground state half lives ($T_{1/2}$) and beta delayed neutron branching (B_n). In addition, proper measurements of the B(GT) distributions (and Q_β values, which can be derived from ground state mass differences) are very important in order to validate the models which are used to estimate $T_{1/2}$ and B_n values of unreachable nuclei (even with EURISOL) where the r-process is supposed to take place. To this end, tape station set-ups, equipped with neutron detectors, gamma high-resolution Ge detectors, gamma total-absorption spectrometers, electron and beta detectors are a mandatory part of EURISOL. X-ray detectors might also be useful. In addition, recent history has shown that in many cases, data coming from beta-decay were the first source of information available on structure for

the most exotic nuclei. This should constitute an extra strong encouragement to envisage the possibility for a beta-decay setup installed at the EURISOL facility. In addition to the physics program which can be achieved by using this robust technique, the equipment described above is an excellent tool for a real evaluation of the effective beam intensities and beam purity evaluation, which is useful in the early stages of commissioning of RIB facilities. In that sense, they can be used as the very first experimental setups where to send the "brandly new beams" as soon as they become available, even before post-acceleration, and can accompany usefully new beam developments.

3 Neutron capture

The determination of neutron capture cross sections on exotic beams is not directly possible, because it would require targets made of exotic nuclei or a collider for neutron and exotic nuclei beams. Indirect methods are available such as the Trojan Horse method (see later) or transfer to the continuum reactions such as (d,p). However information could be provided by models, constrained by spectroscopic information (such as energy, spin, spectroscopic factors of the bound and unbound levels in the $A+1$ nucleus) obtained for example by the (d,p) transfer reactions just mentioned. Some studies on neutron captures at the $N=82$ shell closure are expected to be achieved at the presently available facilities thanks to the high production rate of $N=82$ nuclei around Sn and Cd and the suitable energy for transfer reactions. However there are some more exotic phenomena, such as a new subshell gap predicted at $N=90$ in the Sn isotopic chain, i.e. for ^{140}Sn . Whether it is present or not depends on the proximity of the continuum which would reduce it significantly. Therefore the production of new very neutron-rich nuclei, with higher N/Z ratios than those presently available, would be necessary to see the change of nuclear interaction in a more diffuse potential. The effect could be detected though the presence of low L orbits instead of high L ones at low excitation energy.

4 Response to electromagnetic excitations

Measurements of the Pigmy Dipole Resonance in isotopic chains that include more and more neutron-rich systems may further reduce the uncertainty on the param-

eters (c.f. the symmetry energy) governing the presently available NN model interactions. Indeed it has been shown that valuable information on the nature of the PDR can be obtained by excitation processes involving the nuclear part of the interaction. The use of different bombarding energies, of different combinations of colliding nuclei involving different mixture of isoscalar/isovector components, together with the mandatory use of microscopically constructed form-factors, can provide the clue to reveal the characteristic features of these states. In a similar fashion, the results of detailed study on the collective vs non collective nature of low lying dipole strength point towards a decoherence of the particle-hole excitations involved. One may therefore hope that other important quantities which define our understanding of nuclear physics can be constrained by measurements of the collective strength in exotic nuclei produced at EURISOL which will be more neutron rich and thus further away from stability, than those presently available.

5 Nuclear force and shell structure

For long time it was believed that the nucleus ^{132}Sn could present a strong weakening of the spin-orbit gap and thus represent the limit of applicability of traditional mean field approach. However from the experimental analysis rather "normal" spectroscopic factors have been deduced and thus it is concluded that studies of more exotic species have to be done far beyond ^{132}Sn . Furthermore spectroscopy data on nuclei with both proton and neutron holes, relative to ^{132}Sn are rare. Some β - and isomer-decay studies have been performed on the indium and cadmium nuclei of the region with $N \leq 82$. Shell-model calculations are able to reproduce well the observed decays schemes close to the $N = 82$ shell closure, however the agreement becomes worse when moving further away. These problems may arise due to some collectivity being present in these nuclei or a difference between hole-hole and particle-particle (or particle-hole) interactions. A simple examination of the energies of lowest lying levels of these nuclei would appear to hint at the presence of some collectivity, due to the similarity of the $2^+ \rightarrow 0^+$ and $4^+ \rightarrow 2^+$ transitions energies. Shell-model calculations produce 2^+ energies some 200 or 300 keV too high, however this is a general feature of calculations of this region and the problem exists also for nuclei with $Z \geq 50$ and $N \leq 82$. Coulomb excitation measurements are necessary on these nuclei to search for any collec-

tive effects. More spectroscopy data are also needed to further test the shell-model predictions and to improve the interactions. EURISOL will be able to deliver such beams of the required In, Cd, Ag, and Pd nuclei using the fragmentation of a ^{132}Sn beam. Finally, excited states of nuclei with $Z \leq 50$ and $N > 82$, close to ^{132}Sn are currently unknown. Spectroscopy information here will again allow shell-model predictions to be tested. EURISOL will be able to provide beams of these species using fragmentation reactions of beams such as ^{144}Xe or ^{144}Cs . Such reactions possibly provided the best mechanism to populate and study the nuclei of this region.

6 Reaction dynamics aspects

The collision dynamics in dissipative heavy ion reactions, from low to intermediate energies, is expected to be sensitive to the details of the nuclear interaction away from normal density. Hence dynamical processes involving very exotic beams will allow one to address the study of the nuclear interaction in terms of energy density functionals and, in particular, to constrain the isovector terms and the so-called symmetry energy E_{sym} . This has important implications in the astrophysical context and also for the understanding of the structure of exotic systems. In fact, energy density functionals are probably the only possible framework to describe medium-heavy nuclei and are widely employed also in the study of astrophysical objects, such as compact stars. In investigations of the reaction dynamics, different effective interactions are implemented into transport codes employed to simulate the collision. Then results can be compared to experimental data for specific reactions mechanisms and related observables. A key role in this approach is played by the possibility at EURISOL to study the same reaction in a wide range of incident energy such that different densities will be sampled and corresponding information could be deduced on the equation of state of nuclear matter.

Another example of reactions which need nuclei nowadays out of reach is the use of a radioactive ^{92}Kr beam on a ^{238}U target at an energy of 600 MeV. According to the GRAZING calculations multi-nucleon transfer and deep-inelastic processes following this reaction will populate with relatively high cross-sections neutron-rich Se, Kr, Rb, Sr nuclei presently completely unknown.

Finally we want to stress the extreme importance of more intense beams and

statistics for all studies involving population/excitation of single particle and or collective resonances near threshold with indirect methods like (n,d) transfer, Trojan Horse method, breakup reactions or Coulomb excitation above particle emission threshold.

Update on the physics case for experiments on : The r-process path between the N=50 and N=82 shells

Abstract

The goal originally proposed was to make a systematic study of the basic nuclear structure properties of neutron-rich nuclei on the r-process path between the N=50 and N=82 major neutron shells for measurements at the Nuclear Astrophysics Sector of EURISOL. Measurements of these basic properties will provide the fundamental information for extension to neutron-rich nuclei of the nuclear structure and reaction models needed for full-scale r-process nucleosynthesis studies.

Keywords

r-process nucleosynthesis, nuclear mass, decay properties, shell structure far from stability

Physics case

Nuclear structure properties of neutron-rich nuclei are of paramount importance for the understanding and modelling of the r-process, responsible for the synthesis of approximately half of the elements heavier than iron. Presently available experimental information on basic properties such as masses and decay properties of neutron-rich nuclei do not include nuclei in the r-process path in the regions between the N=50, 82 and 126 shells.

Because of our ignorance on the exact nuclear mechanisms taking place during the r-process, we are bound today to consider as relevant to the r-process all potential nuclear properties for all the thousands of nuclei ranging from the lightest to superheavy nuclei and up to the neutron drip line or even beyond. The properties include ground and excited state properties (masses, deformations, spectra of excited states and nuclear level densities, spontaneous β -decay or fission probabilities, ...) as well as their properties of interactions with nucleons, α -particles and photons. In neutron star environment, the high-density equation of state of asymmetric nuclear matter is also required.

As far as experimental needs are concerned, two major orientations can be envisioned.

- First, the measurement of given properties for a large set of nuclei that would enable a global analysis (and extrapolation) in the framework of microscopic models of properties such as nuclear masses, radii, low-lying excited state, giant resonances.

- Second, the specific measurement of a given property that could bring new insights on the physics of exotic neutron-rich nuclei and could have a significant impact on the extrapolations of existing models. As examples, the following nuclear effects still require further experimental effort: the neutron skin thickness, the $N = 82$ and $N = 126$ shell closures, the imaginary component of the neutron optical potential for n-rich nuclei, the pre-equilibrium contribution to the reaction for exotic n-rich nuclei, the nuclear level densities at high energy and/or for exotic nuclei, the dipole strength at low energies.

Such new measurements will be fundamental in our understanding of the physics of exotic nuclei. As discussed above, it should also be recalled that today we are still far from being capable of make reliable microscopic nuclear predictions on the description of β -decay and the reaction mechanisms, including the equilibrium, pre-equilibrium and direct capture process as well as the radiative neutron capture rates and fission properties of exotic n-rich nuclei.

Observables

Nuclear masses (S_n , and Q_β). Half-lives (β -decay $T_{1/2}$), β -delayed neutron emission probability (P_n), neutron-capture rates (though an indirect method such as the Trojan-horse method), B(GT) distributions. Additional important observables: energies and J^π of excited states, ground-state deformation, and γ -n cross sections.

Proposed experiment

Systematic study of basic nuclear structure properties of neutron rich isotopes of (possibly) all elements from Fe to Sn, covering all "waiting-point" nuclei in the r-process path between the $N=50$ and $N=82$ neutron shells. Depending on beam intensities obtainable, the following isotopes will be studied (mass number range given for each element):

$^{68(*)-74}\text{Fe}$, $^{73-75}\text{Co}$, $^{78}\text{Ni}^*$, $^{79(*)-81}\text{Cu}$, $^{80(*)-84}\text{Zn}$, $^{81(*)-87}\text{Ga}$, $^{84(*)-90}\text{Ge}$, $^{87(*)-95}\text{As}$, $^{90(*)-98}\text{Se}$, $^{91(*)-101}\text{Br}$, $^{96(*)-106}\text{Kr}$, $^{101(*)-107}\text{Rb}$, $^{102(*)-110}\text{Sr}$, $^{105-115}\text{Y}$, $^{108-118}\text{Zr}$, $^{111-123}\text{Nb}$, $^{114-124}\text{Mo}$, $^{121-125}\text{Tc}$, $^{124-126}\text{Ru}$, ^{127}Rh , ^{128}Pd , $^{129}\text{Ag}^*$, $^{130}\text{Cd}^*$, $^{131}\text{In}^*$, $^{132}\text{Sn}^*$.

Nuclides marked with (*) have been already measured and will be used as benchmark cases.

Requirements

Beam properties

Low-energy high purity beams for decay studies and mass measurements, Coulomb barrier energies for Coulex and high energy beams for Coulomb dissociation type of experiments.

Detection

Penning trap mass spectrometer for mass measurements (see e.g. ISOLTRAP). Laser ion-source for purification purposes (e.g. RILIS at ISOLDE). Multi-coincidence set-up with various detection systems, in particular for neutrons and gammas.

Theoretical support

Energy functional method for mass calculations. Modern nuclear structure models for the nuclear mean field. Capabilities for large-scale shell-model calculations (needs the development of appropriate residual interactions to be employed in studies of nuclei far from stability). Coulomb dissociation method. RPA methods to study the nature of resonances. Full dynamical calculation of r-process nucleosynthesis with inclusion of the nuclear physics input obtainable from the experimental data.

The r-process nucleosynthesis

S. Goriely

*Institut d'Astronomie et d'Astrophysique
Université Libre de Bruxelles
Campus de la Plaine, CP 226
1050 Brussels – Belgium*

Abstract. The rapid neutron-capture process, or r-process, is known to be of fundamental importance for explaining the origin of approximately half of the $A > 60$ stable nuclei observed in nature. In recent years nuclear astrophysicists have developed more and more sophisticated r-process models, eagerly trying to add new astrophysical or nuclear physics ingredients to explain the solar system composition in a satisfactory way. The r-process remains the most complex nucleosynthetic process to model from the astrophysics as well as nuclear-physics points of view. The still many nuclear and astrophysics pending questions are discussed.

Keywords: Nucleosynthesis, nuclear reaction, nuclear structure, abundances

PACS: 98.80.Ft, 26.30.+k, 24.60.Dr

ASTROPHYSICS ASPECTS

The r-process of stellar nucleosynthesis is called for to explain the production of the stable neutron-rich nuclides heavier than iron that are observed in stars of various metallicities, as well as in the solar system. A review can be found in Ref. [1].

Nuclear-physics-based and astrophysics-free r-process models of different levels of sophistication have been constructed over the years. They all have their merits and their shortcomings. The ultimate goal is clearly to identify realistic sites for the development of the r-process. The challenge is enormous, and the solution(s) still elude us. Many "realistic" scenarios have been proposed for the last decades. For long, the core-collapse supernova or gamma-ray burst explosions have been envisioned as the privileged r-process location. One- or multi-dimensional spherical or aspherical explosion simulations in connection with the r-process nucleosynthesis are reviewed in [1]. Mass ejection in the so-called neutrino-driven wind from a nascent neutron star or in the prompt explosion of a supernova in the case of a small iron core or an O-Ne-Mg core have been shown to give rise to a successful r-process provided the conditions in the ejecta are favorable with respect to high wind entropies, short expansion timescales or low electron number fractions. Although these scenarios remain promising, especially in view of their significant contribution to the galactic enrichment [2], they remain handicapped by large uncertainties associated mainly with the still incompletely understood mechanism that is responsible for the supernova explosion and the persistent difficulties to obtain suitable r-process conditions in self-consistent dynamical models. In addition, the composition of the ejected matter remains difficult to ascertain due to the remarkable sensitivity of r-process nucleosynthesis to the uncertain properties of the ejecta.

Another candidate site has been proposed as possibly contributing to the galactic

enrichment in r-nuclei. It concerns the decompression of initially cold neutron star matter [3, 4, 5, 6]. In particular, special attention has been paid to neutron star mergers due to their large neutron densities and the confirmation by hydrodynamic simulations that a non-negligible amount of matter can be ejected [7, 8]. Recent calculations of the galactic chemical evolution [2], however, tend to rule out neutron star mergers as the dominant r-process site for two major reasons: First, their relatively long life times and in particular low rates of occurrence would lead to a sudden and late r-process enrichment that is not compatible with the observed r-process enrichment of ultra-metal-poor stars. Second, the significant mass of r-process material ejected by each event should lead to a large scatter of r-element overabundance in solar-like metallicity stars; this scatter is not confirmed observationally. However, this conclusion requires assumptions about the efficiency of mixing in the interstellar medium and is based on uncertain results from numerical models for the total amount of mass that is ejected by a single event. Moreover, it assumes a constant neutron star – neutron star merger rate over the 10 Gyr galactic history that can be questioned. Another uncertainty comes from the disregard of neutron star – black hole mergers that have been estimated to be about 10 times more frequent than their neutron star – neutron star counterparts, although the possibility of mass ejection is still unclear because of the unknown state of supranuclear matter in the neutron star [7, 8]. But the ejection of initially cold, decompressed NS matter might also happen in astrophysical scenarios like the mass ejection in magnetar burst, the explosion of a neutron star below its minimum mass [9] or in the spin-down phase of very rapidly rotating supramassive or ultramassive neutron stars, which could lead to the equatorial shedding of material with high angular momentum.

The identification of the astrophysical site for the r-process remains clearly and by far the most unsatisfactorily understood facet of the r-process modelling, and the one that calls most desperately for progress. Considering the uncertainties remaining on the astrophysical r-process site (and on the involved nuclear physics – see below) any confrontation between predicted r-process yields and observed abundances is obviously risky today.

NUCLEAR PHYSICS ASPECTS

Regarding the nuclear physics needs, the situation might be considered as rather positive in the sense that the mystery of the r-process nucleosynthesis most probably does not stem from nuclear origin, or as negative due to the huge amount of nuclear data needed to model the r-process. Depending on the site considered, different nuclear mechanisms may be at stake, so that it remains difficult to estimate quantitatively the importance of a given nuclear input on the final r-abundance distribution. In the so-called "hot" neutrino-driven wind scenario, the conditions might be such that a $(n, \gamma) - (\gamma, n)$ equilibrium can be established. In this case, at least during the neutron irradiation before the freeze-out phase, only β -decay rates and neutron separation energies need to be estimated and the exact determination of the neutron capture rates may not be required (at least if the rates are high enough to confirm the establishment of the $(n, \gamma) - (\gamma, n)$ equilibrium). In contrast, in low-temperature neutrino-driven winds or the decompression of the inner crust of a neutron star, the nuclear mechanism at stake during

the r-process nucleosynthesis consists in the competition between neutron captures and β -decays. In the scenarios, a detailed knowledge of the neutron capture rates and β -decays by all nuclei potentially involved is necessary. Depending on the strength of the r-process, superheavy nuclei may also be produced and in that case fission recycling may become important. The impact of fission, including spontaneous, neutron-induced and β -delayed fission, on the final abundance pattern strongly depends on the adopted scenario (and the adopted nuclear physics input used to describe fission properties). In particular, it remains totally unclear where fission would stop the r-process flow, what would be the most dominant fission mode and to what extent fission can contribute to the production of r-nuclei with $120 \leq A \leq 160$.

All in all, because of our ignorance on the exact nuclear mechanisms taking place during the r-process, we are bound today to consider as relevant to the r-process all potential nuclear properties for all the thousands of nuclei ranging from the lightest to superheavy nuclei and up to the neutron drip line or even beyond. The properties include ground and excited state properties (masses, deformations, spectra of excited states and nuclear level densities, spontaneous α - and β -decay or fission probabilities, ...) as well as their properties of interactions with nucleons, α -particles and photons. In neutron star environment, the high-density equation of state of asymmetric nuclear matter is also required.

In such circumstances, there is no hope of measuring them in the foreseeable future and there is no other choice as to resort to theoretical predictions. Two major features of the nuclear theory must be contemplated, namely its *accuracy* and its *reliability*. A microscopic description by a physically sound model based on first principles ensures a reliable extrapolation away from experimentally known region. For these reasons, when the nuclear ingredients to the reaction or β -decay models cannot be determined from experimental data, use is made preferentially of microscopic or semi-microscopic global predictions based on sound and reliable nuclear models which, in turn, is accurate enough to compete with more phenomenological highly-parametrized models in the reproduction of experimental data. Global (semi-)microscopic approaches have been developed for the last decades and are now available for nuclear structure properties, nuclear level densities, γ -ray strength functions, optical potentials and fission probabilities. However, many improvements still need to be brought to further increase their predictive powers. Similarly, many new β -decay half-lives have been measured recently and different theoretical approaches have been proposed, but major progress is still needed to improve their reliability far away from the valley of stability. A review on the nuclear needs can be found in Ref. [1]. As an illustration, the impact of nuclear masses and β -decay rates on the r-process nucleosynthesis, we show in Fig. 1 the abundances obtained with 3 mass models and two different β -decay models.

As far as the calculation of reaction rates is concerned, it should be emphasized that all the r-process calculations have made use of neutron capture rates evaluated within the statistical model of Hauser-Feshbach. Such a model makes the fundamental assumption that the capture process takes place through the intermediary formation of a compound nucleus in thermodynamic equilibrium. The formation of a compound nucleus is usually justified if the level density in the compound nucleus at the projectile incident energy is large enough. However, when dealing with exotic neutron-rich nuclei, the number of available states in the compound system is relatively small and the validity of the Hauser-

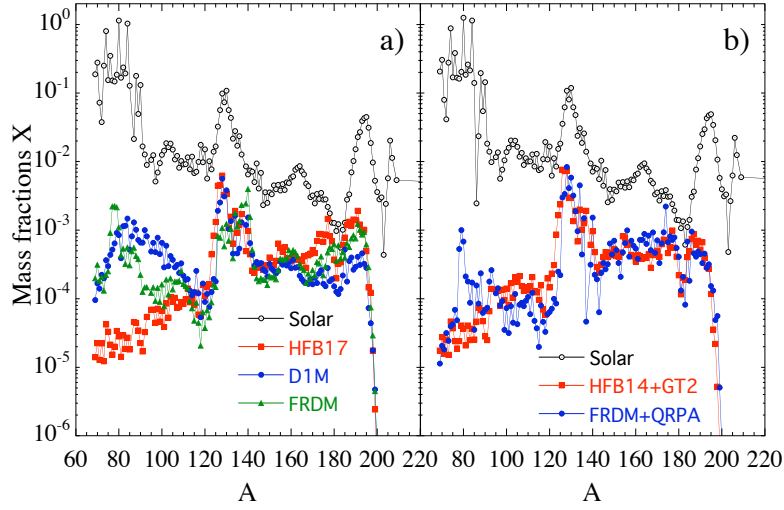


FIGURE 1. (Color online) a) Distribution of the r-nuclide abundances obtained within the neutrino-driven wind corresponding to an entropy $S = 200$, electron fraction $Y_e = 0.48$, mass loss rate $dM/dt = 10^{-6} M_\odot \text{ s}^{-1}$ and breeze solution $f_w = 3$ (see [1] for more details). The three simulations are obtained using 3 different mass models, namely HFB-17 [10], D1M (based on the Gogny force) [11] and FRDM [12]. b) Same as a) for two simulations using 2 different global models of β -decay rates, namely the gross theory (GT2) [13] based on the HFB-14 ground state and the FRDM+QRPA [14].

Feshbach model has to be questioned. In this case, the neutron capture process might be dominated by direct electromagnetic transitions to a bound final state rather than through the formation of a compound nucleus. Direct captures are known to play an important role for light or closed shell systems for which no resonant states are available. The direct neutron capture rates have been re-estimated for exotic neutron-rich nuclei as in [6, 15] using a modified version of the potential model to avoid the uncertainties affecting the single-particle approach based on the one-neutron particle-hole configuration. The direct capture was shown to become larger than the compound contribution for many neutron drip nuclei, but also to be in many cases negligible due to the selection rule forbidding the electromagnetic transitions to any of the available excited levels. As mentioned above, while in high-temperature environment, the reaction rates do not affect the r-process nucleosynthesis, in the cold neutrino-driven wind or during the decompression of neutron star matter the neutron capture is in direct competition with β -decays and a reliable estimate of the rates (including both the resonant and direct contributions) is necessary. The impact of the adopted reaction model is illustrated in Fig. 2

As far as experimental needs are concerned, two major orientations can be envisioned.

- First, the measurement of given properties for a large set of nuclei that would enable a global analysis (and extrapolation) in the framework of microscopic models. This concerns properties such as nuclear masses, radii, low-lying excited state, giant resonances, ...

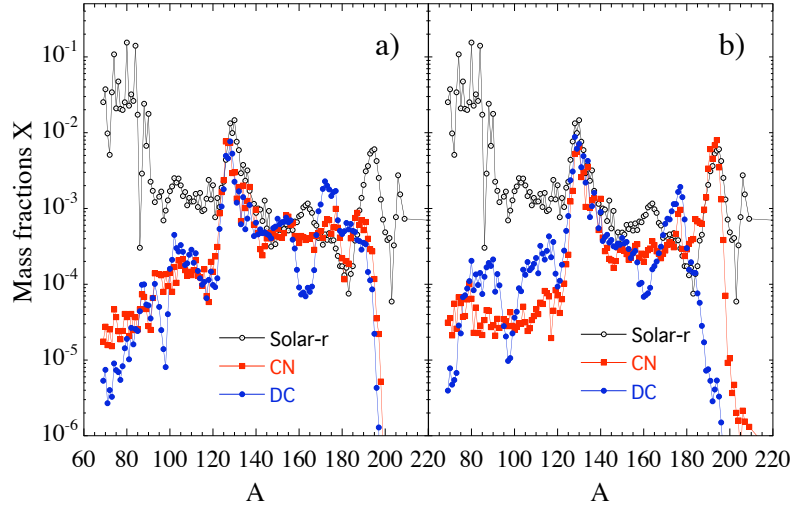


FIGURE 2. (Color online) a) Same simulation as in Fig. 1 for the conditions $S = 200$, $Y_e = 0.48$, $dM/dt = 10^{-6} M_{\odot} \text{ s}^{-1}$ and $f_w = 3$. The two simulations are obtained using either the compound nucleus (CN) contribution to the (n, γ) rates or the direct capture (DC) one. b) Same as a) for $S = 200$, $Y_e = 0.47$, $dM/dt = 10^{-6} M_{\odot} \text{ s}^{-1}$ and $f_w = 1$.

- Second, the specific measurement of a given property that could bring new insights on the physics of exotic neutron-rich nuclei and could have a significant impact on the extrapolations of existing models. As examples, the following nuclear effects still require further experimental effort: the neutron skin thickness, the $N = 82$ and $N = 126$ shell closures, the imaginary component of the neutron optical potential for n-rich nuclei, the pre-equilibrium contribution to the reaction for exotic n-rich nuclei, the nuclear level densities at high energy and/or for exotic nuclei, the dipole strength at low energies, ...

Such new measurements will be fundamental in our understanding of the physics of exotic nuclei. As discussed above, it should also be recalled that today we are still far from being capable of estimating reliably the radiative neutron capture rates, fission properties and β -decay rates of exotic n-rich nuclei.

CONCLUSIONS

A continued theoretical and experimental effort to improve the determination of all nuclear inputs of relevance to the process nucleosynthesis is obviously required. Theoretically, microscopic nuclear predictions is concomitant with new development aiming at improving the description of β -decay and the reaction mechanisms, including the equilibrium, pre-equilibrium and direct capture processes. This theoretical work requires simultaneously new measurements of nuclear properties far away from stability, but also reaction cross sections on stable targets and any experiments that can provide direct

or indirect observables and therefore also new insight on the numerous ingredients of the β -decay and reaction models and their extrapolation far away from stability. At the same time, improved descriptions of the astrophysical sites are eagerly needed to define the conditions in which the r-process nucleosynthesis takes place and consequently the nuclear mechanisms at stake and nuclei involved.

REFERENCES

1. M. Arnould, S. Goriely, K. Takahashi, *Phys. Rep.* **450**, 97 (2007)
2. D. Argast, M. Samland, F.-K. Thielemann and Y. Qian, *Astron. Astrophys.* 416 (2004) 997
3. J.M. Lattimer, F. Mackie, D.G. Ravenhall and D.N. Schramm, *Astrophys. J.* 213 (1977) 225
4. B.S. Meyer, *Astrophys. J.* 343 (1989) 254
5. C. Freiburghaus, S. Rosswog and F.-K. Thielemann, *Astrophys. J.* 525 (1999) L121
6. S. Goriely, P. Demetriou, H.-T. Janka, J.M. Pearson, M. Samyn, *Nucl. Phys.* **A758**, 587c (2005)
7. H.-T. Janka, T. Eberl, M. Ruffert and C.L. Fryer, *Astrophys. J.* 527 (1999) L39
8. S. Rosswog, R. Speith and G.A. Wynn, *Mon. Not. R. Astron. Soc.* 351 (2004) 1121
9. K. Sumiyoshi, S. Yamada, H. Suzuki and W. Hillebrandt, *Astron. Astrophys.* 334 (1998) 159
10. S. Goriely, N. Chamel, J.M. Pearson *Phys. Rev. Lett.* **102**, 152503 (2009)
11. S. Goriely, S. Hilaire, M. Girod, S. Péru *Phys. Rev. Lett.* **102**, 242501 (2009)
12. P. Möller, J. R. Nix, W. D. Myers, W. J. Swiatecki, *At. Nucl. Data Tables* **59**, 185 (1995)
13. T. Tachibana, M. Yamada, N. Yoshida, *Prog. Theor. Phys.* **84**, 641 (1990)
14. P. Möller, J. R. Nix, K.-L. Kratz *At. Nucl. Data Tables* **66**, 131 (1997)
15. S. Goriely, *Astron. Astrophys.* **325**, 414 (1997)

Olivier Sorlin
GANIL, Caen, France

Introduction to the r process nucleosynthesis

The relative abundances of nuclides observed in the solar system (shown in the left part of Figure 1) displays distinct patterns carrying imprints of the processes involved to create these elements. A steep decrease in abundance is seen below Fe. This rapid fall-off witnesses the fact that these elements are mainly produced by fusion reactions, which require the tunnelling through an increasing Coulomb barrier as Z increases. The Fe peak is created at the end of an equilibrium process between charged particles and photodisintegrations reactions which favour the productions of the most bound elements in nature, i.e. around Fe. Above Fe a smooth fall-off in abundance is found, indicating that charged particles are no longer involved there but neutron captures, which are not sensitive to the Coulomb barrier, take over. Therefore the abundance curve stays almost constant as a function of Z or A , except when shell closures are present. There, the neutron-capture cross section decreases by several orders of magnitude immediately after having passed the shell gap. It follows that nuclei at closed shells have a much larger abundances than their neighbours, leading to the presence of three distinct twin peaks superimposed on the smooth abundance curve. Each peak has a narrow width at stable nuclides with magic neutron numbers $N=50, 82,$ and $126,$ and a broader peak shifted to slightly lower mass numbers as shown in the left part of Figure 1. This indicates the existence of (at least) two components, attributed to slow (s) and rapid (r) neutron-capture nucleosynthesis.

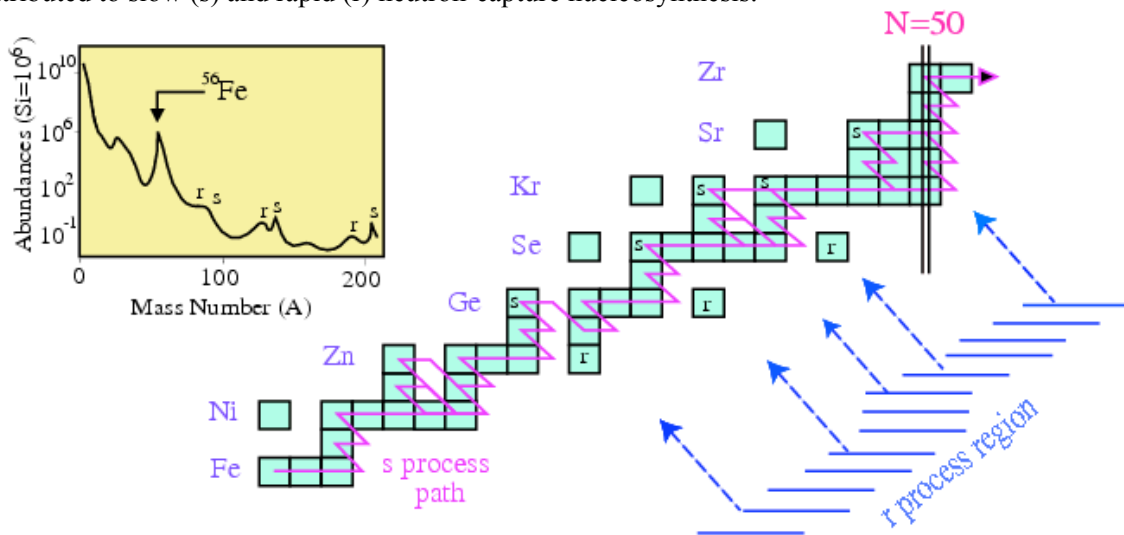


*Figure 1 : **Top Left** : Solar abundance curve of the elements, normalized to Si. **Center** : The s process path, corresponding to given density and temperature, is shown in pink. It develops in the valley of stability. Therefore the most neutron-rich nuclei such as ^{70}Zn , ^{76}Ge and ^{82}Se cannot be reached by this process. Rather the r process, which is driven further from the valley of stability is producing these pure r isotopes.*

A typically expected s process path is shown in Figure 1. It operates in red giant stars at relatively low neutron density of about 10^8cm^{-3} , with neutron captures lifetimes on seed nuclei typically longer than their β -decay lifetimes $T_{1/2}$. As a consequence, the s -process path follows the valley of stability and isotopes with small neutron-capture (n,γ) cross section σ_n are greatly enhanced [Kapp99]. Along the s process path, we find approximately that the product of the cross section and abundance $\sigma_n N_s$ is constant. Small (n,γ) cross sections are encountered for closed shell nuclei, leading to the building of s -process peaks (right part of the twin peaks displayed in Fig. 1) at atomic masses $A=88, 140,$ and 208 . Most of the cross sections of the stable nuclei involved in the s process have been measured with an accuracy of about 10%, with some exceptions. Using these cross sections, the fraction of s elements in

the total abundance curve can be derived. The remaining part of the observed elements above Fe is ascribed to the r process.

The other half of the elements beyond Fe (as in particular the most neutron-rich) is supposed to be produced via neutron captures on very short time scales in neutron-rich environments. In very hot and neutron-dense environments, the r-process proceeds very far off stability. The r-progenitors subsequently β -decay to enrich the stable elements in the valley of stability. As shown in Figure 1, some neutron-rich stable isotopes (^{70}Zn , ^{76}Ge and ^{82}Se) have purely r component as the s process cannot reach them. These stable isotopes are shielding the corresponding isobars from being produced by the r process as well. Therefore ^{70}Ge , ^{76}Se and ^{82}Kr have a pure s process origin.

Despite its importance, the exact site(s) where the r-process(es) occurs still remain one of the greatest mystery in science. The most frequently suggested astrophysical environments are high-entropy ejecta from type II supernovae (SN) [Woos94] and neutron-star mergers [Frei99]. The shock-heated He or C outer layer of type II SN could provide a moderate neutron flux (a weak r-process) through $^{13}\text{C}(\alpha, n)$ reactions which could account for several isotopic anomalies found in pre-solar grains. The key for understanding the r-process(es) resides in a close interaction between astronomy, cosmochemistry, astrophysical modelling of explosive scenarios and nuclear physics. Only the nuclear structure aspects will be discussed here.

To account for the production of r-peaks, shifted to lower atomic masses as compared to the s process, neutron-rich nuclei should be produced. In a very hot and neutron-rich environment, the rate of captures is balanced by that of photodisintegrations induced by the ambient photon bath of the exploding star. The corresponding ratio of nuclei $N(A+1)/N(A)$ depends on the neutron density d_n , the temperature and the neutron separation energy $S_n(A+1)$. Its is given by the so-called Saha equation, which is deduced from the Boltzmann population rule :

$$\frac{N(A+1)}{N(A)} \propto d_n \exp(-S_n(A+1)/kT)$$

This equation means that, for a fixed temperature and neutron density, the abundance in a given isotopic chain is determined by the S_n values. For $d_n \sim 10^{24} \text{ cm}^{-3}$ and $T \sim 10^9 \text{ K}$, it is found that the r process is reaching nuclei with small binding energy ($S_n \sim 2\text{-}3 \text{ MeV}$). As a sharp drop of $S_n(A+1)$ occurs after a major closed shell, an accumulation of nuclei is found there. The process is then stalled at these so-called waiting-point nuclei until beta-decays occur, depleting the nucleosynthesis to the upper Z isotopic chain where a subsequent neutron-capture could immediately occur. After successive beta-decays and neutron captures at the N=82 closed shell, the process is progressively driven closer to stability at higher Z where β -decay lifetimes $T_{1/2}$ become longer (see the red zig-zag line along the N=82 shell in Figure 30). There, around the Sn isotopic chain, neutron captures are expected to proceed faster than photodisintegration and beta-decay rates, possibly driving the r-process nucleosynthesis towards the next shell closure.

At the end of the r-process, radioactive progenitors decay back to stability via beta or beta-delayed neutron emission. The accumulation of r-elements which form the r-peaks at masses $A \sim 80$, ~ 130 and ~ 195 on the abundance curve of the elements is a direct imprint of the existence of waiting point progenitors far from stability. The location, height and shape of the A=130 peak could be traced back from the neutron separation energies (S_n), the half-lives ($T_{1/2}$), the neutron delayed emission probability (P_n), and the neutron-capture cross section (σ_n) of the nuclei located at the N=82 shell closure. These parameters are imbricated in the structural evolution of the nuclei as depicted in the following paragraph.

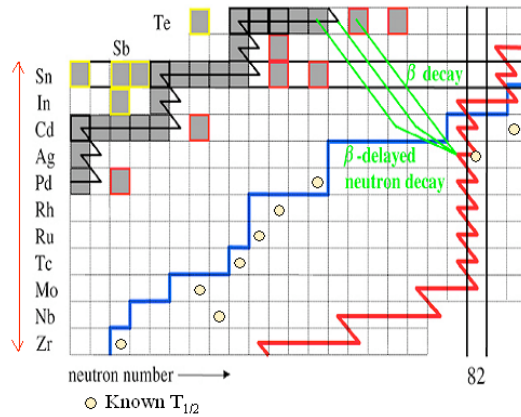
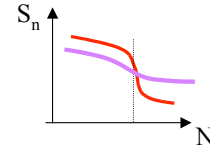
Nuclear physics of the r-process [$d_n \sim 10^{24} \text{cm}^{-3}$, $T \sim 10^9 \text{K}$]

1- Only the 'strongest' nuclei survive :

$$A+1 \begin{array}{c} \leftarrow \\ \uparrow S_n \\ \leftarrow \\ A \end{array} \quad \frac{N(A+1)}{N(A)} \propto d_n \exp(-S_n(A+1)/kT);$$

equilibrium for $S_n \sim 3 \text{MeV}$; 'location' of the r-process

Accumulation of nuclei when S_n drops \rightarrow role of closed shells



'Waiting point' nuclei are main generators of stable nuclei

Predict/determine the behaviour of S_n and shell gaps

Figure 2 : Top Left : Relationship expressing the Boltzmann population of two states (here the abundance of $A+1$ and A nuclei) separated by an energy $S_n(A+1)$ as a function of neutron density d_n and temperature T . **Top Right**: Schematic variation of S_n for a strong shell closure (in red) or for a quenched shell closure (in purple). For the first case, the r progenitors are well located at the shell closure, while for the second the r progenitors are more spread along the isotopic chain. **Bottom Left** : Schematic representation of the location of the r-process path (in red) at the $N=82$ shell closure for a given neutron density value and assuming a strong shell closure. The present experimental knowledge on the atomic masses is indicated by a thick blue line. As far as β -decay lifetimes are concerned, measurements (shown with yellow circles) extend further from stability, reaching in particular the ^{130}Cd [Dill03] and ^{129}Ag waiting-point nuclei [Dill03,Pfei01,Kra05].

Influence of nuclear structure on the r-process nucleosynthesis

The evolution of the $N=82$ shell gap south to the doubly magic nucleus $^{132}\text{Sn}_{82}$ is ruled by the combined effects of the proton-neutron interactions and by the progressive proximity of the continuum states. From $Z=50$ to $Z=40$ only the proton orbit $g_{9/2}$ orbital is progressively emptied (see the right part of Figure 3), therefore all the proton-neutron monopole interactions which intervene in the evolution of nuclear structure between $^{132}\text{Sn}_{82}$ and the close-to-drip-line nucleus $^{122}\text{Zr}_{82}$, involve the same proton orbit. As shown schematically in the right part of Figure 3 some monopole interactions can play an important role to modify the ordering of the neutron orbits, hereby possibly reducing the size of the $N=82$ shell gap as protons are removed from $Z=50$ to $Z=40$. Related to this reduction, the tensor interactions (through the $\pi g_{9/2}-\nu h_{11/2}$ or $\pi g_{9/2}-\nu f_{7/2}$ monopoles) are likely to play the most important roles.

The role of atomic masses

The influence of the S_n values on the r-abundance peaks at the $N=82$ shell closure has been emphasized in Refs. [Chen95,Pfei01]. Using mass models which give rise to strong shell closures (as FRDM or ETFSI-1), one obtains a local increase of the S_n values around $N=70$ and a very abrupt drop immediately after $N=82$. They originate from a predicted strong quadrupole deformation around ^{110}Zr and a strong shell closure at $N=82$, respectively. As a result, neutron captures are stalled for a while around $A=110$, $N=70$ and are subsequently directly driven to the closed shell $N=82$. This leaves few r-

progenitors in between these two regions, leading to a significant trough in the fit of the abundance curve of the elements at $A \sim 120$ in Fig. 2¹. On the other hand, models exhibiting less strong shell closures (called "quenched" mass models as ETFSI-Q or HFB/SkP) lead to a smoothed variation of S_n values, bringing back r-progenitors before reaching the $N=82$ shell closure². Thus the trough at $A \sim 120$ is filled in closer agreement with the solar r-abundance curve³. The recent determination of the Q_β -value in the β -decay of the ^{130}Cd [Dill03] waiting-point nucleus as well as the study of the ^{131}In isomer [Gors09] accredit this weakening which should however be confirmed by further investigations. From these arguments, it follows that the determination of the S_n values at the $N=82$ shell closure is essential. So far theoretical models diverge soon after departing from the last measured nucleus, as discussed for instance in Ref. [Lunn03], meaning that the underlying physics which could modify the binding energies of the orbits is poorly known and far from being consensual. **The remaining masses to be measured are located south to $Z=50$, $N=82$ and at the $N=126$ shell closure where only few information relevant to the r process is known. It is also important to measure the atomic masses of several isomers located at low excitation energy. When present at low excitation energy, typically about 100keV, these isomers can be thermally populated during the explosion of the star.**

Sensitivity of nuclear structure at $N=82$ on the r abundance curve

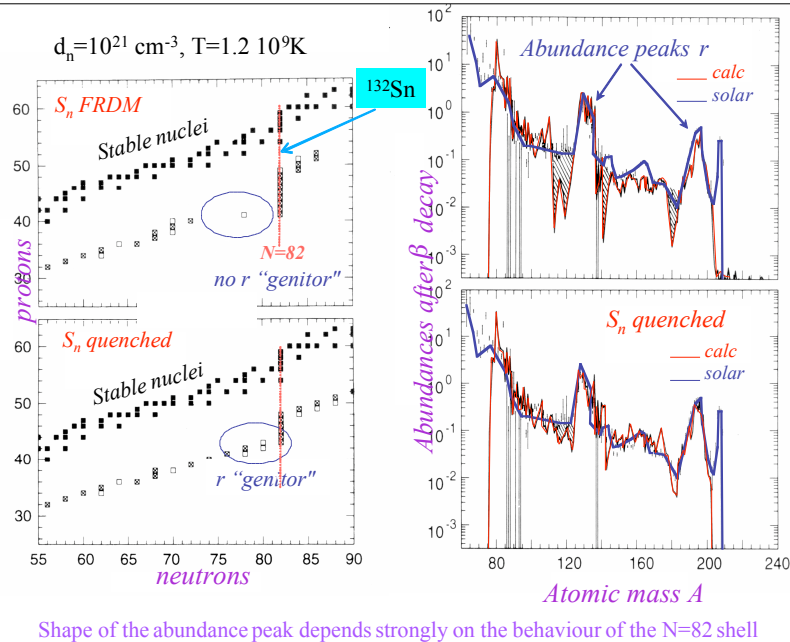


Figure 3 : Left Major r process progenitors are indicated with open squares (with a cross 90%, without 10% of total abundance) for given neutron-density and temperature conditions, assuming a strong $N=82$ shell closure, as found by the Finite Range Droplet Model [Moll85], or by the HFB/SkP [Doba96] model which gives quenched shell gaps.

Right : The corresponding calculated abundances of the elements using the Saha equation (compared to solar abundances). For the strong shell closure hypothesis (upper part), the neutron capture flow is immediately driven to the $N=82$ shell, leaving few progenitors before. This produces a hole in abundance before the major r peaks. Rather the quenched mass formula is filling these holes (adapted from Ref. [Pfei01]).

¹ Noteworthy is the fact that if ^{110}Zr were a doubly magic nucleus, a sudden drop of S_n value at $N=70$ would be found, leading to the build up of r-process elements at $A \sim 110$.

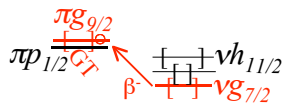
² The reduction of the shell gap can occur from the action of proton neutron two-body forces, combined with the change of single particle energies induced by the increased diffuseness of the nuclear potential well for the neutrons. Here the term "quench" includes both effects, which still have to be proven experimentally.

³ Note that this better agreement does not necessarily documents for quenched shell closures, as a specific stellar origin could account for the filling of these mass regions as well.

The role of β -decay lifetimes

Likewise, the strength of the tensor interaction influences strongly the β -decay lifetimes of the $N=82$ nuclei through the $\pi g_{9/2}$ - $\nu g_{7/2}$ monopole, as depicted in Figure 2. The reason for so is that the β -decay of $N=82$ nuclei south to $Z=50$ proceeds mainly through the Gamow-Teller (GT) transition $\nu g_{7/2} \rightarrow \pi g_{9/2}$ transition, as described in Refs. [Dill03,Cuen07]. The $\nu h_{11/2} \rightarrow \pi g_{9/2}$ first forbidden decay transition is expected to contribute to less than 10% of the beta-decay lifetime [Cuen10]. As protons are progressively removed from the $g_{9/2}$ orbit, the neutron $g_{7/2}$ orbit becomes gradually less deeply bound due to the missing proton-neutron interactions $\pi g_{9/2}$ - $\nu g_{7/2}$. Consequently, the aforementioned GT transition will occur at gradually smaller excitation energy E^* in the daughter nuclei, leading to a drastic shortening of β -decay lifetimes $T_{1/2}$, which scales with $1/(Q_\beta - E^*)^5$.

2- Weak interactions to produce heavy elements :



$T_{1/2}$ scales with energy of the transition and strength of the force

Nuclei accumulated at waiting points according to $T_{1/2} \rightarrow$ peak height, duration of r process

P_n values : probability to emit a neutron during β decay \rightarrow smoothens the r peaks

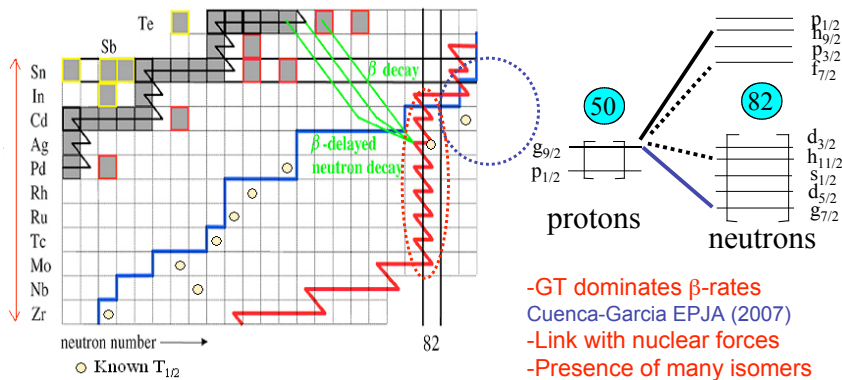


Figure 4 : Schematic view of the proton-neutron interactions which play a role for the evolution of the β decay lifetime $T_{1/2}$. Right : The interaction between the $\pi g_{9/2}$ and $\nu g_{7/2}$ orbits, indicated by a full line, is expected to be the largest among all other interactions involved, see text for explanation and consequences. The dashed (full) lines indicate proton-neutron interaction containing a repulsive (attractive) tensor force. This tensor part will influence the absolute value of the nuclear interaction. The loci indicated in red and blue on the chart of nuclides correspond to the approximate locations where lifetimes play the most important role.

When short-lived nuclei are paving the r -process path, the abundance peaks of the r -elements are barely formed and a total duration of the explosive process of few milliseconds could be long enough to reach the heaviest elements of the chart of nuclides. At the opposite, long-lived nuclei located in the r -process path are the major genitors of stable r -nuclei in the universe, after series of β or β -neutron decays to stability, and are responsible for the existence of significant peaks in the abundance curve of the elements. Therefore accurate half-life predictions or measurements are required along the r -process both to explain the shape of observed peaks but also to constrain the duration of the r -process. When the β -decay partly proceeds above the neutron emission threshold of the daughter nucleus with a probability P_n , a neutron is emitted after the conversion of a neutron into a proton by the β^- decay process. In such a process a nucleus (A,Z) is therefore converted to $(A-1,Z+1)$ with the fraction P_n , and to $(A,Z+1)$ with the probability $1-P_n$. This delayed neutron emission probability smoothens the abundance curve of the elements as the decay proceeds to masses A and $A-1$. It follows that the abundance curve of the elements no longer exhibits an odd-even effect abundance pattern as for the s peak. A review of the measured lifetimes relevant for the r process, as well as the role of isomers which can be thermally populated in exploding stars, can be found in Ref. [Kra05]. So far, most of the lifetime measurements relevant for the r process have been achieved at the ISOLDE/CERN facility.

As mentioned for the atomic masses, the remaining lifetimes to be measured are located south to $Z=50$, $N=82$ and at the $N=126$ shell closure. When a beta-decay isomer is present at low excitation energy, it can be thermally populated during the explosion of the star, making it important for the r process duration and for the building of r peaks.

The role of continuum

Added to the properties of the NN interactions which are assumed for the moment to be unchanged whatever the respective binding energies of protons and neutrons, self-consistent mean-field calculations which encompass the treatment of continuum states show a quenching of the $N=82$ shell gap when approaching the neutron drip-line [Doba94]. This is primarily caused by the lowering of the low j orbits relative to high- j values. The low- j neutron orbits, such as the $vp_{1/2}$ and $vp_{3/2}$ ones, may progressively become the valence states immediately above the $N=82$ gap. Such effects were ascribed to the fact that, close to the drip-line, the low- j neutron orbits of the continuum interact strongly with bound states, whereas the interaction with the high- j ones is much less effective. Qualitatively, the nuclear mean field close to the drip-line could be mimicked by a Nilsson potential without the ℓ^2 term [Doba]. At exploding star temperatures of typically 10^9K (or neutron energies of about 100keV) neutrons can hardly overcome large centrifugal barriers created by high ℓ orbits. Therefore, the presence of low- j or low- ℓ neutron valence orbits at low excitation energy would enhance the neutron capture cross-sections σ_n by several orders of magnitudes, shortening the neutron capture time at the waiting point nuclei accordingly.

The role of neutron capture cross sections

Neutron capture cross-sections are often calculated in the framework of the statistical Hauser-Feshbach model [Haus52,Cow91,Raus97], which assumes the presence of a high density of states above the neutron separation energy with various spin and parity values (see Figure 4). However the use of this statistical approach is no longer appropriate to calculate neutron capture cross sections for neutron-rich nuclei at closed shell, since the neutron-separation energy is small and the level density is low. In such cases, the main contribution is obtained from direct captures on few bound states of low ℓ values, mainly through s or p waves, or/and by resonant captures slightly above the neutron-energy threshold (see Figure 4).

The fact that the neutron p orbits become the few first valence states above $N=82$ is therefore extremely important. This feature is discussed in Ref. [Raus98] for the ^{133}Sn nucleus. In Figure 4, it is shown that predictions on direct neutron capture rates can differ by up to two orders of magnitude in this mass region. As the direct capture cross section proceeds mainly through the same $vp_{3/2}$ and $vp_{1/2}$ states from $Z=50$ down to $Z=40$, the evolution of their energy and spectroscopic factors determines how neutron-capture cross sections will change along the $N=82$ shell closure. It indicates to which extent the r-process will be blocked at this shell closure when the temperature of the exploding system decreases and photodisintegration become negligible. Since the direct determination of neutron-capture cross sections on very unstable nuclei A is technically not feasible, their determination should be provided by models, constrained by spectroscopic information (such as energy, spin, spectroscopic factors of the bound and unbound levels in the $A+1$ nucleus) obtained by (d,p) transfer reactions. Such pioneering studies have been undertaken for the $N=28$ shell closure in the neutron-rich ^{48}Ca and ^{46}Ar nuclei where similar p states come into play in the neutron-capture cross sections [ngdp]. These studies on neutron captures at the $N=82$ shell closure are expected to be achieved at the SPIRAL2 facility thanks to the high production rate of $N=82$ nuclei around Sn and Cd and the suitable energy for transfer reactions.

Nuclear physics of the r-process [$d_n \sim 10^{24} \text{cm}^{-3}$, $T \sim 10^9 \text{K}$]

3- Role of neutron capture rates ?

Shuffle the material to more neutron-rich when the star expands
 Could move the r process to next peak

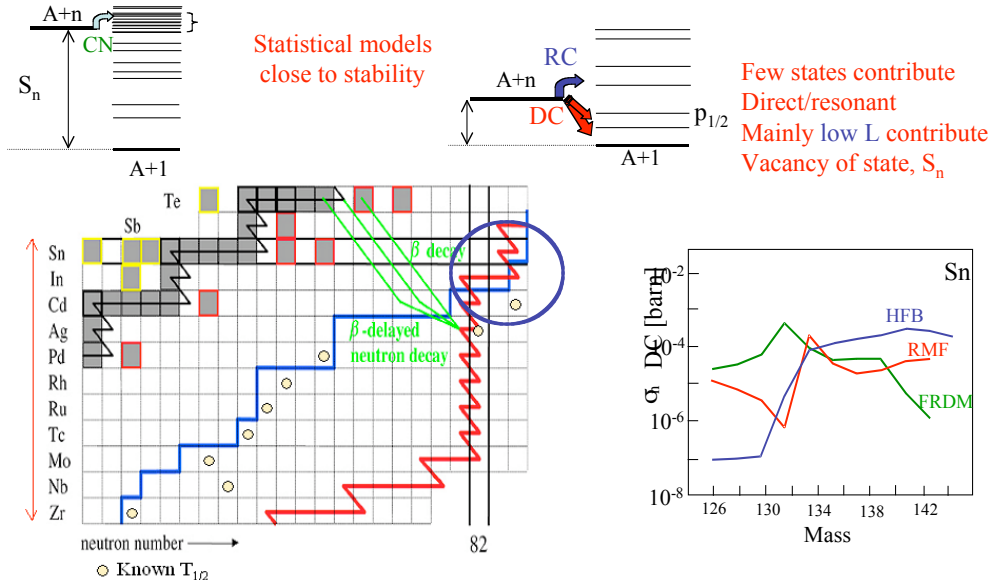


Figure 5 : **Top** : Schematic views of the processes through which neutron captures can occur are shown. On the **left**, the formation of a compound nucleus is favoured, leading to a treatment of the neutron capture by the Hauser-Feshbach statistical model. On the **right**, the resonant and the direct capture processes dominate for neutron-rich nuclei at closed shells. Capture to low ℓ states gives larger cross sections, as the centrifugal barrier is low. **Bottom right** : Neutron capture predictions using various mean field models show discrepancies of up to two orders of magnitude, emphasizing the importance of having reliable nuclear physics values of the energy of the states, spectroscopic factors and atomic masses [Raus98].

However it is not sure that the drip line can be reached with the SPIRAL2 facility. In particular a new subshell gap is predicted at $N=90$ in the Sn isotopic chain, i.e. for ^{140}Sn . Whether it is present or not depends on the proximity of the continuum which would reduce it significantly. Therefore very neutron-rich nuclei should be available to see the change of nuclear interaction in a more diffuse potential. The effect could be seen by the presence of low L orbits instead of high L ones at low excitation energy.

To summarize this astrophysical part, experimental and theoretical achievements aiming at a comprehensive understanding of the evolution of the $N=82$ and $N=126$ shell closure will provide significant insight to the understanding of the r-process nucleosynthesis, as these topics are intimately entwined.

- [Chen95] B. Chen et al., *Phys. Lett. B* **355** (1995) 37
- [Cow91] J. J. Cowan, F.-K. Thielemann and J. W. Truran, *Phys. Rep.* **208** (1991) 267
- [Cuen07] J. J. Cuenca-Garcia et al., *Eur. Phys. J. A* **34** (2007) 99
- [Cuen10] J. J. Cuenca-Garcia et al., GSI scientific report 2008, p168, Nustar-theory-04
- [Dill03] I. Dillmann et al., *Phys. Rev. Lett.* **91** (2003) 162503
- [Doba94] J. Dobaczewski et al., *Phys. Rev. Lett.* **72** (1994) 981,
- [Frei99] C. Freiburghaus, S. Rosswog and F.-K. Thielemann, *Ap. J.* **525** (1999) L121
- [Gade06] A. Gade et al., *Phys. Rev. C* **74** (2006) 034322
- [Gade08] A. Gade and T. Glasmacher, *Prog. Part. Nucl. Phys.* **60** (2008) 161
- [Haus52] W. Hauser and H. Feshbach, *Phys. Rev.* **87** (1952) 366
- [Kapp99] F. Kaeppler et al., *Prog. Part. Nucl. Phys.* **43** (1999) 419
- [Kra05] K.-L. Kratz et al., *Eur. Phys. J. A* **25**, s01 (2005) 633 - 638.
- [Krat07] K. -L. Kratz et al., *Prog. Part. Nucl. Phys.* **59** (2007) 147
- [Lunn03] D. Lunney et al., *Rev. Mod. Phys.* **75** (2003) 1021
- [ngdp] F. Kaeppler et al. *Ap. J.* **347** (1989) L43,
 E. Kraussmann et al. *Phys. Rev. C* **53** (1996) 469,
 L. Gaudefroy et al. *Eur. Phys. J. A* **27** (s01) (2006) 302,
 O. Sorlin et al. *C. R. Phys.* **4** (2003) 541.
- [Pfei01] B. Pfeiffer et al., *Nucl. Phys. A* **693** (2001) 282
- [Raus97] T. Rauscher et al., *Phys. Rev. C* **56** (1997) 1613
- [Raus98] T. Rauscher et al., *Phys. Rev. C* **57** (1998) 2031
- [Woos94] S. e. Woosley et al., *Ap.J.* **433** (1994) 229

The role of nuclear physics in r-process nucleosynthesis

Gabriel Martínez Pinedo (GSI - Darmstadt)

For many years the neutrino-driven wind has been considered as the favoured site for r-process nucleosynthesis. However, all simulations so far have failed to obtain the conditions necessary for the production of heavy r-process elements including U and Th. There may be some important physical ingredient still missing in the models, but alternative sites should also be considered for the production of r-process elements. These may be associated to the formation of a rotating neutron star after the supernova explosion and the appearance of an accretion disk and jets; the merging of two neutron stars; and the ejection of neutron-rich matter from black hole accretion disks associated with g-ray bursts. A major step in solving the r-process puzzle has been the detection of r-process elements in a few very metal-poor stars located in the halo of the galaxy. These stars formed a long time ago when the galaxy was still iron poor and provide us with a snapshot of the nucleosynthesis yield resulting from, hopefully, a single nucleosynthesis event. All observations so far show that the production of r-process elements with $A > 130$ is very robust and results in elemental abundances consistent with the solar r-process abundances. Elements with $A < 130$ show much larger variations from star to star suggesting the need for two different processes responsible for the production of elements heavier and those lighter than $A = 130$. This is also supported by the abundances of some extinct r-process nuclides (e.g. ^{129}I and ^{182}Hf) in the early Solar System, inferred from measurements of isotopic anomalies in meteoritic materials, which cannot be explained by one single process. Large-scale astronomical surveys of r-process stars, and further studies of meteoritic material, will help to clarify the situation and will help in understanding the enrichment of the galaxy with heavy elements.

From the nuclear physics point of view the r-process is a sequence of neutron captures, photodissociations and β -decays occurring at such large neutron densities that nuclei near the neutron drip line are produced. Most of these nuclei have never been produced in the laboratory and consequently their properties remain largely unknown. In order to interpret future observations it will be necessary to compare them with predictions of different r-process model calculations. These require reliable nuclear input in order to relate the observed abundances with the particular astrophysical conditions of the r-process site. A dramatic change in our understanding of the r-process is expected to occur once future radioactive beam facilities become operational, as they will produce a wealth of r-process nuclei and consequently greatly constrain the astrophysical models. To fully exploit the potential offered by these facilities, a concerted effort between experimental and theoretical efforts, involving both the nuclear and astrophysical modelling, will be required.

The understanding of r-process nucleosynthesis represents one of the largest challenges in nuclear astrophysics. r-process calculations require the determination of different nuclear properties of several thousand nuclei. Most of these

nuclei have never been produced in the laboratory and consequently their properties and relevant reactions must be determined theoretically. This includes neutron captures, photodissociations and β -decays. Additionally, in environments with large neutron-to-seed ratios, fission reactions including neutron-induced fission, γ -induced fission, β -delayed fission and spontaneous fission become important and should be supplemented with reliable predictions of fission yields.

A basic input for the calculation of neutron capture rates is the γ -strength function. Several experiments and theoretical calculations have shown the appearance of a new low energy mode in neutron-rich nuclei known as the pygmy dipole resonance. Future Coulomb dissociation experiments will improve our understanding of this mode and together with theoretical calculations help to determine their impact in neutron capture rates and r-process nucleosynthesis. It should be noted that both experiments and current theoretical models determine the γ -strength distribution built on the ground state of the nucleus. However, in many cases the capture cross section is dominated by g transitions to excited states in the nucleus. Currently, it is assumed that the γ -strength distribution of excited states fulfils the Brink hypothesis, which states that the strength depends only on the g energy and not on the nuclear state. The validity of this approximation for the astrophysically relevant γ -energies, 2-3 MeV, is by no means warranted and consequently it will be necessary to develop theoretical models for the calculation of γ -strength functions on excited states of the nucleus.

The β -decay of r-process nuclei determines the speed at which the nucleosynthesis flow moves from light r-process nuclei to heavy nuclei. Experimentally, β -decays of r-process nuclei have been determined for only a few key nuclei around the N=50 and N=82 shell closures. These include ^{78}Ni , ^{130}Cd and ^{129}Ag . These measurements have greatly helped to constrain theoretical calculations for these nuclei that are currently based on a variety of approaches including the Shell-Model, Density Functional plus QRPA, macroscopic/microscopic models plus QRPA, HFB plus QRPA, and relativistic mean-fields plus RPA. Most of the theoretical calculations are currently limited to spherical nuclei. Extensions of the different models to deformed nuclei are consequently necessary. The recent developments of new in-beam analysis techniques have contributed to the determination of β -decay half-lives of nuclei approaching the N=126 r-process region. The use of these techniques together with progress in high intensity Uranium beams will open to experiment the so far unknown N=126 r-process nuclei. This is particularly relevant as current theoretical predictions have a large spread in values. At the same time it is expected that first-forbidden contributions will contribute significantly, a prediction that needs to be confirmed experimentally.

Future experiments are expected to provide valuable information about the evolution of the N=82 and N=126 shell closures far from stability and the impact on r-process nucleosynthesis. In addition, the development of new fragment separators will open to experimental study the region of neutron-rich nuclei beyond Uranium and Thorium. Understanding the shell structure in this region and in particular the survival or not of the neutron shell closures N=152 and

$N=162$ is of particular importance in order to understand the mechanism responsible for the actinide boost observed in the U and Th elemental abundances of some metal-poor stars.

A special phenomenon relevant in astrophysical environments is the influence of free electrons in the plasma on reactions and decays. Decay lifetimes can be altered not only by thermal excitation of a nucleus, but also electron captures will depend on the electron density surrounding the nucleus. In reactions, nuclear charges are screened by the electron cloud. This is fundamentally different from screening in atoms or molecules. Nevertheless, these latter types of screening have to be understood as well, because they have an impact on precision measurements of low-energy cross sections of light targets, e.g., for hydrostatic burning. Screening in the plasma can be treated in the weak and strong screening approximations but more accurate treatments for intermediate or dynamic screening and the dependence on the plasma composition have to be developed. This is important not just for nucleosynthesis but also for the SNIa explosion mechanism. Explosive nucleosynthesis calculations require the development of huge nucleosynthesis networks. In the particular case of r-process nucleosynthesis they comprise around 6000 nuclear species on the neutron-rich side and several 100,000 reactions if fission is included. On the proton-rich side, p-, rp- and np-process nucleosynthesis also require networks extending far into the unstable region (up to $A100$ all the way to the dripline) and including 10,000s of reactions. A simultaneous solution of the changes in hydrodynamical properties and composition represents a very challenging problem. Fortunately, in many scenarios reduced nuclear networks can be used to account for the energy generation while the detailed changes in composition can be described in a post processing approach. Currently, all stellar models studying nucleosynthesis are 1-D. Multi-dimensional effects such as convection or the impact of rotation are implemented phenomenologically. Nevertheless, coupling full reaction networks to these calculations is already computationally expensive and often reduced networks combined with postprocessing are used. Future improved models and advanced computing will lead to more detailed astrophysical predictions requiring more accurate nuclear input.

In addition to the stable beam facilities, construction of the next generation of radioactive beam facilities are now underway fragmentation beams at FAIR and ISOL beams at SPIRAL-2, HIE-ISOLDE and SPES. These new beams will revolutionise our capability and allow a concerted attempt to understand nucleosynthesis in explosive sites where the evolution is dominated by reactions between unstable nuclei. The timely completion of these projects is vital to allow the exciting range of nuclear astrophysics experiments outlined above to begin. This next generation of facilities will enable great advances during the next decade, but beyond that the higher intensity, wider beam reach of EURISOL will be required. As this EURISOL project develops it is essential that the nuclear astrophysics community remain fully engaged in the project to ensure that the technical specifications of the facility remain in line with what is needed for this field.

Experiments close to stability contributing to our understanding of the r-process

René Reifarth

Gesellschaft für Schwerionenforschung mbH, Darmstadt, D-64291, Germany
J.W. Goethe Universität, Frankfurt a.M, D-60438, Germany

E-mail: r.reifarth@gsi.de

Abstract. Almost all of the heavy elements are produced via neutron capture reactions in a multitude of stellar production sites (s- and r-process). The predictive power of the underlying stellar models is currently limited because they contain poorly constrained physics components such as convection, rotation or magnetic fields.

Neutron captures measurements on heavy radioactive isotopes close to stability provide a unique opportunity to largely improve these physics components, and thereby address important questions of nuclear astrophysics. Such species are branch-points in the otherwise uniquely defined path of subsequent neutron captures along the s-process path in the valley of stability. These branch points reveal themselves through unmistakable signatures recovered from pre-solar meteoritic grains that originate in individual element producing stars.

In addition, a better understanding of the s-process abundance distribution will directly benefit our understanding of the r process, since the observed abundances are the superposition of s- and r-process contributions.

In particular the upcoming FRANZ facility allows the investigation of radioactive isotopes with half-lives down to tens of days, while present facilities require half-lives of years. This means the need for sample production facilities increases. EURISOL would certainly be a very good candidate.

1. Experimental situation concerning the s process

Almost all of the heavy element abundances beyond iron are produced via neutron capture reaction, about equally shared between the slow neutron capture nucleosynthesis (*s* process) and the rapid neutron capture nucleosynthesis (*r* process).

Starting at iron-peak seed, the *s*-process mass flow follows the neutron rich side of the valley of stability via a sequence of neutron captures and β^- decays synthesizing the elements between iron and bismuth.

If different reaction rates are comparable, the *s*-process path branches and the branching ratio reflects the physical conditions in the interior of the star. Such nuclei are most interesting, because they provide the tools to effectively constrain modern models of the stars where the nucleosynthesis occurs. As soon as the β^- decay is significantly faster than the typically competing neutron capture, no branching will take place. Therefore experimental neutron capture data for the *s* process are only needed, if the respective neutron capture time under stellar conditions is similar or smaller than the β^- decay time, which includes all stable isotopes. Depending on the actual neutron density during the *s* process, the "line of interest" is closer to or farther away from the valley of stability.

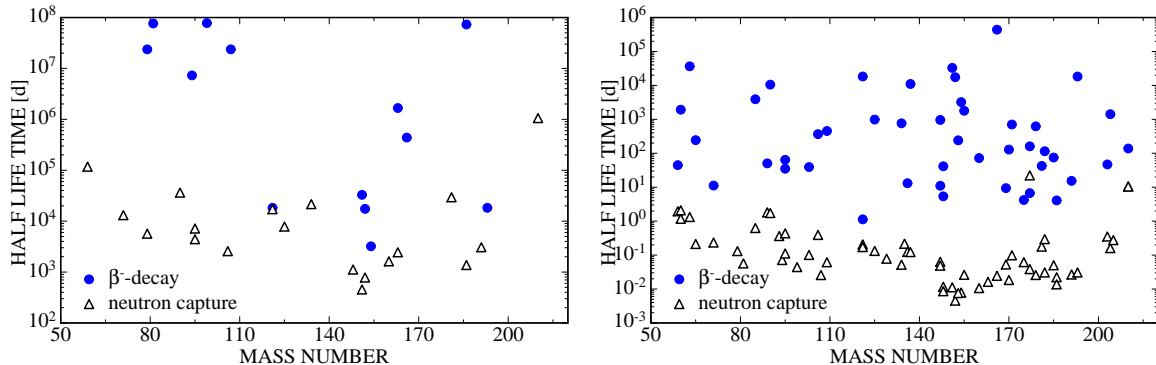


Figure 1. Left: Half life times with respect to neutron capture (open triangles) for a neutron of density 10^7 cm^{-3} and terrestrial β^- half life times (filled circles) for unstable isotopes on the s-process path as a function of mass number. Shown are only isotopes where the neutron capture is faster than the β^- -decay at $kT = 5 \text{ keV}$. The neutron capture cross sections are taken from [4] and the half lives under stellar conditions from [5]. Right: Same as left, but for a neutron of density 10^{12} cm^{-3} and β^- -decays at $kT = 30 \text{ keV}$

The modern picture of the main *s*-process component refers to the He shell burning phase in AGB stars [1]. Nuclei with masses between 90 and 209 are mainly produced during the main component. The highest neutron densities in this model occur during the $^{22}\text{Ne}(\alpha, n)$ phase and are up to 10^{12} cm^{-3} with temperatures around $kT = 30 \text{ keV}$. The other extreme can be found during the $^{13}\text{C}(\alpha, n)$ phase where neutron densities as low as 10^7 cm^{-3} and temperatures around $kT = 5 \text{ keV}$ are possible. Similarly to the main component, also the weak component referring to different evolutionary stages in massive stars has to phases [2, 3]. Mainly nuclei with masses between 56 and 90 are mainly produced during the weak component. The first phase occurs during the helium core burning with neutron densities down to 10^6 cm^{-3} and temperatures around $kT = 25 \text{ keV}$. The second phase happens during the carbon shell burning with neutron densities up to 10^{12} cm^{-3} at temperatures around $kT = 90 \text{ keV}$.

The left part of Figure 1 shows a summary of the neutron capture and β^- decay times for radioactive isotopes on the neutron rich side of the valley of stability, under the condition that the neutron capture during the $^{13}\text{C}(\alpha, n)$ occurs faster than than the β^- decay at stellar temperature. Obviously the vast majority of isotopes, where an experimental neutron capture cross section is desirable, have terrestrial β^- half-lives of at least thousands of days. The right part Figure 1 shows the same as the left part, but for the higher neutron density and temperature. Now isotopes with half-lives down to a few days can be of interest for the *s*-process reaction network.

Improved experimental techniques, especially as far as the neutron source and sample preparation are concerned, are necessary to perform direct neutron capture measurements on such isotopes [6]. Though the activation method or accelerator mass spectroscopy of the reaction products could be applied in a limited number of cases, experimental facilities like DANCE at LANL (USA) [7], n-TOF at CERN (Switzerland) [8] and the upcoming projects like SARAF (Israel) [9] and FRANZ at the Goethe University in Frankfurt (Germany) [10] are addressing the need for such measurements on the basis of the more universal method of detecting the prompt capture γ -rays, which is required for the application of the neutron time-of-flight (TOF) technique.

In particular the FRANZ facility allows the investigation of radioactive isotopes with half-

lives down to tens of days, while present facilities require half-lives of a few hundred days. This means the need for sample production facilities increases. A very good candidate would EURISOL.

2. The connection between s- and r-process

Nowadays, the s-process as a nucleosynthesis process is well understood and established. Current research uses the s-process as a link between abundance observations and stellar models. The underlying physics needs to be better determined by investigating the important branch points.

Massive stars are not only the host of the weak component of the s process, but are also a candidate for the stellar site of the r process. A better understanding of the physical conditions during the weak component of the s process and the ejection processes after the supernova explosion will therefore improve our knowledge of the stellar site of the r process. Furthermore, since the weak component is typically dominating the production of isotopes between masses 60 and 90, small uncertainties in the s-process predictions result in huge uncertainties in the predicted r-process abundance, since the observed abundances are the sum of the different nucleosynthesis processes.

References

- [1] Lugaro M, Herwig F, Lattanzio J C, Gallino R and Straniero O 2003 *Ap.J.* **586** 1305
- [2] Travaglio C, Gallino R, Arnone E, Cowan J, Jordan F and Sneden C 2004 *Ap. J.* **601** 864
- [3] Heil M, Käppeler F, Uberseder E, Gallino R and Pignatari M 2007 *Prog. Nucl. Part. Phys.* **59** 174
- [4] Bao Z Y, Beer H, Käppeler F, Voss F, Wisshak K and Rauscher T 2000 *Atomic Data Nucl. Data Tables* **76** 70
- [5] Takahashi K and Yokoi K 1987 *Atomic Data Nucl. Data Tables* **36** 375
- [6] Reifarth R, Haight R C, Heil M, Käppeler F and Vieira D J 2004 *Nucl. Instr. Meth. A* **524** 215
- [7] Reifarth R, Bredeweg T A, Alpizar-Vicente A, Browne J C, Esch E I, Greife U, Haight R C, Hatarik R, Kronenberg A, O'Donnell J M, Rundberg R S, Ullmann J L, Vieira D J, Wilhelmy J B and Wouters J M 2004 *Nucl. Instr. Meth. A* **531** 528
- [8] Abbondanno U, Aerts G, Alvarez-Velarde F, Alvarez-Pol H, Andriamonje S, Andrzejewski J, Badurek G, Baumann P, Becvar F, Benlliure J, Berthoumieux E, Calvino F, Cano-Ott D, Capote R, Cennini P, Chepel V, Chiaveri E, Colonna N, Cortes G, Cortina D, Couture A, Cox J, Dababneh S, Dahlfors M, David S, Dolfini R, Domingo-Pardo C, Duran I, Embid-Segura M, Ferrant L, Ferrari A, Ferreira-Marques R, Fraiss-Koelbl H, Furman W, Goncalves I, Gallino R, Gonzalez-Romero E, Goverdovski A, Gramegna F, Griesmayer E, Günsing F, Haas B, Haight R, Heil M, Herrera-Martinez A, Isaev S, Jericha E, Käppeler F, Kadi Y, Karadimos D, Kerveno M, Ketlerov V, Koehler P, Konovalov V, Krticka M, Lamboudis C, Leeb H, Lindote A, Lopes I, Lozano M, Lukic S, Marganiec J, Marrone S, Martinez-Val J, Mastinu P, Mengoni A, Milazzo P M, Molina-Coballes A, Moreau C, Mosconi M, Neves F, Oberhummer H, O'Brien S, Pancin J, Papaevangelou T, Paradela C, Pavlik A, Pavlopoulos P, Perlado J M, Perrot L, Pignatari M, Plag R, Plompen A, Plukis A, Poch A, Policarpo A, Pretel C, Quesada J, Raman S, Rapp W, Rauscher T, Reifarth R, Rosetti M, Rubbia C, Rudolf G, Rullhusen P, Salgado J, Soares J C, Stephan C, Tagliente G, Tain J, Tassan-Got L, Tavora L, Terlizzi R, Vannini G, Vaz P, Ventura A, Villamarin D, Vincente M C, Vlachoudis V, Voss F, Wendler H, Wiescher M and (n TOF Collaboration) K W ((n-TOF Collaboration)) 2004 *Phys. Rev. Letters* **93** 161103 (pages 5)
- [9] Nagler A, Mardor I, Berkovits D, Piel C, vom Stein P and Vogel H 2006 *LINAC 2006* (Knoxville, TN: Joint Accelerator Conferences Website) p MOP054
- [10] Meusel O, Chau L P, Mueller I, Ratzinger U, Schempp A, Volk K and Zhang C 2006 *LINAC 2006* (Knoxville, TN: Joint Accelerator Conferences Website) p MOP051

Optical techniques for r-process nuclei

Bradley Cheal
(bradley.cheal@manchester.ac.uk)

Schuster Building, Brunswick Street, The University of Manchester, M13 9PL, UK

Nuclear structure research across the nuclear chart is underpinned by measurements of fundamental ground state and isomeric properties. Shell structure and level migrations can be probed using valence properties such as the nuclear spin and magnetic moment, and collective properties by the quadrupole shape and mean-square charge radius. These can all be studied in a model-independent way using laser spectroscopy [1].

Laser ion sources use lasers to resonantly ionise and selectively enhance the yield of a chosen element. At ISOLDE, CERN, the Resonant Ionisation Laser Ion Source, RILIS [2], is now used for most experiments and similar systems are under development elsewhere. An optical spectrum can be produced by recording the yield as the laser frequency is scanned. Although a fast and efficient method, the resonance peaks are Doppler broadened due to the velocity spread of the atoms

Higher resolution is required to fully resolve the hyperfine components—particularly important for the quadrupole moment, precision and measurements of the nuclear spin. This is achieved by overlapping the extracted (fast) ion beam with the laser beam in a collinear geometry. While the energy spread of the ions remains a constant under acceleration, the ~ 30 keV kinetic energy suppresses the velocity spread in the forward direction and thus the Doppler broadening. Fluorescence photons are detected as a Doppler tuning voltage is scanned.

Such experiments are conducted almost entirely at ISOL facilities such as ISOLDE, CERN and at the JYFL IGISOL, Jyväskylä, Finland. This latter type of facility gains an advantage for refractory elements and short lived (sub-millisecond) states, since the products recoil into a gas stopper from thin foil targets.

Background counts in collinear spectra arise principally from the continuous scattering of laser light into the photomultiplier tube. An ion beam cooler-buncher (a gas-filled segmented linear rf quadrupole) not only reduces the emittance (improving the ion-laser spatial overlap with a long and narrow beam waist) but also offers the ability to accumulate the ions and release them in bunches. By only accepting photon counts in coincidence with the passing of an ion bunch through the detection region, the background is suppressed by four orders of magnitude. Such devices have been employed for this purpose at JYFL [3] and more recently ISCOOL at ISOLDE [4]. Hyperfine structures have been measured with ion fluxes down to 100 ions/s using this method [5].

The Collinear Resonance Ionisation Spectroscopy (CRIS) project [6], currently under construction at ISOLDE, seeks to combine the high resolution of the collinear method with the sensitivity of particle detection. In this technique, the ions are neutralised and selectively re-ionised in a multi-step optical excitation process. A spectrum is then formed by scanning the frequency of the first step while measuring the ion counts (or subsequent decay). Since only pulsed lasers have the required power for the ionisation step, a bunched ion beam is essential to avoid duty cycle losses in efficiency.

Exploration of r-process nuclei is hampered by the rapid fall in yield with neutron

number. Although each generation of future facility will offer higher production intensities, the sensitivity of the method should continue to be further improved to reach the most exotic of cases possible and with the most efficient use of beam time. For fluorescence detection, prior to the bunching technique, the photon background was suppressed by vetoing all photon counts not detected in coincidence with a (single) corresponding ion [7]. With the use of segmented photomultiplier tubes, a timing resolution of a few nanoseconds is achievable, and a theoretical sensitivity of a few ions per second. However, in practice the technique suffers without beam purity.

A new technique of optical pumping in an ion beam cooler exploits the focal point of slowly travelling ions for efficient excitation. This has been used to populate metastable states to broaden the range of transitions available to collinear fast-beam techniques—in some cases making elements available to such studies for the first time [8]. In the future, multi-step laser excitations schemes will be investigated which excite the singly charged ions in the cooler to a doubly charged state. On the release of an ion bunch, these will be time-of-flight separated and a pure beam of a single element (already mass analysed) will be formed. In the case of laser spectroscopy, this will allow the full potential of photon-ion coincidence spectroscopy to be exploited. Initial development work on this technique will take place in the new laboratory extension at JYFL (where a new cyclotron is being installed for IGISOL experiments) before porting to other facilities, including future facilities such as EURISOL.

References

- [1] J. Billowes and P. Campbell, *J Phys. G* **21** (1995) 707
- [2] U. Köster, V. Fedoseyev *et al.*, *Nucl. Instr. and Meth. B* **160** (2000) 528
- [3] P. Campbell *et al.*, *Phys. Rev. Lett.* **89** (2002) 082501
- [4] E. Mané *et al.*, *Eur. Phys. J. A* **42** (2009) 503
- [5] M.L. Bissell *et al.*, *Phys. Lett. B* **645** (2007) 330
- [6] K.T. Flanagan *et al.*, CERN-INTC-2008-010
- [7] D.A. Eastham *et al.*, *Opt. Commun.* **82** (1991) 23
J.M.G. Levins *et al.*, *Phys. Rev. Lett.* **82** (1999) 2476
- [8] B. Cheal *et al.*, *Phys. Rev. Lett.*, **102** (2009) 222501

New ideas in the nuclear energy density functional approach

Jacek Dobaczewski

IFT - University of Warsaw
JYFL - University of Jyväskylä

in collaboration with the FIDIPRO team:

M. Borucki, G. Carlsson, J. Dobaczewski, M. Kortelainen, N. Michel,
K. Mizuyama, A. Pastore, F. Raimondi, R. Rodríguez-Guzmán,
J. Toivanen, P. Toivanen, and P. Veselý

Abstract of the talk given at the first EURISOL UG topical meeting:
The formation and structure of r-process nuclei between $N = 50$ and 82 (including ^{78}Ni and ^{132}Sn areas)
December 9-11, 2009, INFN-LNS, Città Universitaria, Catania, Italy

In Ref. [1], it was proposed to shift attention and focus of the energy density functional (EDF) methods [2] from ground-state bulk properties (e.g. total nuclear masses) to single-particle (s.p.) properties, and to look for a spectroscopic-quality EDFs that would correctly describe nuclear shell structure. Proper positions of s.p. levels are instrumental for good description of deformation, pairing, particle-core coupling, and rotational effects, and many other phenomena.

Up to now, methods based on using EDFs, in any of its variants like local Skyrme, non-local Gogny, or relativistic-mean-field [2] approach, were mostly using adjustments to bulk nuclear properties. As a result, shell properties were described poorly. After so many years of investigations, a further increase in precision and predictability of all methods based on the EDFs may require extensions beyond forms currently in use [3, 4]. Before this can be fully achieved, it was proposed to first take care of the s.p. properties, and come back to precise adjustment of bulk properties once these extensions are implemented.

To illustrate the current status of the description of the s.p. levels, in Fig. 1 we show the neutron and proton levels above the $Z = 50$ and $N = 50$ shell gaps, calculated by using typical three Skyrme functionals. The parametrization SkP [5] gives, on average, the best description of the s.p. levels [3], which is due to its effective mass of $m^*/m = 1$. The parametrization SLy4 [6] gives, on average, the best description of the bulk nuclear properties, and that of SkO_T [1] was adjusted to reproduce the spin-orbit and tensor properties of light nuclei. First of all, one sees that these three parametrizations give rather different and inconsistent positions of the s.p. levels. Second, none of this parametrizations gives results compatible with experimental data, see e.g. Ref. [7]. As a particular example of such a discrepancy, let us quote the incorrect splitting between the neutron $2d_{5/2}$ and $1g_{7/2}$ orbitals near ^{100}Sn , which is experimentally known to be only 172 keV [8, 9].

Within the standard 12-parameter form of the Skyrme functional [2], an improvement of spectroscopic properties cannot be obtained [3], and extensions of this form seem to be mandatory. One possible way could be the inclusion of density dependence into all the 12 coupling constant of the standard functional [10]. Another one, which was recently proposed in Ref. [4], aims at including gradient corrections up to next-to-next-to-next-

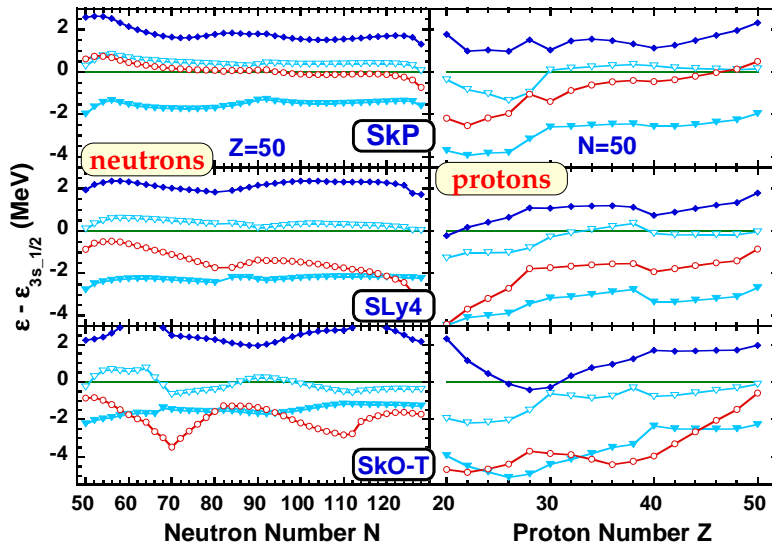


Figure 1: Neutron s.p. levels for $Z = 50$ (left panels) and proton s.p. levels for $N = 50$ (right panels) as functions of the numbers of neutrons and protons, respectively. Top, middle, and bottom panels show results obtained for the SkP [5], SLy4 [6], and SkO_T [1] Skyrme functionals. The s.p. energies, relative to those of the $3s_{1/2}$ orbital, are plotted for the $2d_{5/2}$ (full triangles), $2d_{3/2}$ (open triangles), $1g_{7/2}$ (open circles), and $1h_{11/2}$ (full diamonds) orbitals.

to-leading order ($N^3\text{LO}$ – sixth order). Work along these lines is now in progress.

At present, to gain progress and precision in the description of nuclear properties across the nuclear chart, it is required to use concerted efforts of large theoretical groups. The amount of work, which is needed to build new and better approaches, exceeds by far the capabilities of present-day small and dispersed groups of theorists working in nuclear structure and nuclear reactions. In Europe, since many years the only effort to build a new substantial theoretical group has been realized within the FIDIPRO project [11] at the University of Jyväskylä. A much larger initiative has been recently undertaken in the US within the UNEDF proposal [12].

Nevertheless, even these recently increased efforts are not sufficient for building commensurable support for planned and constructed new-generation experimental facilities. Indeed, over the past twenty odd years, the community of nuclear theorists has dangerously shrunk. Although the domain has been continuously receiving a significant influx of young talent, the possibilities to employ and keep these highly trained people were not available, due to grossly inadequate funding of theory. As a result, we have now to cope with the age gap of theorists being between 30 and 45 years old.

The present situation puts the entire domain of low-energy nuclear physics in jeopardy. Indeed, because of the shortage thereof, it can be increasingly difficult to involve theorists in preparations of white-papers and proposals for new investments in experimental projects. Regretfully, in the past such an involvement was not followed by matching funds allocated for the development of theory. More importantly, it can be increasingly difficult to consume the experimental progress in measuring more and more nuclei far from stability, and to cast it into an increased understanding of global nuclear forces and many-body properties. In the situation where costly nuclear-physics projects, like EURISOL, will fiercely compete with other large-scale endeavours in science, the domain must demonstrate that the projected measurements will contribute to the progress in understanding nuclei, which requires excellent theory.

In practice, a balanced science portfolio in nuclear physics can only be build by earmarking for theory 5–10% of the capital investment of any experimental project. This contribution should be understood at the same level as covering the running and maintenance costs of new facilities, and should be similarly undisputable. Such a contribution, at the level of 5.7%, has recently been projected within the ENSAR proposal, which was submitted at the beginning of December 2009. To fully correct for the past trend, the EURISOL preparatory phase should

be focused on theory to a much higher degree – we have time for that, and we should not miss this window of opportunity. It is increasingly encouraging, that a support to theory begins to be strongly advocated by the experimental community. It is obvious that such an investment cannot be called for by theorists alone.

On the practical level, the most promising scheme of expansion could be to create several strong groups at major European universities; at those which already now have a substantial experience in conducting research in this domain of physics. Indeed, theory groups best flourish in the stimulating and competitive environment of a university, where they have a chance to profit from cross-links and cross-fertilization from theory groups in other domains of physics. These groups could form a virtual European Institute for Theoretical Nuclear Physics, which could be funded on the European level, and would provide for (i) post-doc and junior temporary positions and (ii) bridge positions at the senior level co-financed with the hosting universities. A network of several groups of this kind could be strong enough to coherently undertake serious projects aiming at a quantitatively better and unified nuclear-structure and nuclear-reactions theory.

References

- [1] M. Zalewski, J. Dobaczewski, W. Satuła, and T.R. Werner, Phys. Rev. C **77**, 024316 (2008).
- [2] M. Bender, P.-H. Heenen, and P.-G. Reinhard, Rev. Mod. Phys. **75**, 121 (2003).
- [3] M. Kortelainen, J. Dobaczewski, K. Mizuyama, and J. Toivanen, Phys. Rev. C **77**, 064307 (2008).
- [4] B.G. Carlsson, J. Dobaczewski, and M. Kortelainen, Phys. Rev. C **78**, 044326 (2008).
- [5] J. Dobaczewski, H. Flocard and J. Treiner, Nucl. Phys. **A422**, 103 (1984).
- [6] E. Chabanat, P. Bonche, P. Haensel, J. Meyer, and R. Schaeffer, Nucl. Phys. A **635**, 231 (1998).
- [7] N. Schwierz, I. Wiedenhover, and A. Volya, arXiv:0709.3525.
- [8] D. Seweryniak, M.P. Carpenter, S. Gros, A.A. Hecht, N. Hoteling, R.V.F. Janssens, T.L. Khoo, T. Lauritsen, C.J. Lister, G. Lotay, D. Peterson, A.P. Robinson, W.B. Walters, X. Wang, P.J. Woods, and S. Zhu, Phys. Rev. Lett. **99**, 022504 (2007); Acta Phys. Pol. **B40**, 621 (2009).
- [9] I.G. Darby *et al.*, submitted to Nature (2009).
- [10] M. Kortelainen *et al.*, to be published.
- [11] <http://www.jyu.fi/accelerator/fidipro/>.
- [12] <http://unedf.org/>.

Ari Jokinen
University of Jyväskylä

1. Background/motivation/Status/Present situation, ...

During the last few years, an application of Penning trap techniques in nuclear laboratories working with radioactive isotopes has resulted in a vast amount of new precise data. On neutron-rich side, especially among medium mass nuclei connecting two waiting point regions (A 80 and A 130), the new data is mainly coming from two ISOL facilities, IGISOL in the Accelerator laboratory in the University of Jyväskylä and ISOLDE at CERN.

In the Penning trap mass determination of the nucleus is based on the cyclotron frequency (ω_c) of the ion of interest $\omega_c = (1/2\pi)(q/m)B$, provided magnetic field B is calibrated by measuring the cyclotron frequency ($\omega_{c,\text{ref}}$) of a precisely known reference mass. Frequent switching between the unknown and reference isotope allows precise calibration of the magnetic field and thus high precision in atomic mass deduced. Typical precision obtained at ISOLTRAP and JYFLTRAP is of the order of few keV even for the most exotic isotopes reached so far.

Parallel to increasing amount of ion trap data, vast amount of new data have been collected at storage ring at GSI. In some isotopic chains, the storage ring can reach out further from the stability, but the precision obtained is typically one to two orders of magnitude worse, i.e. at least few tens of keV or more.

Direct mass measurements have shown serious deviations compared to the evaluated atomic mass data. The discrepancy tends to get larger while moving further from the stability. This probably due to the fact that the old data relying on the beta decay Q-value often underestimates the decay energies due to the poor knowledge of the decay schemes far from the stability. Over the long isobaric chain, an error on the ground-state masses accumulates when moving further from the stability. This observation is not only important for the evaluated atomic mass data, but implies that the mass predictions tuned to reproduce the evaluated data, should be refitted to the new data available.

In addition to a pure atomic mass interest, the obtained data can be and has been used to extract nuclear decay and structure data, providing an important complimentary source to spectroscopic studies. Nuclear structure data is obtained by following the systematic trends of binding observables, like the two-neutron separation, shell gap energies and pairing energies. A series of precise atomic masses of neutron-rich nuclides were measured to map the mass surface around the well-known region of sudden onset of deformation at Z=40 and N=60. Another nuclear structure interest is related to the evolution of N=50 shell gap as a function of decreasing element number. Very recently similar studies have been performed in the vicinity of ^{132}Sn allowing to probe evolution of N=82 shell gap as well as binding along the Sn-chain. A further motivation for mass measurements in the neutron-rich side is to provide accurate mass values for a better understanding of the rapid-neutron capture process (r-process).

In addition to pure mass measurements, JYFLTRAP setup has been widely used to improve the sensitivity and the selectivity of the conventional decay

spectroscopy resulting in for example, new decay scheme of ^{115}Ru , new results on the decay of odd $109,111\text{Mo}$ isotopes and collective structure of ^{114}Ru isotopes via beta decay ^{114}Tc . Other spectroscopic techniques coupled to the JYFLTRAP include Total absorption spectroscopy, beta-delayed neutron spectroscopy and in-trap detection of charged particles.

2. Mass measurements in EURISOL era

The recent achievements pave the way for a study of ground-state properties of the most exotic nuclei, achievable only with the next generation facilities, like EURISOL. Measurement techniques have already been developed beyond the necessary precision for nuclear structure studies. In the forthcoming years and with new facilities the main two issues in terms of atomic mass measurements are:

1) What is the gain in production of exotic isotopes in new facilities compared to the present ones? The present ion trap facilities have demonstrated that required precision can be achieved in few tens of ms. Typical beta decay half-lives of medium mass nuclei are still in the range of 100 ms and moving few neutrons further from the stability will not change the situation drastically. Thus the half-lives are not the limiting factor, but the reach of exotic isotopes is mainly defined by the production yields in the future facilities.

2) Ion manipulation and purification prior to the trap measurements becomes increasingly important in the future. Ion traps have limited capacity for isobaric contaminations and isobaric background tends to increase with the new facilities, like EURISOL. Thus the technical challenge lies in the purification of the sample. This is general problem which holds for many spectroscopic studies, not only for trap measurements, with future facilities.

All in all, there is still room for precision mass measurement of neutron-rich nuclei in the future facilities, like EURISOL. It is expected that storage ring facilities, like FAIR or RIKEN will provide large sets of new data and most probably they can reach further from the stability. However, there are a couple of issues supporting ion trap techniques at future ISOL facilities: Firstly, the precision obtainable will always be superior compared to storage ring approaches and secondly, storage ring data rely on the precise calibrations from the Penning trap measurements.

Mass measurements on neutron-rich nuclei at ISOLTRAP: Present status and future perspectives (Alexander Herlert, CERN)

The mass of a nucleus plays an important role in the investigation of nuclear structure and nuclear astrophysics. For the latter it is a key ingredient to perform network calculations on nucleosynthesis processes. Especially the rapid neutron capture process (r process) requires the knowledge of nuclear masses, half-lives, branching ratios, and neutron capture cross sections of very neutron-rich nuclei far away from the valley of stability. For the nuclear masses, different mass models can be employed, which however show large deviations for extrapolated mass values. A wide survey of the mass surface with Penning trap mass spectrometers helps to improve the accuracy and precision of the known nuclides, partly by including the data into a global atomic mass evaluation, but also helps to explore the region of unknown isotopes.

The ISOLTRAP Penning trap mass spectrometer is the pioneering experiment for the precision mass determination of radionuclide masses and up to date five other systems are operated worldwide at RIB facilities: CPT at Argonne National Lab, SHIPTRAP at GSI, JYFLTRAP in Jyväskylä, LEBIT at NSCL/MSU, and TITAN at TRIUMF. All systems are in general capable to reach a relative mass uncertainty down to $\delta m/m = 1 \times 10^{-8}$ (and even below) and can investigate nuclides with a half-life of just a few tens of milliseconds. New techniques for the preparation of the ions as well as their detection have been developed in the past and the efficiencies have increased over the last years such that more and more exotic nuclides could be addressed. Especially both the ISOLTRAP and JYFLTRAP mass spectrometers have contributed each several hundred mass values, partly reaching to the edge of the region of known nuclides where the masses had just been extrapolated from trends in the mass surface. This allowed one to obtain important information on neutron-rich nuclides relevant for the calculation of the r -process path, for example mass measurements on the major waiting point ^{80}Zn and beyond, neutron-rich krypton nuclides up to ^{97}Kr , or neutron-rich tin nuclides beyond ^{134}Sn . In some cases the same isotopes have been studied and the data showed within the uncertainties a very good agreement, which demonstrates the high quality and accuracy of mass values obtained with Penning traps.

All Penning trap mass spectrometers use the same technique to determine the atomic mass of the exotic nuclides. A few ions, ideally only one ion, of the ion of interest are stored in the Penning trap and by mass-selective manipulation of the ion motion with external radiofrequency fields the cyclotron frequency is determined using a destructive ion-cyclotron-resonance time-of-flight technique. The calibration of the magnetic field is done by measuring the cyclotron frequency of a well-known nuclide. For the purification a second Penning trap is employed which also uses the mass-selective manipulation of the ion motion within a buffer-gas environment. The achievable mass resolving power is of the order of 10^5 and is thus superior to the standard mass separators, e.g., at ISOLDE.

Recent target an ion-source development at ISOLDE aimed at better RILIS schemes for selective laser ionization and an improved ionization efficiency for plasma ion sources. In the latter case the so-called versatile arc discharge ion source (VADIS) gave in certain

cases a factor 10 higher ionization efficiencies which allowed the ISOLTRAP mass spectrometer to probe very neutron-rich krypton isotopes thus crossing the $N=60$ line. The new data showed no sign of deformation in that region of the mass surface in contrast to isotopes with higher Z .

The main limitations for Penning traps measurements are related to the purity of the delivered beam, the intensity of the radionuclide beam, and the half-life of the nuclide of interest. The purity comprises two aspects: first, the presence of long-lived excited state isomers, which are sometimes more abundant than the ground state; second, the other isobaric contaminations which are also coming with the radioactive beam. For the removal of isomers, which can be only a few tens of keV away from the ground state, it very much depends on the half-life of the ion of interest. The longer the rf excitations can be applied to perform the mass-selective manipulation, the higher is the resolving power. Thus, the purification for very short-lived ions is limited. Isobaric contamination can usually be removed with the mass-selective cleaning procedure in a Penning trap (also limited by the half-life with respect to the achievable resolving power). However, for large abundances of isobaric contamination in the trap, the presence of space-charge influences the ion motion and prevents the application of the cleaning procedure. A first systematic study of these space-charge effects has been done and more measurements are planned.

In order to circumvent the problem of large yields of contaminating isobaric ions, it is planned to use an electrostatic ion trap as an isobar separator. Inside this trap, the different ion species are reflected between two electrostatic mirrors and after a certain waiting time (up to a few milliseconds) the ion species are separated in different ion bunches and can be separated after ejection with a very fast beam gate. First off-line tests with stable CO and N_2 ions have been successful and after the implementation at ISOLTRAP further tests are planned.

Besides the increase of ionization efficiencies at the targets and efficiencies of the Penning trap systems (not only for the final ion detection but also the stopping of the radionuclide ions and their transfer to the trap) the improvement of production yields is very important. Higher yields at the future RIB facilities, e.g., also at EURISOL, will help to further reach to very neutron-rich nuclides. However, a mass separator with a very high mass-resolving power is needed in order to avoid the subsequent preparation steps in the various ion traps to produce clean ion bunches. The resulting shorter experiment cycles will also help to reach short-lived nuclides even when production yields are dropping as well. Furthermore, single ion detection in cryogenic Penning traps is being applied and might be useful for the investigation of exotic nuclides with very low production rates. Thus, Penning traps will also play an important role in the future.

Structure of nuclei “North and Northeast of ^{78}Ni ”: contribution from beta-decay

David Verney

IPN, Orsay, France.

1-Introduction

Considerable efforts have been recently deployed in order to experimentally reach the region in the immediate vicinity of ^{78}Ni to assess the doubly magic character of this very neutron rich nucleus. One of the most interesting questions related to the persistence of the $Z = 28$ and $N = 50$ shell gaps far from stability is whether ^{78}Ni can be considered as an inert core (a good core) for the nuclear shell model.

2-The Tandem/ALTO facility at IPN Orsay

An experimental campaign aiming at studying the stiffness of the $N=50$ major shell gap in direction to ^{78}Ni via γ -spectroscopy following β -decay has been undertaken at the Tandem/ALTO facility installed at the Institut de Physique Nucléaire, Orsay. Mass separated beams of ^{238}U -fission fragments were obtained at the PARRNe mass separator using ISOL techniques. During the first experiments, the radioactive species were created by irradiating the UCx target/ion source ensemble with the 26-MeV deuteron beam delivered by the 15-MV MP-Tandem, and then, with a primary electron beam of 50 MeV $10\mu\text{A}$ delivered by the ALTO electron LINAC (part of the former LEP-injector). Gamma rays following the beta decays of ^{83}Ga and ^{81}Zn were observed during the deuteron campaign and from ^{84}Ga beta-decay during the first ALTO runs ($1\mu\text{A}$ electrons).

3- β -decay experimental setup

Typical γ -detection system used in this campaign consisted of one coaxial large volume HPGe detector (70% relative efficiency) of the non-tapered CHATO type with a resolution of 2.3 keV at 1.3 MeV and one small EXOGAM CLOVER detector from the prototype series (100% relative efficiency) with a typical resolution for the central signal of a single crystal of 2.0 keV at 1.3 MeV. These two detectors were placed in a 180° geometry close to the point where the beam was collected onto the tape. In this configuration a total photopeak efficiency of 3% at 1.3 MeV was achieved. This collection point was surrounded by a tube-shaped plastic scintillator for β -detection (ϵ_{β} 30-50%). The main function of the tape cycling is to provide a complementary piece of information to help in the Z -identification of unknown new lines which are expected to appear in the spectra by analyzing their time dependence. The second purpose of this device is to allow evacuation of longer-lived activities of the daughter nuclei.

We focus in this report on results which have been obtained on γ -spectroscopy following β -decays studies of $^{83,84}_{31}\text{Ga}_{52,53}$.

4-Results from the study of the $^{83}\text{Ga}_{52}\text{-}^{83}\text{Ge}_{53}$ β -decay $^{84}\text{Ga}_{52}\text{-}^{83}\text{Ge}_{53}$ $\beta\text{-n}$ -decay : possible discovery of a new subshell gap at $N=58$.

Two γ -lines were attributed to transitions in ^{83}Ge at 867.4 keV and 1238.5 keV in the study of ^{83}Ga β -decay and one at 247.8 keV in the study of ^{84}Ga $\beta\text{-n}$ decay allowing to establish a first level scheme for this very exotic nucleus, though very scarce. When placed into the systematic of low lying levels of the heavier $N=51$ odd-isotones it appears that the two levels at 867.4 keV and 1238.5 keV could be associated to two members of the multiplet of states originating from the coupling of the 2^+ of the even-even singly magic ($N=50$) core and the first filled neutron orbital beyond $N=50$ viz $\nu 2d_{5/2}$. The first excited state of the $N=51$ odd-isotones starting from stability (Sr) has $J^\pi=1/2^+$ and can be associated to the main fragment of the neutron single particle state $\nu 3s_{1/2}$. As confirmed by recent direct reaction

measurements performed at HRIBF-Oak Ridge. We have used the core-particle coupling approach in the Thankappan and True way and using a dipole-dipole + quadrupole-quadrupole coupling strength between the core and the particle in order to extract effective neutron single particle energies from the existing level pattern for ^{89}Sr , ^{87}Kr , ^{85}Se and ^{83}Ge . The results of the calculation reproduce with good precision the excited state energy sequence but also the measured spectroscopic factors and electromagnetic quantities when available. It emerges clearly from this analysis of the existing data on the $N=51$ odd-isotones starting from stability down to $Z=32$ that there is a down sloping of the $\nu 3s_{1/2}$ single particle which separates markedly from the $\nu 2d_{3/2}$ and $\nu 1g_{7/2}$ to get very close to the $\nu 2d_{5/2}$ giving rise to a new and unexpected subshell gap at $N=58$. It is worth mentioning at that point that such a behavior of the neutron single particle evolution towards ^{78}Ni , and in particular the occurrence of a new subshell gap, was not clearly (if not at all) predicted or foreseen in the framework of existing structure theoretical studies.

5-Results from the study of the ^{84}Ga - ^{84}Ge β -decay : possible onset of collectivity in the vicinity of ^{78}Ni .

Two γ -lines were attributed to transitions in ^{84}Ge at 624.3 keV and 1046.1 keV in the study of ^{84}Ga β -decay and were attributed to the $2+_{0+}$ and $4+_{2+}$ transitions. There is an increase of the experimental $E(4+_{1})/E(2+_{1})$ values for the $N = 52$ isotones from stability ($Z = 40$) toward neutron excess. The inclusion of the new value at $Z = 32$ obtained in the present work reveals some acceleration in this tendency (similar to the one between $Z = 40$ and 38) which should, most generally speaking, be interpreted as a sudden increase of collectivity. Interestingly, a local minimum at $Z=32$ in the $N=50$ gap has been put in evidence by the most recent mass measurements. This local minimum is well explained in beyond mean field approach which also reproduces with very good accuracy the observed $2+$ and $4+$ level energies. When looking closer to the HFB+GCM calculations a sudden transition between spherical shape for the singly magic ^{82}Ge and complete gamma-softness for $N=52$ is indeed expected.

5-Conclusion and perspectives for β -decay studies of stopped fission fragment beams in the framework of EURISOL.

As a conclusion, beta-decay studies performed close to ^{78}Ni allowed to discover new and unexpected trends in nuclear structure in this mass region for the first time. This mass region has been the object of a very intensive experimental work in recent years using all available techniques and it appears clearly that beta-decay studies are still quite competitive. Recent history has show that in many cases, data coming from beta-decay were the first source of information available on structure for the most exotic nuclei. This should constitute a strong encouragement to envisage the possibility for a beta-decay setup installed at the EURISOL facility. In addition to the physics program which can be achieved by using this robust technique, systems like tape stations equipped with beta and gamma (plus X-rays, electrons etc) detectors are excellent tools for a real evaluation of the effective beam intensities and beam purity evaluation, which is useful in the early stages of commissioning of RIB facilities. In that sense, they can be used as the very first experimental setups where to send the "brandly new beams" as soon as they become available, even before post-acceleration, and can accompany usefully new beam developments.

REGISTRATION BETA-DELAYED 1, 2-NEUTRONS EMISSION FROM PHOTOFISSION FRAGMENTS OF ^{238}U AT MK-25 AND PARNNE

*D. Testov¹⁾, S. Ancelin²⁾, F. Ibrahim²⁾, M. Niikura²⁾, Yu. Penionzhkevich¹⁾,
V. Smirnov¹⁾, E. Sokol¹⁾, B. Tastet²⁾, D. Verney²⁾*

¹⁾ – *Flerov laboratory of Nuclear Reactions, Joint Institute for Nuclear Research, Dubna, Russia*

²⁾ – *Institute de Physique Nucléaire d'Orsay, France*

ANNOTATION

The project of an extension of the experiment which was carried out at electron accelerator MK-25 (JINR, Dubna) of registration β -delayed 2-neutrons emission from fragments of ^{238}U using the on-line separator PARNNe (IPN, Orsay) is proposed. New experimental studies of the ground-state and β -decay properties of very neutron-rich nuclei near the exotic shell-closures have been a motivation for these experiments. The Sn isotopes keep their magic character from $N=50$ to $N=82$. Studies its integral properties ($T_{1/2}$ and P_n) put a first-sight constraint on the ground state properties of very isospin asymmetric nuclei: the masses, Q-values, deformations, etc.

SCIENTIFIC CASE

When moving further and further away from the valley of stability, the Q values for β decay increase more and more. Close to the drip line, β -delayed particle emission is observed. Even further away, β -delayed two-nucleon emission can be observed and studied. There are a lot of experimental data concerning multiple (up to 4 neutrons) neutron emission in light nuclei range [1, 2] and only double neutron emission for $^{98,100}\text{Rb}$ has been measured in experiment [3] in ranges of medium and heavy nuclei. However, correlations between the two neutrons haven't been searched for these nuclei. Also there are predictions of existence $\beta 2n$ emitters in the ranges of medium and heavy nuclei [4, 5].

These correlations can give valuable information, inaccessible otherwise, about the pairing of nucleons inside the atomic nucleus. This information isn't accessible otherwise. Neutrons are not disturbed by the Coulomb barrier and correlation should be observable outside the nucleus therefore, two-neutron emission has a decisive advantage over two-proton emission.

In additional to interest of correlation studies, the decay characteristics of these nuclei are also of paramount importance for the understanding and modeling the astrophysical rapid-neutron caption process, which is responsible for the synthesis of approximately half of the elements heavier than Iron. Presently available experimental information about basic properties such as masses and decay schemes of neutron-rich nuclei doesn't include nuclei in the r-process path in the regions between the $N=50$, 82 and 126 shells. Systematic study of basic nuclear structure properties of neutron rich isotopes for (possibly) all elements from Fe to Sn, covering all "waiting-point" nuclei in the r-process path is very important.

Most of our understanding of nuclear structure relies on the existence of shell gap appearing for specific nucleon numbers called magic numbers. The study of the evolution of these gaps far from stability has been a motivation for many experiments. The magic number $Z=50$ is already known for its continuity far from stability. Actually, the Sn isotopes keep their magic character from $N=50$ to $N=82$. Probing the persistence of the shell gap at $N=50$ from $Z=50$ down to $Z=28$ represents an extremely active field of investigation in nuclear structure nowadays. Furthermore,

^{80}Zn is a critical nucleus in the calculation of the r process of stellar nucleosynthesis, and the most general calculation of this process require detailed knowledge of the properties of this nucleus.

To sum up there are three areas where two β -delayed neutron emission is possible. For the lightest nuclei the β -delayed two neutrons emission was experimentally well established. Search for β -delayed two neutrons emission in Br-Rb and Sb-Sn regions of the nuclide chart is an interesting experimental task.

The majority of the new P_n values were deduced from the ratios of simultaneously measured β - and delayed-neutron activities. It was only in a few cases that spectroscopic data were used to determine the one or other decay property (e.g. independent P_n determinations for ^{93}Br , ^{100}Rb and ^{135}Sn). Most of the new data were obtained at the on-line mass-separator facility ISOLDE at CERN. Data in the Fe-group region were obtained at the fragment separators LISE at GANIL and at the LISOL separator at Louvain-la-Neuve. Data in the refractory-element region were measured at the ion-guide separator IGISOL at Jyvaskyla. Finally, some new data in the ^{132}Sn region came from the OSIRIS mass-separator group at Studsvik.

B-DELAYED NEUTRON EMISSION FROM FISSION PRODUCTS IN THE ^{132}SN MASS REGION

Measuring the β -delayed neutron emission probability along the chains of very neutron-rich isotopes the effects which could be detected is possible irregularities in the A -dependence of the P_{total} -values after crossing the major neutron shell with $N=82$. Suppression of the delayed neutron emission probability has been predicted in [6, 7] for nuclei whose neutron excess is bigger than one major shell. It should not exist e.g. in Pd to In isotopes, but should appear in Sn and Sb isotopes with neutron numbers $N>82$.

The two-neutron separation energies S_{2n} reveal a smooth A -dependence except after the major neutron shell-crossing, while the Q_{β} -values show an odd-even staggering. It translates to the staggering of the phase-space $Q_{\beta-2n}$ available for the two-neutron β -delayed emission. This may affect the probability of the two-neutron β -delayed emission.

The neutron β -delayed emission is a threshold effect. Thus, interesting is the case of the decay to the collective states located close to the S_{2n} -position in the daughter nuclei. The amount of the β -strength entering the $Q_{\beta-2n}$ -window may differs for the neighboring isotopes. In a favorable situation some increase of the P_{2n} -values may be expected. The degree of the P_{2n} -values staggering carries important information on the interplay of nuclear deformation and pairing. It should be also influenced by the so-called “shell-quenching” effect widely discussed recently.

A favorable situation for dedicated studies can be found in the region of the Sn isotopes with the neutron numbers $N>82$ where typically $Q_{\beta-2n}=2-5$ MeV.

Our DF3+CQRPA calculation gives a factor of 3 to 5 suppression of the P_n -values from nearly 100% expected from pure GT-approximation [7].

METHODOLOGY

For identification new two-neutron emitters and for studying their decays, these isotopes have to be implanted into a catcher, which is surrounded by a high-efficiency, high-granularity β -, γ - and neutron detection systems. The half-life of the nucleus, the energy of the betas, gammas and neutrons and in particular the angle between the two neutrons could be measured.

Helium counters detect neutrons by the reaction $^3\text{He} + n \rightarrow ^3\text{H} + p + 780$ keV, with the cross section for thermal neutron $\sigma_{\text{th}}=5320$ barns. A neutron is detected just once because it is captured in this moment; it means that the “cross talk” effect is excluded in principle. Since thermal neutrons are involved, the energy threshold is almost zero. The helium counters are practically insensitive to gamma rays. The detailed descriptions of main features of the detectors are presented in the articles [8].

THE FIRST TRIAL EXPERIMENT

The unique experimental detection system created with at ALTO [10] (IPN Orsay) consisted of three kinds of the detectors were constructed. 90 ^3He counters were used together with a detector of gammas and beta. The schematic view of the setup is shown at the Fig 1a., and at the Fig. 1b the photo is given.

The neutron detector efficiency measured from spontaneous fission source in the geometry presented was up to 35%. Life time of neutrons inside the detector is 35 μs was also measured.

Three-partial coincidence trial experiment was carried out at a mass separated beam ($A = 136$). The P_n probability for ^{136}Te was measured and compared with the table one. Due to low statistics the result obtained has quite big errors however it proves availability of the unique system created for direct measurements of delayed multi neutron emissions from neutron rich fission fragments.

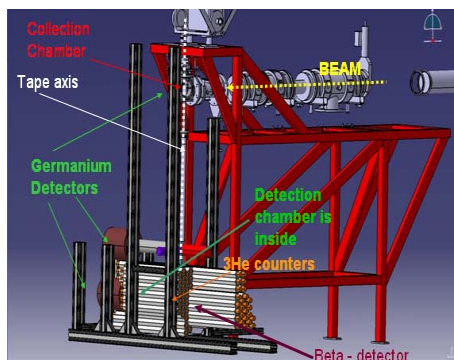


Fig 1a. The schematic view of the experimental setup



Fig 1b. The overview of the experimental installation

Continuing with a mass separated beam of $A=136$ our research could be late expanded to systematic studies of β -delayed multiple (and single as by product) neutron emission for different Z and N ranges. Candidates for undergoing two-neutron decay are the isotopes $^{88,89}\text{As}$, $^{136,137,138}\text{Sb}$, ^{139}Te and ^{142}I . In addition to the measurement of the neutron multiplicity and the probability of emission, the granular neutron detector will allow measurement of neutron correlations that will give information on the possible existence of multi neutron systems in extremely neutron-rich nuclei. Studies of radioactivity of neutron-rich fragments in $\beta\gamma n$ and $\beta\gamma 2n$ experiments are also planned.

- [1] G.Audi, O.Bersillon, J.Blachot, A.H.Wapstra, Nucl. Phys. A 729(2003)3.
- [2] Nuclear Physics A 729 (2003) 3–128
- [3] B.Jonson, H.A.Gustafsson, P.G.Hansen, P.Hoff, P.O.Larsson, S.Mattsson, G.Nyman, H.L. Ravn, D. Schardt, Proc. 4th Int. Conf. Nuclei far from Stability, 1981, CERN 81-09, 265.
- [4] P.Moller, J.Nix, K.-L.Kratz, Atomic Data & Nucl.Data Tabl., 66, 131 (1997)
- [5] Yu.Lyutostansky and I.Panov, Z.Phys.A, 313,235 (1983)
- [6] I.N. Borzov, Phys.ReV. C71 (2005) 065801
- [7] I.N. Borzov, Phys.ReV. C67 (2003) 025802.
- [8. A. Testov, Ch. Briancon, S. N. Dmitriev et. al. Nuclear Physics A 729 (2003) 3–128.
- [9] Yu.P.Gangrsky, K.Gladnishki, V.I.Zhemenik, G.V.Myshinsky, Yu.E.Penionzkevich, E.A. Sokol, Bulletin of the Russian Academy of Sciences, Physics, 69(2005)629 (in Russian)
- [10] M. Cheikh Mhamed et al., Nucl. Instr. And Meth. B 266 (2008) 4092-4096

Search for the pygmy dipole resonance in the nucleus ^{68}Ni

Angela Bracco

Dipartimento di Fisica, Università degli Studi di Milano
and INFN, Sez. di Milano, via Celoria 16, 20133 Milano (Italy)

Extended abstract of the talk given at the first EURISOL UG topical meeting:
The formation and structure of r-process nuclei between $N = 50$ and 82 (including ^{78}Ni and ^{132}Sn areas)
December 9-11, 2009, INFN-LNS, Catania, Italy

Giant resonances are basic building blocks of nuclear structure. Because they dominate the nuclear response at low excitation energies, investigations of their main features such as centroid and widths have been carried out for many years in experimental nuclear physics. In the case of the simplest mode, the giant dipole resonance (GDR) a reasonable knowledge of its systematic features has been achieved. However it is not generally known its fine structure which carries unique information on the underline nature of the mode and on the decay mechanisms. A very interesting long standing question is the nature of the so-called electric pygmy dipole resonance close to the neutron threshold in medium-to-heavy nuclei. It is predicted to result from a neutron excess density vibration relative to the $N \approx Z$ core. This mechanism interpreted the sizable low-lying E1 strength in very light neutron-rich nuclei. A good understanding of the properties of soft E1 modes (or pygmy) is important particularly in connection with exotic neutron rich nuclei. In fact, this allows to test predictions showing that the structural features of the GDR changes for extreme neutron-to-proton ratios. Furthermore, the presence of a resonance of E1 character close to particle threshold has important astrophysical implications because it considerably modify the thermal equilibrium of (γ, n) and (n, γ) reactions in explosive nucleosynthesis scenarios [1]. A powerful tool to study the low lying E1 strength of unstable neutron rich nuclei is the scattering of high-energy radioactive beams in inverse kinematics. At beam energies of several hundred MeV/nucleon, the rapidly varying electromagnetic field of a high Z target experienced by the fast moving projectile, generates dipole transitions with relatively large cross sections up to excitation energies of the order of 20 MeV and thus opens the possibility of studying the dipole response of exotic nuclei. So far, experimental information on the E1 response in unstable nuclei is rather limited and the existing results are based on neutron breakup measurements [2, 3, 4]. A complementary approach is the virtual-photon-scattering method so far employed to study ^{20}O up to excitation energy of 7 MeV [5]. Here a report is given of the first measurement made for ^{68}Ni that uses the virtual-photon-scattering at much higher energy than that of ^{20}O in order to excite with the Coulomb field the region well above the nucleon binding energy. An important point is also that at this bombarding energy the excitation of vibrations of electric dipole character is dominating over other excitation modes [6]. The unstable nucleus ^{68}Ni represents a good case to search for pygmy structures being this nucleus located in the middle of the long isotopic Ni chain having at the extremes the doubly magic ^{56}Ni and ^{78}Ni . In addition, it is experimentally accessible with the present radioactive beam facilities. In addition, different theoretical predictions on the pygmy dipole strength are available for this mass region [7, 8, 9]. A search of the pygmy resonance in ^{68}Ni was made using the virtual photon technique. The experiment was carried out using the radioactive beam ^{68}Ni at 600 A MeV impinging on a Au target. The ^{68}Ni beam, produced at GSI with fragmentation of ^{86}Kr at 900 A MeV on a ^9Be target, was separated the Fragment Separator and the gamma-rays produced at the interaction with the Au target were detected with the RISING set-up including also the

HECTOR array. The measured gamma-ray spectra show a peak centered at approximately 11 MeV, whose intensity can be explained in term of an enhanced strength of the dipole response function (pygmy resonance). A pygmy structure of this type was also predicted by different models for this unstable neutron rich nucleus [10]. The data have allowed to deduce the neutron skin radius with the model dependent approach discussed by Colò .

References

- [1] S. Goriely, Phys. Lett. **B436**, 10 (1998) and S. Goriely and E. Khan, Nucl. Phys. **A706** 217 (2002).
- [2] A. Klimkiewicz, *et al.*, Phys. Rev. **C76**, 051603 (2007).
- [3] A. Leistenschneider *et al.*, Phys. Rev. Lett. **86**, 5442 (2001).
- [4] P. Adrich *et al.*, Phys. Rev. Lett. **95**, 132501 (2005).
- [5] E. Tryggestad *et al.*, Phys. Lett. **B541**, 52 (2002).
- [6] T. Aumann, Eur. Phys. J. **A26**, 441 (2005).
- [7] D. Vretenar *et al.*, Nucl. Phys. **A692**, 496 (2001).
- [8] L. Cao and Z. Ma Mod. Phys. Lett. **A19**, 2845 (2004).
- [9] N. Paar *et al.*, 2007 Rep. Prog. Phys. **70** 691.
- [10] O. Wieland *et al.*, Phys. Rev. Lett. 102, 092502 (2009).

Electromagnetic Excitation of Neutron-Rich Ni Isotopes *

T. Le Bleis^{1,2,3}, D. Rossi⁴, P. Adrich¹, F. Aksouh¹, H. Alvarez-Pol⁵, T. Aumann¹, J. Benlliure⁵, M. Boehmer⁶, K. Boretzky¹, E. Casarejos⁵, M. Chartier⁷, A. Chatillon¹, D. Cortina-Gil⁵, U. Datta Pramanik⁸, H. Emling¹, O. Ershova^{1,3}, B. Fernandez-Dominguez⁷, H. Geissel¹, M. Gorska¹, M. Heil¹, H. Johansson^{1,9}, A. R. Junghans¹⁰, A. Klimkiewicz^{1,11}, O. Kiselev^{1,4}, J.V. Kratz⁴, N. Kurz¹, M. Labiche¹², R. Lemmon¹³, Y. Litvinov¹, K. Mahata¹, P. Maierbeck⁶, T. Nilsson⁹, C. Nociforo¹, R. Palit¹⁴, S. Paschalis⁷, R. Plag^{1,3}, R. Reifarth^{1,3}, H. Simon¹, K. Sümmerer¹, A. Wagner¹⁰, W. Walus¹¹, H. Weick¹, and M. Winkler¹

¹GSI, Darmstadt, Germany; ²IPHC, Strasbourg, France; ³Univ. Frankfurt, Germany; ⁴Univ. Mainz, Germany; ⁵Univ. Santiago de Compostela, Spain; ⁶TU Munich, Germany; ⁷Univ. Liverpool, UK; ⁸SINP Kolkata, India; ⁹Chalmers Göteborg, Sweden; ¹⁰FZ Dresden Rossendorf, Germany; ¹¹Jagiellonian Univ., Krakow, Poland; ¹²Univ. Paisley, UK; ¹³Daresbury, UK; ¹⁴TIFR Mumbai, India

As a response to an external electromagnetic field, a nucleus can be collectively excited to a Giant-Resonance state. The Giant Resonances, and in particular the isovector Giant Dipole Resonance (GDR), have been extensively studied both theoretically and experimentally in stable nuclei. In the early 1990s, theoretical studies predicted the presence of low-lying dipole strength below the GDR region in isospin-asymmetric nuclei. This new dipole mode, usually referred to as Pygmy Dipole Resonance (PDR), has been attributed to the oscillation of a neutron- or a proton-skin against an isospin-saturated core [1]. More recently, experimental developments allowed the investigation of the dipole response of short-lived nuclei. In particular, neutron-rich Sn isotopes were studied using heavy-ion-induced electromagnetic excitation at relativistic energies in inverse kinematics at the LAND-R³B setup at GSI. The differential cross section $d\sigma/dE^*$, which is obtained from invariant-mass reconstruction, shows the presence of low-lying strength in the dipole response that cannot be explained by the GDR alone, and which has been associated with the Pygmy Resonance mentioned above [2].

In order to study the dipole response of neutron-rich Ni isotopes including ⁶⁸Ni, a similar experiment has been performed by the LAND collaboration using the Coulomb excitation technique. The neutron-evaporation channels have been investigated and the strength distribution was obtained. Measurements were performed with three different targets (C, Sn and Pb) in order to distinguish electromagnetic and nuclear-induced excitations. A measurement without target yielded the background contribution. While electromagnetic excitation occurs at impact parameters larger than the sum of the radii of the colliding nuclei, the nuclear contribution stems from a narrow impact-parameter range close to the grazing impact parameter b_c . This determines the target dependence of the nuclear cross section σ_N scaling basically with the sum of the two radii, i.e., $\sigma_N \propto A_T^{1/3} + A_P^{1/3}$. In addition to this 'black-disc' approach, we have considered a model taking into account

the transparency of the nuclei for an impact-parameter range Δb , yielding $\sigma_N \propto [b_c - \frac{\Delta b}{2}] \Delta b$. Here, we adopt the parametrization of b_c based on empirical nuclear densities and Eikonal calculations, which has been checked against measured cross sections for electromagnetic dissociation of stable nuclei [3]. The charge dependence of the electromagnetic contribution $\sigma_C \propto Z_T^\alpha$ was determined from a semi-classical calculation resulting in, e.g., $\alpha = 1.61(2)$ for the $1n$ cross section of ⁶⁸Ni. Fits to the obtained cross sections with the three targets show that both models lead to the same results. It is then possible to determine the nuclear component of the interaction with Pb using the results obtained on C, e.g., $\sigma_N^{Pb} = 1.57(20)\sigma^C$ for ⁶⁸Ni.

The preliminary analysis of both integrated and differential cross sections for electromagnetic dissociation of ⁶⁷⁻⁶⁹Ni shows that the cross sections cannot be explained only by the excitation of the GDR with parameters from various systematics. In particular, a larger cross section in the low-energy part of the spectrum is observed, which can be described by the addition of extra dipole strength exhausting 5 to 10% of the energy-weighted sum rule. The comparison of our result, which refers to the dominant neutron-decay, with a recent (γ, γ') measurement for ⁶⁸Ni [4] yields a decay branching ratio of about 3% for the gamma back-decay of the Pygmy resonance in this nucleus.

Although the analysis is still on-going, we can say in summary that evidence for the presence of a low-energy component in the dipole-strength distribution of neutron-rich Ni isotopes has been obtained indicating, a systematic nature of the PDR mode.

References

- [1] N. Paar *et al.*, Rep. Prog. Phys. 70 (2007) 691 and references cited therein.
- [2] P. Adrich *et al.*, Phys. Rev. Lett. 95 (2005) 132501. A. Klimkiewicz *et al.*, Phys. Rev. C 76 (2007) 051603(R).
- [3] T. Aumann *et al.*, Phys. Rev. C 51 (1995) 416; C.J. Benesh *et al.*, Phys. Rev. C 40 (1989) 1198.
- [4] O. Wieland *et al.*, Phys. Rev. Lett. 102 (2009) 062502.

* This work is supported in part by BMBF grant 06MZ2221, by the HGF Young Investigators Project VH-NG-327, and by the Alliance Program of the Helmholtz Association (HA216/EMMI).

Coulomb excitation of neutron-rich nuclei around ^{132}Sn at REX-ISOLDE

Th. Kröll (TU Darmstadt) for the IS411/IS415/IS477 collaborations

1 Motivation

The explanation of the magic numbers for nuclei in the valley of stability was one of the milestones in the understanding of nuclear structure. Important interest nowadays is the question if they persist or will be altered going away from the valley of stability because the residual interactions responsible for their existence may change. We report here on Coulomb excitation studies of nuclei around ^{132}Sn , the heaviest doubly-magic nucleus off stability which is accessible for experiments so far. A particular interest in these nuclei comes from nuclear astrophysics as the r-process is expected to pass this region.

An indication for a change in nuclear structure came some years ago from $B(E2)$ values for neutron-rich Sn and Te nuclei in the vicinity of ^{132}Sn [1], in particular ^{136}Te , which were lower than expectations from systematics and predictions from most theories. However, a recent re-analysis of the data [2] and a life-time measurement performed at ISOLDE applying the advanced ultrafast-timing technique [3] revealed for ^{136}Te a 20% larger value, now well in agreement with shell model predictions. Aiming to extend such investigations, we studied neutron-rich Cd, Xe, and Ba isotopes at the REX-ISOLDE facility at CERN.

2 Experimental method

The radioactive nuclei have been produced at the ISOLDE facility at CERN by the 1.4 GeV proton beam from the PS Booster impinging on a UC_x target. For some isotopes neutron induced fission has been applied using a neutron converter target to reduce the proton-rich isobaric contaminants. For each beam the target and the ion source have been optimised for elemental selectivity. The extracted ions were mass separated, cooled and bunched in the Penning trap REX-TRAP, and sent to an EBIS for charge breeding. Eventually, the energy was boosted to around 2.85 MeV/u by the REX-LINAC.

We employed γ -spectroscopy following “safe” Coulomb excitation of the radioactive beams. The γ -rays deexciting the populated states were detected by the highly efficient MINIBALL spectrometer, consisting of 8 triple clusters of six-fold segmented HPGe detectors equipped with fully digital electronics in coincidence with the scattered particles. Since most ISOL beams are not pure beams, several methods to determine the beam composition have been applied.

The $B(E2)$ values of radioactive beams are determined relative to those of the target whose electromagnetic properties are well known. For the beam nuclei, the $B(E2; 0^+ \rightarrow 2^+)$ values have been varied until the calculated cross sections agree with the experimental values. Effects like reorientation, in fact the determination of the quadrupole moment, deorientation, or the off-centre position and the size of of the beam spot are included in the analysis.

3 Experiments and results

Beams of $^{122,124,126}\text{Cd}$ have been produced using a heated quartz transfer line and the highly selective RILIS laser ion source in order to suppress isobaric contaminants. The beam purities ranged from 60% to 83%. For ^{122}Cd , the error for $B(E2)$ value has been reduced significantly compared to a previous measurement. For $^{124,126}\text{Cd}$, $B(E2)$ values have been determined for the first time [5]. The preliminary values are well in agreement with simple systematics, given by a modified Grodzin's formula [4], as well as with predictions from the shell model [6] and beyond-mean-field calculations [7]. For the waiting-point nucleus ^{130}Cd exist contradicting results [8, 9] leading to interpretations like a quenching of the $N = 82$ gap or the existence of deformation just two protons below ^{132}Sn . This will be investigated further by the study of ^{128}Cd at REX-ISOLDE where a larger $B(E2)$ value would evidence the onset of deformation.

For the Xe isotopes previously no $B(E2)$ had been measured above $N = 82$, except the two contradicting values for ^{140}Xe . Xe beams have been produced using a cold plasma source where all elements less volatile than noble gases stick to the wall. The only isobaric contaminants are therefore, and only for the short-lived isotopes, their own decay products. We determined $B(E2)$ values for $^{138,140,142,144}\text{Xe}$ [5]. For ^{140}Xe , our result supports the larger value from literature [10]. The preliminary results clearly follow the expectations from simple systematics, but agree also well with predictions from QRPA calculations [11] as well as from the Monte Carlo Shell Model (MCSM) [12]. Both models give lower $B(E2)$ values for ^{138}Xe , however still within the preliminary error.

Aiming to extend these studies to more deformed nuclei, maybe even involving octupole correlations, we studied also Ba isotopes. Ba beams have been produced by ingesting fluorine gas to the ISOLDE target and extracting BaF^+ molecules which are later cracked in the EBIS. However, the preparation of the very exotic $^{148,150}\text{Ba}$ beams failed. Surprisingly, molecules like NdF^+ , leading to a ^{148}Nd beam, have been extracted which are not existing as neutral molecules. For the $N = 84$ isotope ^{140}Ba , the error of the $B(E2)$ value could be reduced significantly [13]. Its value as well as those for the heavier isotopes up to ^{148}Ba known from previous measurements agree well with the simple systematics and predictions from the MCSM [12].

A more direct probe the wave functions are g-factors. As first experiment, we studied the g-factors of the first 2^+ states in the ^{138}Xe and ^{140}Ba $N = 84$ isotones. For the ^{138}Xe , we performed an experiment applying the transient field method to be sensitive to the sign of the g-factor [14]. The Ba has been studied applying recoil-in-vacuum method (^{142}Ba , which has been measured also, with a known g-factor served as calibration) [13]. So far, the preliminary results have too large errors to draw conclusions.

4 Summary and Outlook

We have studied neutron-rich Cd, Xe, and Ba isotopes around ^{132}Sn by γ -ray spectroscopy following “safe” Coulomb excitation at REX-ISOLDE. The obtained $B(E2)$ values are well in agreement with both expectations from simple systematics and predictions from theory. The possible existence of a “ $B(E2)$ value anomaly” in this region could not be confirmed. For the first time, a g-factor has been measured for an excited state of a radioactive nucleus applying the transient field method.

The REX-ISOLDE facility will be upgraded to HIE-ISOLDE until 2015 enabling higher beam energies up to 10 MeV/u, higher intensities, and an improved beam quality. This will open new experimental opportunities in particular concerning heavy beams and transfer reactions. The later will allow to study also single-particle properties and pairing correlations in nuclei of this region with one- and two-neutron transfer reactions in inverse kinematics applying the T-REX Si detector array [15] in combination with MINIBALL.

Work supported by BMBF (Nr. 06MT238, 09DA9036I), EU (EURONS Nr. 506065), HIC for FAIR (LOEWE), DFG (Excellence Cluster Universe), MLL, and the MINIBALL/REX-ISOLDE collaborations.

References

- [1] D. C. Radford et al., *Phys. Rev. Lett.* 88, 222501 (2002).
- [2] D. C. Radford, Workshop GAMMA08, RIKEN (2008).
- [3] L. M. Fraile, H. Mach et al., *Proc. of INPC2007*, *Nucl. Phys. A* 805, 218 (2008).
- [4] D. Habs, R. Krücken et al., CERN Proposal INTC-P-156 (2002).
- [5] T. Behrens, Ph.D. thesis (TU München, 2008).
- [6] A. Scherillo et al., *Phys. Rev. C* 70, 054318 (2004).
- [7] T. Rodriguez, J. L. Egido, A. Jungclaus, priv. communication.
- [8] I. Dillmann et al., *Phys. Rev. Lett.* 91, 162303 (2003).
- [9] A. Jungclaus et. al., *Phys. Rev. Lett.* 99, 132501 (2007).
- [10] A. Lindroth et al., *Phys. Rev. Lett.* 82, 4783 (1999).
- [11] J. Terasaki et al., *Phys. Rev. C* 66, 054313 (2002).
- [12] N. Shimizu et al., *Phys. Rev. Lett.* 86, 1171 (2001), *Phys. Rev. C* 70, 054313 (2004), and *J. Phys. Conf. Ser.* 49, 178 (2006).
- [13] C. Bauer, Master thesis (TU Darmstadt, 2009).
- [14] J. Leske et al., Annual Spring Meeting of DPG, Giessen (2007).
- [15] V. Bildstein et al., *Prog. Part. Nucl. Phys.* 59, 386 (2007).

Coulomb excitation in the neighbourhood of ^{68}Ni using MINIBALL at REX-ISOLDE

J. Diriken

for the MINIBALL Collaboration

The region around the $Z = 28$, $N = 40$ nucleus ^{68}Ni is an interesting region to test nuclear structure models (e.g. the shell model). Systematic studies have shown a maximum in the excitation energy of the first excited 2^+ state [1] and a minimum in the reduced transition probability ($B(E2)$ -value) of this transition to the ground state [2, 3] leading to interpretations in terms of magicity and a $N = 40$ -subshell closure [4, 5]. Measurements of two-neutron separation energies on the other hand do not show any irregularity around $N = 40$ [6], raising questions about the true nature of this $N = 40$ -subshell closure. The low $B(E2; 2^+ \rightarrow 0^+)$ in ^{68}Ni has been interpreted as being due to the fact that the bulk part of the $B(E2)$ strength resides at high energy [3].

Recent shell model calculations have pointed out the importance of the size of the $N = 40$ gap between the νpf -shell and $\nu g_{9/2}$ orbital on the structure in this region. By determining $B(E2)$ -values a deeper insight in structural changes and the influence of this $\nu g_{9/2}$ intruder orbital in this specific mass region can be obtained. These values can be compared with those extracted from large scale shell model calculation as to test and finetune the models [7, 8, 9] and to verify different calculated shell effects predicted by these models.

These $B(E2)$ -values can be obtained by using the technique of Coulomb excitation. The way this is done at the ISOLDE on-line isotope mass separator facility is by producing radioactive species by irradiation a UC_x target with a 1.4 GeV proton beam. After ionization (preferentially by resonant laser ionization [10]) and mass selection in one of the two available separators the continuous beam is bunched (REX-TRAP) and brought to a higher charge state (EBIS) to enhance the post-acceleration efficiency. After post-acceleration the beam is delivered to the MINIBALL set-up with a maximum energy of 3 MeV/u. This energy range allows to perform "safe" Coulomb excitation as the interaction is purely electro-magnetic, without or little interference of any nuclear effect.

The MINIBALL set-up itself consists of an interaction target and a CD shaped segmented silicon detector to detect the scattered projectile and target particles [13]. Outside of the scattering chamber the MINIBALL γ -array is positioned, consisting of 8 clusters, each with 3 hyperpure germanium crystals, each of them sixfold electronically segmented [14]. $B(E2)$ -values can be extracted by normalising observed γ -rates of transitions in the projectile particles to those of the known target [3, 17, 18, 27].

In this report an overview of the work using this technique in the mass region around ^{68}Ni will be presented, which comprises neutron-rich manganese, iron, copper, zinc and gallium isotopes.

Coulomb excitation of neutron-rich zinc isotopes was performed to further investigate the indications of increased collectivity in the zinc chain above $N > 40$ [11, 12]. The obtained $B(E2)$ -systematics can also be used to further investigate the importance of excitations through the $Z = 28$ [15] and/or $N = 50$ [16] shell gaps far from stability. Highlights of the campaign include the first observation of the 2_1^+ state in the $N = 50$ nucleus ^{80}Zn and determination of $B(E2)$ -values for the $2_1^+ \rightarrow 0_1^+$ transition up to $N = 50$. Both $B(E2)$ -systematics for the $Z = 30$ isotopes and $N = 50$ isotones show a decrease in collectivity when approaching $N = 50$ and $Z = 28$ respectively. This observation shows no strong weakening of these gaps when approaching ^{78}Ni which might have implications for the r-process. More details about this experiment can be found in [17, 18].

The possible mechanism for a reduction of the $Z = 28$ shell gap beyond $N = 40$ is the tensor interaction between neutrons filling the $\nu g_{9/2}$ orbital and the πpf -shell [15], a phenomenon commonly referred to as monopole migration. The manifestation of this interaction was seen in the β -decay studies which revealed a decrease of the $5/2_1^-$ state in the odd-A copper isotopes passed $N = 40$ [19]. This is in contrast with the clear core coupled character of this $5/2_1^-$ below $N = 40$. Measurements of the $B(E2)$ -values in the Cu isotopes ($Z = 29$) were performed and provided useful information on the character of these states. The results of this experiment show that in the odd mass copper chain beyond $N = 40$ three different types of excitation exist as compared to a core coupled scheme below $N = 40$ [20]. Beyond $N = 40$, a strongly excited $7/2^-$ state was observed and the $B(E2; 7/2^- \rightarrow 3/2^-)$ matched very well the $B(E2)$ of the neighboring even nickel isotopes, suggesting a core coupled structure. Furthermore, low lying $1/2^-$ state was observed that exhibited a large $B(E2; 1/2^- \rightarrow 3/2^-)$ matrix element. Recent shell model calculations do reproduce these findings [21]. Both the $5/2_1^-$ and $1/2_1^-$ change structure where the former becomes essentially single-particle and thus confirms the interpretation from the β -decay study, while the latter shows a sharp increase in collectivity. This last observation indicates the role of the $\nu g_{9/2}$ orbital on the structure in this region.

Due to surface ionization in the ion source the ^{73}Cu beam was severely contaminated with ^{73}Ga and allowed to measure $B(E2)$ -values for transitions in this nucleus as well. The motivation for the analysis of the available Coulomb excitation data on ^{73}Ga is twofold: firstly, in the past it was found that the $^{71}\text{Ga}(t,p)^{73}\text{Ga}$ $L=0$ strength splits in nearly three equal parts, indicating a shape transition [22]. Secondly, it was recently found that the ^{73}Ga ground state has a spin and parity assignment of $1/2^-$ [23]. The results show a shift of the $E2$ -strength to lower energies as compared to the isotopes below $N = 40$ where two groups of excited states can be distinguished: two single-particle states ($\pi f_{5/2}$ and $p_{1/2}$) and a set of 4 states resulting from the core-coupling scheme. The bulk of the $E2$ -strength in ^{73}Ga resides at energies considerably smaller than the energy of the 2_1^+ state in ^{72}Zn , supporting the proposed shape transition. However, the $B(E2)$ is substantially smaller compared to the $B(E2; 2^+ \rightarrow 0^+)$ of the underlying ^{72}Zn core of 19(5) W.u. [24]. The data proves the existence of a ground state doublet in ^{73}Ga as the observed Doppler broadening

of the 199 keV transition -which depopulates the first $5/2^-$ level- cannot be explained without the presence of a $3/2^-$ state near the $1/2^-$. Based on the available Coulomb excitation data and published β -decay data an upper limit of 2 keV could be imposed on the excitation energy of this $3/2^-$ state [25].

The paragraphs above suggest an increase in collectivity above $Z = 28$ and beyond $N = 40$. Also below $Z = 40$ different large-scale shell model calculations show the importance of neutron orbitals above $N = 40$ as there is a clear difference in $B(E2; 2_1^+ \rightarrow 0^+)$ -values for neutron rich iron isotopes calculated with and without the inclusion of the νgd -orbitals [9]. Iron beams, however, cannot be produced directly at ISOLDE. In an indirect way an iron beam can be produced after β -decay of short-lived manganese isotopes. These nuclei can be produced at ISOLDE and if they decay to iron in one of the traps where the beam is prepared prior to the post-acceleration, an iron beam can be produced [26]. Tests with different combinations of trapping and charge breeding times were performed and it was found that the fraction of iron in the beam is larger for long charge breeding times and short trapping times. Experiments have been performed with $^{61,62}\text{Mn}/\text{Fe}$ beams and the analyzed results for mass 61 show the need for the inclusion of the $\nu g_{9/2}$ -orbital in the large scale shell model calculations as it influences the quadrupole collectivity even at low excitation energy [27]. Data on mass 62 are still under analysis. One of the key points of this experiment is that it demonstrates the option of producing and post-accelerating certain beams of nuclei that can't be produced directly at ISOLDE. Possible candidates for future experiments are ^{50}Ca (decay of ^{50}K), $^{98,100}\text{Sr}$ (decay of $^{98,100}\text{Rb}$) and $^{62-65}\text{Fe}$ (decay of $^{62-65}\text{Mn}$).

References

- [1] M. Bernas et al. J.Phys.Lett. 45, L-851 (1984)
- [2] O. Sorlin et al. Phys.Rev.Lett. 88, 092501 (2002)
- [3] N. Bree et al. Phys.Rev.C 78, 047301 (2008)
- [4] R. Broda et al. Phys.Rev.Lett. 74, 868 (1985)
- [5] O. Perru et al. Phys.Rev.Lett. 96, 232501 (2006)
- [6] S. Rahaman et al. Euro.Phys.Jour.A 34, 5 (2007)
- [7] M. Hjorth-Jensen et al. Phys.Rep 261, 125 (1995)
- [8] A. Lisetskiy et al. Phys.Rev.C 70, 044314 (2004)
- [9] E. Caurier et al. Euro.Phys.Jour.A 15, 145 (2002)
- [10] U. Köster et al. Nucl.Instr.Meth.B 204, 347 (2003)

- [11] O. Perru et al. Phys.Rev.Lett 96, 232501 (2006)
- [12] J. Van Roosbroeck et al. Phys.Rev.C 71, 054307 (2005)
- [13] A. Ostrowski et al., Nucl.Instr.Meth.A 480, 448 (2002)
- [14] J. Eberth et al. Prog.Part.Nucl.Phys. 46, 389 (2001)
- [15] T. Otsuka et al., Phys.Rev.Lett. 95, 232502 (2005)
- [16] T. Otsuka et al., Phys.Rev.Lett. 97, 162501 (2006)
- [17] J. Van De Walle et al. Phys.Rev.Lett 99, 142501 (2007)
- [18] J. Van De Walle et al. Phys.Rev.C 79, 014309 (2009)
- [19] S. Franchoo et al. Phys.Rev.C 64, 044321 (2002)
- [20] I. Stefanescu et al. Phys.Rev.Lett 100, 112502 (2008)
- [21] M. Honma et al. Phys.Rev.C 80, 064323 (2009)
- [22] M. N. Vergnes et al. Phys.Rev.C 19, 1276 (1979)
- [23] B. Cheal et al. To be published
- [24] S. Leenhardt et al. Eur.Phys.J. A 14,1 (2002)
- [25] E. Runte et al. Nucl.Phys.A 399, 163 (1983)
- [26] D. Voulot et al. Nucl.Instr.Meth.B 266, 4103 (2008)
- [27] J. Van De Walle et al. Eur. Phys. J. A 42, 401 (2009)

On the nature of the Pygmy Dipole Resonance

E. G. Lanza ⁽¹⁾, A. Vitturi ⁽²⁾, M.V. Andrés ⁽³⁾, F. Catara ⁽¹⁾ and D. Gambacurta ⁽¹⁾

⁽¹⁾ *Dipartimento di Fisica and INFN, Catania, Italy*

⁽²⁾ *Dipartimento di Fisica and INFN, Padova, Italy*

⁽³⁾ *Departamento de FAMN, Facultad de Física, Sevilla, Spain*

We study the nature of the low-lying dipole strength in neutron-rich nuclei, often associated to the Pygmy Dipole Resonance. The states are described within the Hartree-Fock plus RPA formalism, using different parametrizations of the Skyrme interaction. We show how the information from combined reactions processes involving the Coulomb and different mixtures of isoscalar and isovector nuclear interactions can provide a clue to reveal the characteristic features of these states.

In the last years the properties of collective states in neutron-rich nuclei have been studied with special attention to the presence of dipole strength at low excitation energy. This strength has been often associated to the possible existence of a new collective mode of new nature: Pygmy Dipole Resonance (PDR) (see, for example ref. [1] and reference quoted in).

From an experimental point of view the evidence for these states has come from high-energy Coulomb excitation processes[2]. As known, these can only provide values of the multipole $B(E\lambda)$ transition rates. Much more information, like wave function and transition densities, can be obtained by resorting to reactions where the nuclear part of the interaction is involved. This can be done because of the strong isoscalar component of the PDR state. By tuning the projectile mass, charge, bombarding energy and scattering angle one can alter the relative role of the nuclear and Coulomb components, as well as of the isoscalar and isovector contributions.

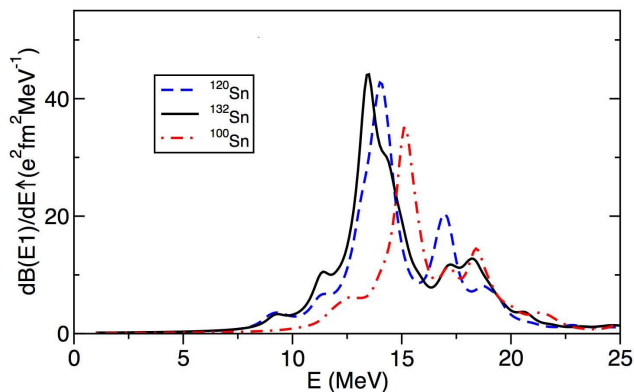


FIG. 1: Isovector strength distributions for dipole states for tin isotopes calculated with the SGII interaction. The bars are the RPA $B(E1)$ values. The solid curves represent $dB(E1)/dE$ as obtained by adopting a smoothing procedure described in the text. In the lower right figure we report the same continuous lines shown in the other frames.

From a theoretical point of view the presence of this low-lying strength is predicted by almost all microscopic models, ranging from Hartree-Fock plus RPA with Skyrme interactions to relativistic Hartree-Bogoliubov

plus relativistic quasiparticle RPA. All these approaches predict similar amounts of strength, but often disagree on the collective (or not) nature of these states, on their fragmentation and on their isoscalar/isovector contents[1].

We will use here the results obtained in the simplest discrete non-relativistic RPA approach with Skyrme interactions, consistently used both at the level of mean-field Hartree-Fock and of RPA. We have performed calculations for several Sn isotopes[3]. To better appreciate the isotope dependence, three distributions of dipole strength are shown together in Fig. 1. As soon as we increase the mass number some low-lying strength (carrying a fraction of the EWSR of the order of few per cent) below 10 MeV appears[4]. These are precisely the states that are candidates to be interpreted as Pygmy Dipole Resonances: they are generally associated with the occurrence of neutron skins in the nuclear densities and their oscillations with respect to the proton+neutron cores.

One important question is how much collective are these dipole states. One measure of the collectivity is the number of particle-hole components entering in the RPA wavefunction with an appreciable weight. For a state ν the contribution of a particle-hole configuration can be calculated by defining the quantity

$$A_{ph} = |X_{ph}^\nu|^2 - |Y_{ph}^\nu|^2 \quad (1)$$

in terms of the X and Y RPA's amplitudes, with the normalization condition

$$\sum_{ph} A_{ph} = 1 \quad (2)$$

Then, one can see what is the contribution, in percentage, of a p-h configuration to the formation of the state ν . Such criterion does not take into account the other fundamental concept that underlies collectivity that is coherence. The reduced transition probability from the ground state to the excited state ν can be written as

$$B(E\lambda) = \left| \sum_{ph} b_{ph}(E\lambda) \right|^2 = \left| \sum_{ph} (X_{ph}^\nu - Y_{ph}^\nu) T_{ph}^\lambda \right|^2 \quad (3)$$

where T_{ph}^λ are the 2^λ multipole transition amplitudes associated with the elementary p-h configurations. The previous analysis, based only on the magnitude of the

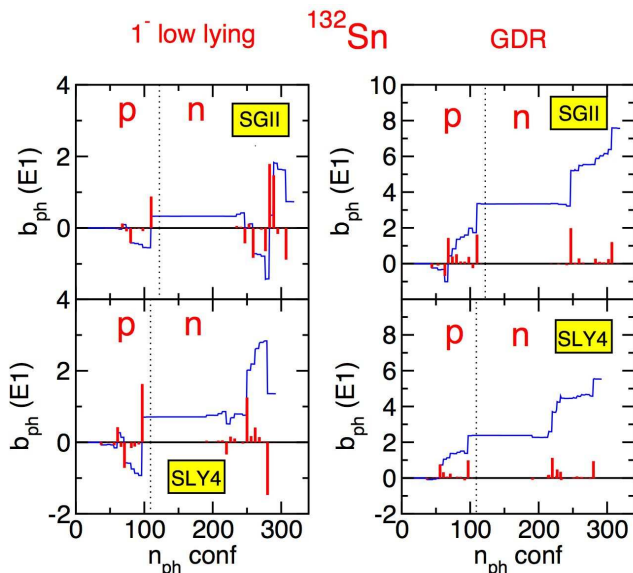


FIG. 2: Partial contributions b_{ph} of the reduced transition probability vs. the order number of the p-h configurations used in the RPA calculations for the two Skyrme interactions. The dotted lines divide the protons from the neutron configurations. The order goes from the most to the less bound ones. The bars corresponds to the individual b_{ph} contributions while the continuous thin line is the cumulative sum of the contributions.

A_{ph} 's, can be misleading because it does not take into account the amplitude T_{ph}^λ nor the relative signs of the separate contributions. Indeed, if we look also to the b_{ph} 's we note that configurations with a small percentage may give big contribution to the reduced transition probability. In Fig. 2 we plot the partial contributions b_{ph} versus the order number of the p-h configurations used in the RPA calculations for two Skyrme interactions. The bars corresponds to the individual values of the b_{ph} while the continuous thin (blue) line is the cumulative sum of the contributions. The dotted lines divide the protons from the neutron configurations. The order goes from the most bound configurations to the higher ones. The figures on the left column are for two low lying dipole states while the ones on the right column are for the GDR states. They are obtained with the two Skyrme interaction as indicated in the figure. From the figure we can clearly see how the $B(E1)$ of the GDR states are built up by the small contributions of many p-h configurations which add coherently. For the low-lying states we have a different behaviour: there are several p-h configurations participating to the formation of the $B(E1)$ but some of them have opposite sign giving rise to a final value which is small. From our novel analysis, it emerges that although the low-lying states cannot be considered as collective as the GDR states they cannot be described as single p-h configuration.

More precise information on the specific nature of the

states is contained in their transition densities. As an example we show in Fig. 3 the RPA transition densities associated with the GDR (right frame) and with a state in the PDR region (left frame) in ^{132}Sn . Neutron and proton components of the transition densities are separately shown, together with their isoscalar and isovector combinations. The two cases clearly display very different behaviours. The one associated with the GDR shows the usual opposite-phase behaviour of the proton and neutron components, leading to a dominant isovector character. The situation is rather different in the

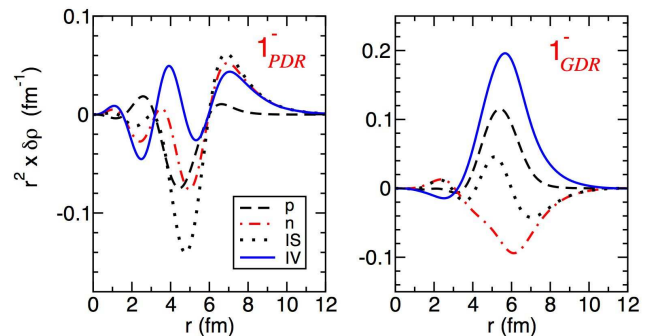


FIG. 3: Transition densities for the low-lying dipole state (PDR) (left) and for the GDR (right) for the ^{132}Sn isotope calculated with the SLY4 interaction. We show the proton, neutron, isoscalar and isovector components (as indicated in the legend).

case of the other state at lower energy. Here neutron and proton components seem to oscillate in phase in the interior region, while in the external region only the neutrons give a contribution to both isoscalar and isovector transition densities which have the same magnitude. Such behaviour, which has been found also in all the other microscopic approaches[1, 6], can be taken as a sort of definition of PDR.

This brings in the question of the interpretation of this state, macroscopically described as the oscillation of the neutron skin with respect to the proton+neutron cores. A macroscopic description of such a mode assumes a separation of the neutron density into a core part ρ_N^C with N_C neutrons and a valence part ρ_N^V with N_V neutrons ($N = N_C + N_V$), with a proton density ρ_P with Z protons. This leads to neutron and proton transition densities given by

$$\begin{aligned} \delta\rho_N(r) &= \beta \left[\frac{N_V}{A} \frac{d\rho_N^C(r)}{dr} - \frac{N_C + Z}{A} \frac{d\rho_N^V(r)}{dr} \right] \\ \delta\rho_P(r) &= \beta \left[\frac{N_V}{A} \frac{d\rho_P(r)}{dr} \right] \end{aligned} \quad (4)$$

with β a proper strength parameter. The microscopic RPA and the macroscopic transition densities, normalized to the same $B(E1)$ value, are compared in Fig.4. Although some similarities are present, a full interpreta-

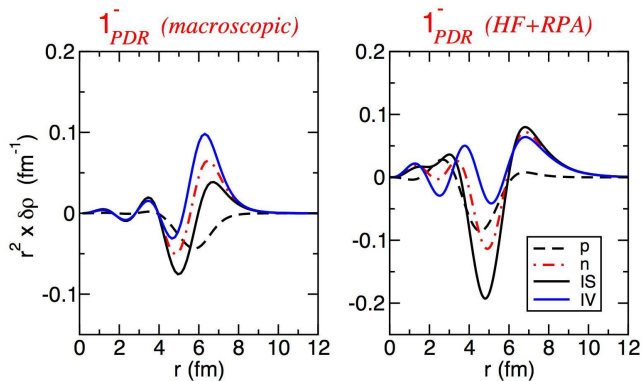


FIG. 4: Transition densities for the low-lying dipole state for the ^{132}Sn isotope. The frame on the left show the macroscopic transition densities according to eq. (4), the ones on the right are calculated microscopically with the HF + RPA. We show the proton, neutron, isoscalar and isovector components (as indicated in the legend).

tion of the state in the above macroscopic terms is not obvious. It should be noted that, besides the requirement of the shape of the transition density, the macroscopic picture should also involve a collective nature of the state, which was not found to be fulfilled at least in our calculations.

The transition densities are the basic ingredients to construct the nuclear formfactors describing nuclear excitation processes. These formfactors can be obtained by double folding [7] the transition densities with the density of the reaction partner and the $N - N$ interaction (taken in our case as M3Y), including both isoscalar and isovector terms. The change of reaction (and of the bombarding energy), with the consequent change of the relative role of nuclear and Coulomb components as well as of the isoscalar/isovector nuclear components) will alter the relative population of the different states. We will consider here the excitation of the Pygmy and Giant dipole states in ^{132}Sn by different partners: α , ^{40}Ca and ^{48}Ca . The corresponding formfactors (nuclear, Coulomb and total) and shown in Fig. 5.

With ion-ion potential and formfactors we can now calculate cross sections (for example within the semiclassical approach as done in ref. [3]). In order to reduce the number of states for which we calculated the cross section, we bunch together states with significant strength and whose energy is lying in a limited interval. The bunching is done by taking as energy the average energy of the states belonging to the group with the condition that the EWSR must be preserved.

The energy differential total cross sections for the dipole states are shown in Fig. 6. The different contributions from Coulomb and nuclear formfactors are separately show. It is clear that the balance between PDR and GDR vary in the different reactions. The ratios can be further modified by looking at the differential angular

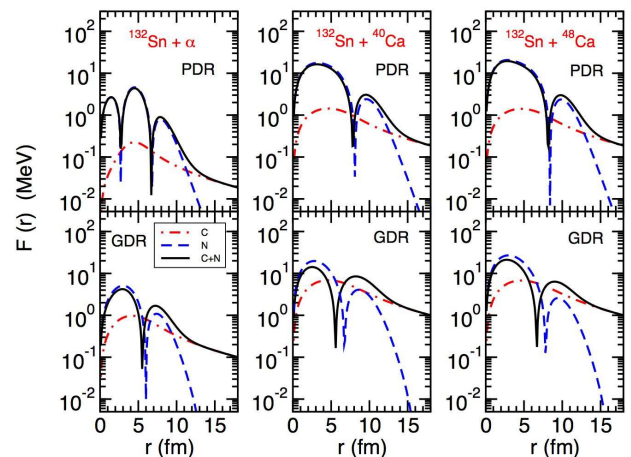


FIG. 5: Formfactors for three different systems $^{132}\text{Sn} + \alpha$, $^{132}\text{Sn} + ^{40}\text{Ca}$, $^{132}\text{Sn} + ^{48}\text{Ca}$. The upper parts refer to the PDR states while the lower ones are for the GDR. The different component are shown together with the total one (solid black line).

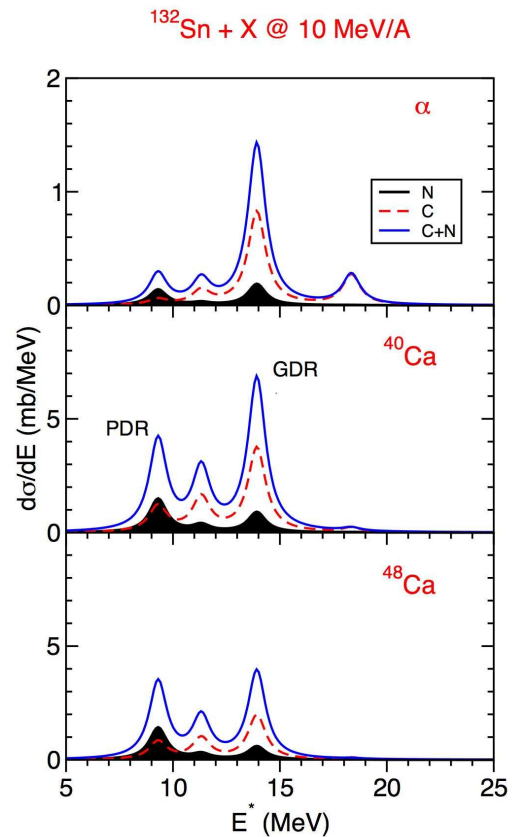


FIG. 6: Differential cross sections as function of the excitation energy for the systems $^{132}\text{Sn} + \alpha$, ^{40}Ca , ^{48}Ca at 10 MeV per nucleon. The Coulomb contribution is shown as (red) dashed line. The shaded (black) area corresponds to the nuclear contribution.

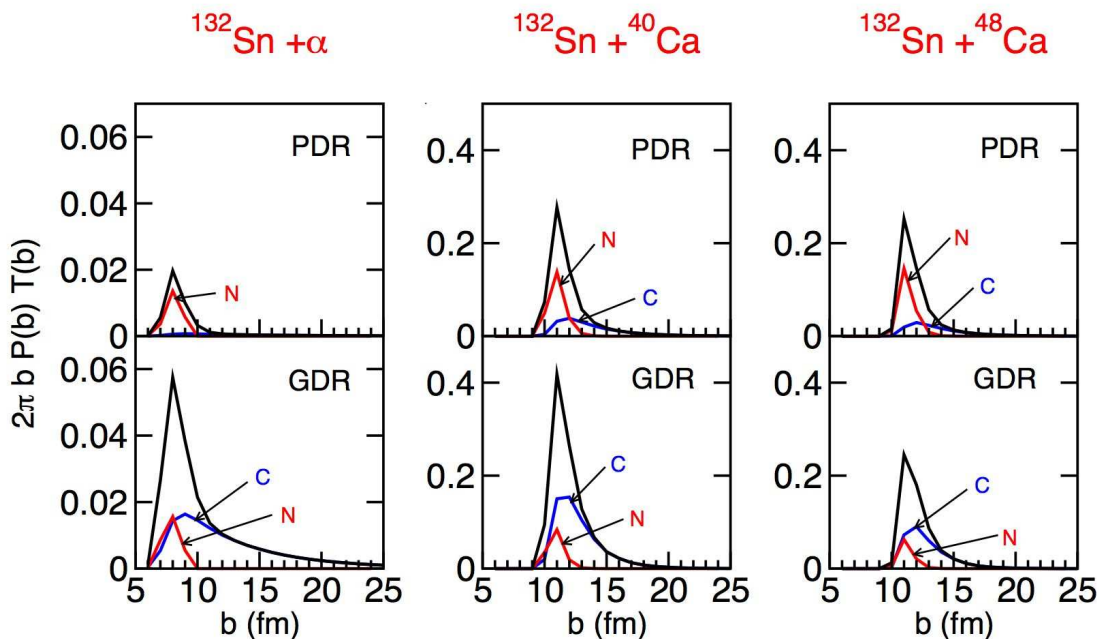


FIG. 7: Partial wave cross sections as function of the impact parameter b for the systems $^{132}\text{Sn} + \alpha$, ^{40}Ca , ^{48}Ca at 10 MeV per nucleon. The Coulomb (C) and nuclear (N) contributions are indicated in the figures. The curves with the highest maximum are the total cross section.

distributions. In the semiclassical picture, these are associated to different ranges of impact parameters. Nuclear contributions are known to be enhanced at grazing angles, corresponding to grazing impact parameters. This is clearly evidenced in Fig. 7, where the partial-wave cross sections are shown as a function of the impact parameter.

In conclusion we can say that valuable information on the nature of the PDR can be obtained by excita-

tion processes involving the nuclear part of the interaction. The use of different bombarding energies, of different combinations of colliding nuclei involving different mixture of isoscalar/isovector components, together with the mandatory use of microscopically constructed form-factors, can provide the clue to reveal the characteristic features of these states.

-
- [1] N. Paar, D. Vretenar, E. Khan and G. Colò, *Rep. Prog. Phys.* **70**, 691 (2007) and references therein.
- [2] P. Adrich et al. (LAND-FRS Collaboration), *Phys. Rev. Lett.* **95** 132501 (2005); A. Klimkiewicz et al. (LAND-FRS Collaboration), *Nucl. Phys. A* **788** 145 (2007); A. Klimkiewicz et al. (LAND Collaboration) *Phys. Rev. C* **76** 051603(R) (2007).
- [3] E.G. Lanza, F. Catara, D. Gambacurta M.V. Andres and Ph. Chomaz, *Phys. Rev. C* **79** 054615 (2009).
- [4] F. Catara, E.G. Lanza, M.A. Nagarajan and A. Vitturi *Nucl. Phys. A* **614** 86 (1997); *Nucl. Phys. A* **624** 449 (1997).
- [5] J.A. Christley, E.G. Lanza, S.M. Lenzi, M.A. Nagarajan, and A. Vitturi, *J. Phys. G: Nucl. Part. Phys.* **25** 11 (1999).
- [6] N. Tsoneva and H. Lenske, *Phys. Rev. C* **77** 024321 (2008).
- [7] G.R. Satchler and W.G. Love, *Phys. Rep.* **55** 183 (1979).

Relationship between the multipole response in neutron-rich nuclei and the nuclear equation of state: the dipole case

Gianluca Colò

Dipartimento di Fisica, Università degli Studi di Milano
and INFN, Sez. di Milano, via Celoria 16, 20133 Milano (Italy)

collaborators

Andrea Carbone, Angela Bracco, Li-Gang Cao, Pier Francesco Bortignon,
Franco Camera, Oliver Wieland

Extended abstract of the talk given at the first EURISOL UG topical meeting:
The formation and structure of r-process nuclei between $N = 50$ and 82 (including ^{78}Ni and ^{132}Sn areas)
December 9-11, 2009, INFN-LNS, Catania, Italy

Dipole states have attracted considerable interest in nuclear physics for many decades, since the discovery of the Giant Dipole Resonance (GDR) [1]. In fact, this is one of the most well known manifestations of nuclear collective motion [2], arising if an external electromagnetic field acts on the protons, displacing them with respect to the neutrons: the strong proton-neutron attraction provides the restoring force. Usually, in stable nuclei, the nuclear dipole response is restricted to a single resonance peak, which exhausts essentially all the associated sum rule. In other words, most of the nucleons do participate to a single, very collective oscillation.

Recently, the interest in the properties of the nuclear response has been renewed, due to the peculiar features that it may assume in neutron-rich nuclei. With increasing neutron number, protons become more bound since the proton potential becomes deeper; the neutron potential itself is not strongly affected, but the neutrons occupy levels that are more and more close to the continuum. Then, the neutron Fermi energy may become significantly higher than the proton Fermi energy, and the neutron and proton particle-hole (p-h) excitations can assume different characters: the proton ones are bound-to-bound transitions, whereas the neutron ones may be transitions from weakly bound states to continuum states. In this case one expects a decoupling between neutron and proton excitations. In particular, dipole strength is expected to show up at low energy; this strength is mainly made up by neutron excitations and consequently, it has mixed isoscalar/isovector character.

This pattern is different from what is found in stable nuclei where all the dipole strength is concentrated in the GDR. The name “Pygmy Dipole Resonance” (PDR) has been introduced to indicate any kind of strength below the GDR energy region. As reviewed e.g. in Ref. [3], one should nonetheless avoid simplistic generalizations. In light nuclei, sometimes one or few neutron states contribute to the so-called PDR but close to the drip line the combination of weak binding and low angular momentum can produce a peak which is classified as a threshold effect. In heavier nuclei, and more far from the drip line, this character is completely absent. The decoupling between the so-called PDR and the GDR may be weaker, and the energy difference smaller.

We focus in this contribution on the so-called PDRs in medium-heavy nuclei that have been experimentally measured. The goal is in fact to explore cases in which some collectivity is present and a link with more

general nuclear properties can be extracted. In $^{130,132}\text{Sn}$ the LAND collaboration has identified strength below the GDR, which amounts to about 1-5% of the Thomas-Reiche-Kuhn (TRK) sum rule [4, 5]. The detailed theoretical nature of this strength has been somewhat debated: Relativistic Mean Field (RMF) models tend to predict more collectivity than nonrelativistic ones. Of course the reason should not be found in the covariant or non-covariant formulation, rather in the different strength, or density-dependence, characterizing the neutron-proton effective interaction. In this contribution we also compare with the experimental datum on the PDR in the nucleus ^{68}Ni (cf. Ref. [6]).

From the theoretical point of view, this low-lying dipole strength could be studied within different models. The advantage of self-consistent mean-field (SCMF) models lies in the fact that they can be applied both to finite nuclei and uniform matter and consequently they allow making links between multipole response studies and the equation of state (EOS) of nuclear matter, which in turn has implications for the physics of neutron stars. At present, there is an enormous effort aimed at determining the parameters that govern the asymmetric matter EOS, using both experimental and theoretical tools.

The energy per particle in a nuclear system characterized by a total density ρ (sum of the neutron and proton densities ρ_n and ρ_p), and by a local asymmetry $\delta \equiv (\rho_n - \rho_p) / \rho$, is usually written as

$$\frac{E}{A}(\rho, \delta) = \frac{E}{A}(\rho, \delta = 0) + S(\rho)\delta^2. \quad (1)$$

The above equation defines the so-called symmetry energy $S(\rho)$. Information on the symmetry energy can be obtained from various sources, none of them being so far conclusive by itself. The main parameters that govern the density dependence of the symmetry energy are: (i) the symmetry energy at saturation, $S(\rho_0)$, which is denoted usually by a_4 or J ; (ii) the derivative of the symmetry energy at saturation which is related to the widely used ‘‘slope’’ parameter L by $S'(\rho)|_{\rho=\rho_0} = L/3\rho_0$.

We have found correlations between the properties of the PDR and the slope parameter L . Random Phase Approximation (RPA) calculations of the dipole strength have been carried out. Our implementation based on nonrelativistic Skyrme forces is fully self-consistent and discussed, e.g., in Ref. [7]. We also perform relativistic calculations based on the formalism described in Refs. [8, 9]. The resulting correlations are shown in the upper part of Fig. 1 for both nuclei ^{68}Ni and ^{132}Sn . The straight lines correspond to linear fits. We have considered the measured values of the EWSR percentage, and deduced a range of acceptable values for L , by taking care both of the experimental error and of the error associated with the fit.

Our result is that the slope parameter L is constrained to be in the interval 50.3-89.4 MeV or 29.0-82.0 MeV, if we use either the ^{68}Ni results, or the ^{132}Sn results (cf. the lower left panel of Fig. 1). The weighted average, $L = 64.8 \pm 15.7$ MeV, is displayed in the lower right panel of Fig. 1 (it corresponds to the shaded box). In this panel, the correlation of J and L is provided, so that we can deduce our best value of J which is 32.3 ± 1.3 MeV.

The main interest of our analysis lies in the fact that our results for L and J are in quite good agreement with those extracted from the analysis of heavy-ion collisions [10, 11, 12] and from other kinds of studies [13, 14, 15]. In particular, we have solved, to a good extent, the problem that the result from Ref. [5] was not overlapping significantly with the results obtained by the different analysis of heavy-ion collisions.

Measurements of the PDR in isotopic chains that include neutron-rich systems may further reduce the uncertainty on the parameters governing the symmetry energy. In a similar fashion, one may hope that other important quantities which define our understanding of nuclear physics can be constrained by measurements of the collective strength. For instance, the quadrupole strength in neutron-rich nuclei can give information on the evolution of the (isoscalar) effective mass m^* .

References

- [1] B.L. Berman and S.C. Fultz, Rev. Mod. Phys. 47, 713 (1975).
- [2] M.N. Harakeh and A.M. van der Woude, *Giant Resonances: Fundamental High-Frequency Modes of Nuclear Excitation* (Oxford University Press, Oxford, 2001); P.F. Bortignon, A. Bracco, and R.A. Broglia, *Giant Resonances; Nuclear Structure at Finite Temperature* (Harwood Academic, New York, 1998).
- [3] N. Paar, D. Vretenar, E. Khan, G. Colò, Rep. Prog. Phys. 70, 691 (2007).

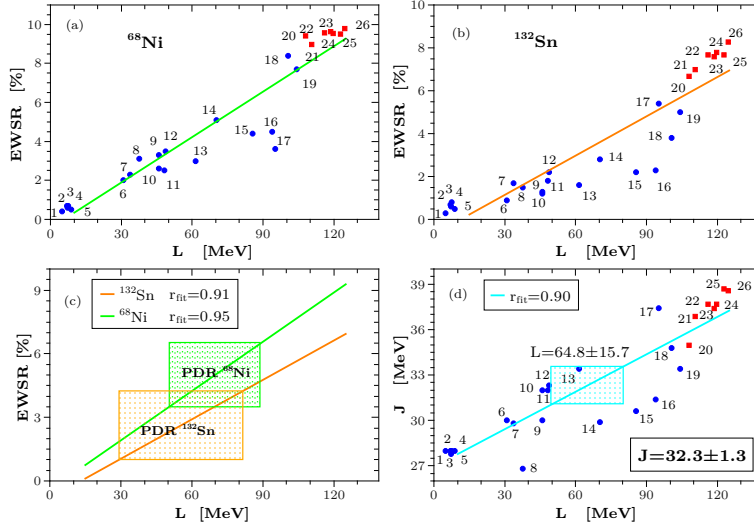


Figure 1: (Color online) In panels (a) and (b), the correlation between L and the percentage of TRK sum rule exhausted by the PDR, respectively in ^{68}Ni and ^{132}Sn , is displayed. The computed data points are labelled, here and in what follows, by numbers. The correspondence with the parameter sets used is: 1= ν 090, 2=MSk3, 3=BSk1, 4= ν 110, 5= ν 100, 6=SkT6, 7=SkT9, 8=SGII, 9=SkM*, 10=SLy4, 11=SLy5, 12=SLy230a, 13=LNS, 14=SkMP, 15=SkRs, 16=SkGs, 17=SK255, 18=SkI3, 19=SkI2, 20=NLC, 21=TM1, 22=PK1, 23=NL3, 24=NLBA, 25=NL3+, 26=NLE. The straight lines correspond to the results of the fits. In panel (c) we show the same straight lines displayed in (a) and (b), together with the correlation coefficient r and the constraints from experiments [5, 6]. In panel (d) the correlation between L and J is shown. The box corresponds to the value of L deduced from the weighted average of the two values extracted from ^{68}Ni and ^{132}Sn .

- [4] P. Adrich *et al.*, Phys. Rev. Lett. 95, 132501 (2005).
- [5] A. Klimkiewicz *et al.*, Phys. Rev. C76, 051603(R) (2007).
- [6] O. Wieland *et al.*, Phys. Rev. Lett. 102, 092502 (2009).
- [7] G. Colò *et al.*, Nucl. Phys. A788 (2007) 173c.
- [8] P. Ring *et al.*, Nucl. Phys. A694, 249 (2001).
- [9] Z.Y. Ma *et al.*, Nucl. Phys. A703, 222 (2002).
- [10] L.W. Chen *et al.*, Phys. Rev. Lett. 94, 032701 (2005).
- [11] M.B. Tsang *et al.*, Phys. Rev. Lett. 102, 122701 (2009).
- [12] D.V. Shetty *et al.*, Phys. Rev. C76, 024606 (2007).
- [13] M. Centelles *et al.*, Phys. Rev. Lett. 102, 122502 (2009); M. Warda *et al.*, Phys. Rev. C80, 024316 (2009).
- [14] P. Danielewicz and J. Lee, Nucl. Phys. A818, 36 (2009).
- [15] P. Danielewicz, Nucl. Phys. A727, 233 (2003).

M.Górska et al.,

"Structure of heavy Cd and In isotopes up to N=82"

The general trend towards investigating exotic nuclei and the need for new experimental data to provide benchmarks for modern nuclear structure models have stimulated experiments with radioactive beams at world leading facilities for nuclear physics. In particular, the in-flight method for the production of radioactive beams at high energies has become important for nuclear structure studies. The Coulomb excitation, knockout and fragmentation reactions or isomeric beams at intermediate and relativistic energies provide considerable new information about the ground and excited states energies, lifetimes, spectroscopic factors, decay transition strengths and other observables which yield further understanding of the nuclear wave functions.

The beams of the most exotic (and least abundant) nuclei are used to investigate decay modes and learn about nuclear structure properties of their daughters, i.e. on the ground state wave function of the decaying nucleus, or excited isomeric states provided that the lifetime of the state is long enough that it survives the flight through the experimental apparatus.

The study of exotic nuclei is driven by the many theoretical predictions [1] and first experimental observations [2] of shell evolution. Shell evolution is the direct proof that the nucleon-nucleon interaction has to be modified far off the stability line. The tensor component of the nuclear interaction, not included properly in the model calculation, is presently being carefully analysed by different theoretical groups. The corresponding effect, valid for neutron-deficient as well as for neutron-rich nuclei, is known as monopole migration. It is responsible for the doubly-magic character of ^{24}O with $Z=8$ and $N=16$, deformation in ^{32}Mg [1,3], the collapse of the $N=28$ shell in ^{42}Si [4], as well as for enhanced transition probabilities in the light Sn isotopes [5] among many other examples as summarised in Ref. [6] and references therein. **However, the monopole migration is predicted not to be strong enough to cause a quenching of the N=82 shell gap at Z=40. There, the modified spin-orbit force, predicted by mean-field calculations [7] is assumed to be responsible for a possible shell-gap disappearance at ^{122}Zr .**

The experimental data presented here stems from the combination of the GSI FRagment Separator (FRS) [8] which separate and selects secondary radioactive beams, and highly efficient Ge array to form the RISING project [9,10]. In particular in this article the results from the "stopped beam campaign" of RISING are reported. The various primary beams of typically several hundred MeV/u are used to undergo fragmentation or fission on Be targets of 4 g/cm² and 1 g/cm² thickness, respectively.

The secondary beams were separated and identified event-by-event with respect to their nuclear charge Z and mass A using the FRS and implanted at the final focal plane in a passive or an active stopper. The active stopper was realised in a multi-layer Si DSSSD array. This allows one to measure γ -ray radiation emitted both from isomeric states and following ground state γ decay. Gamma rays emitted in the isomeric decay process were measured in an array of 15 Cluster detectors [11] from the former Euroball spectrometer [12], which surrounds the stopper in a compact geometry, such that high detection efficiency could be achieved with high granularity. The photo-peak efficiency for the RISING array in the configuration used in the stopped beam campaign covered a range from 3.0(3)% at 45 keV, passing a maximum of 25(1)% at ~ 65 keV and falling off to 5.1(2)% for a 3.8 MeV γ ray. More details on the Ge array are given in Ref.[10].

On the neutron-rich side of the nuclear chart the N=82 shell evolution/quenching played the major role in the RISING nuclei of interest. The investigation of the neutron-rich Zr isotopes towards N=70 is crucial for the predicted shell quenching of N=82 at Z=40 [7]. These previously inaccessible nuclei from that region are under SM analysis and future experimental goals are being considered [13]. On the other hand the discussion of the shell quenching was already initiated with the example of ^{130}Cd [14]. The study of excited states for this nucleus within the RISING project [15] has proven that such quenching is not present. The analogy of the 8^+ isomeric decay pattern in two nuclei with identical valence space, namely ^{98}Cd [16,17] and ^{130}Cd , with two proton holes in ^{100}Sn and ^{132}Sn , respectively is clearly visible. The experimental data both for level energies and the isomeric transition strength compare well to the shell model calculations for both nuclei. The calculations use the same interaction matrix elements with only

simple scaling of the core nucleus. The monopole matrix elements were in both cases adjusted to fit the experimentally known effective single particle states.

Moreover, the data on ^{131}In where the β decay of a core excited state was observed [18] proved that the change in the $N=82$ shell gap between ^{132}Sn and ^{130}Cd is caused only by the residual interaction causing a monopole migration and further an effective gap reduction of about 600 keV within the accuracy of the interaction. Results obtained with the interaction used for this extrapolation are convincing when comparing experimental and theoretical level energies in a benchmark nucleus ^{132}Sn . As the experiment for stretched configurations, which are less affected by model space truncation, is well reproduced, the interaction is assumed to be appropriate for this extrapolation. **Further SM extrapolation of the shell gap towards ^{122}Zr give no indication of a strong shell quenching in this nucleus.**

In summary, in-flight separation and event-by-event identification of radioactive beams combined with an efficient β -ray spectroscopy setup has proved to be very successful in investigating the nuclear structure of exotic nuclei within the RISING project at GSI. The experimental method is constantly improved by the collaboration and provides a unique facility worth studying the nuclei addressed in this contribution. **The major step forward in this research of neutron rich nuclei from the experimental side will be reached in exploring intense radioactive beam from fission sources in combination with high efficiency and granularity gamma ray spectroscopy.**

- [1] T. Otsuka et al., *Phys. Rev. Lett.* **87**, 082502 (2001).
- [2] T. Motobayashi et al, *Phys. Lett.* **B 346**, 9 (1995).
- [3] T. Otsuka et al., *Phys. Rev. Lett.* **95**, 232502 (2005).
- [4] B. Bastin et al., *Phys. Rev. Lett.* **99**, 022503 (2007).
- [5] P. Doornenbal et al. *Phys. Lett.* **B 647**, 237 (2007).
- [6] H. Grawe, K. Langanke and G. Martínez-Pinedo, *Rep. Progr. Phys.* **70**, 1525 (2007).
- [7] J. Dobaczewski, I. Hamamoto, W. Nazarewicz and J. A. Sheikh, *Phys. Rev. Lett.* **72**, 981 (1994).
- [8] H. Geissel et al., *Nucl. Instrum. Methods Phys. Res.* **B70**, 286 (1992).
- [9] H.-J. Wollersheim et al., *Nucl. Instrum. Methods Phys. Res.* **A537**, 637 (2006).
- [10] S. Pietri et al., *Nucl. Instrum. Methods Phys. Res.* **B261**, 1079 (2007).
- [11] J. Eberth et al., *Nucl. Instrum. Methods Phys. Res.* **A369**, 135 (1996).
- [12] J. Simpson, *Z. Phys.* **A358**, 139 (1997).
- [13] A. Bruce et al., experimental proposal at GSI
- [14] I. Dillmann et al., *Phys. Rev. Lett.* **91**, 162503 (2003).
- [15] A. Jungclaus et al., *Phys. Rev. Lett.* **99**, 132501 (2007).
- [16] M. Górska et al., *Phys. Rev. Lett.* **79**, 2415 (1997).
- [17] A. Blazhev et al., *Phys. Rev.* **C69**, 064304 (2004).
- [18] M. Górska et al., *Phys. Lett.* **672**, (2009) 313

A. Gargano¹, L. Coraggio¹, A. Covello^{1,2}, and N. Itaco^{1,2}

¹*Istituto Nazionale di Fisica Nucleare, Complesso Universitario di Monte S. Angelo, I-80126 Napoli, Italy*

²*Dipartimento di Scienze Fisiche, Università di Napoli Federico II, Complesso Universitario di Monte S. Angelo, I-80126 Napoli, Italy*

During the last decade there has been substantial progress in the experimental study of nuclei far from the stability line. These new data pose challenging questions about the evolution of the shell structure and may lead to a better understanding of the action of nuclear forces. In particular, the study of exotic nuclei around doubly closed shells, such as ^{78}Ni , ^{100}Sn , and ^{132}Sn , yield direct information on the two basic ingredients of the shell model: single-particle energies and matrix elements of the effective interaction. This makes them the best testing ground for realistic shell-model calculations where the effective interaction is derived from the nucleon-nucleon (NN) potential.

In recent years a considerable effort has been made to gain information on neutron-rich nuclei “north-east” of ^{132}Sn , and the new available data have stimulated several shell-model studies in this region with the main aim to verify if some observed peculiar properties should be seen as the onset of a shell-structure modification. We have studied [1–4] several nuclei beyond ^{132}Sn in terms of the shell model, employing realistic effective interactions derived from the CD-Bonn nucleon-nucleon potential [5]. The very good agreement between theory and experiment shows that our realistic effective interaction is well suited to describe the spectroscopic properties of the nuclei considered, leading to the conclusion that to explain the presently available data on exotic nuclei in the ^{132}Sn region there is no need to invoke shell-structure modifications. These results makes it very interesting and timely to perform shell-model calculations not only to try to explain the existing data, but also to make predictions which may stimulate further experimental efforts.

We have first performed realistic shell-model calculations for the two-valence particle nuclei ^{134}Sn , ^{134}Te , and ^{134}Sb , which represent the best systems for a direct test of the neutron-neutron, proton-proton, and proton-neutron matrix elements of the effective interaction. We have then studied nuclei with more valence nucleons to further verify the predictive power of our calculations and to interpret the new emerging data in the region. For instance, we have performed calculations for nuclei with two additional protons or neutrons with respect to ^{134}Sb , namely ^{136}Sb and ^{136}I , focusing on proton-neutron multiplets. The spectroscopic results of exotic nuclei near ^{132}Sn have been also discussed [6, 7] in connection with the strict resemblance between them and their counterparts in the stable ^{208}Pb region. In particular, in both regions the role of core polarization effects has been emphasized, showing their relevance in determining the matrix elements of the effective interaction which lead to the right $0^- - 1^-$ spacing in odd-odd nuclei and to a weakening of the neutron-neutron pairing gap with respect to the proton-proton one.

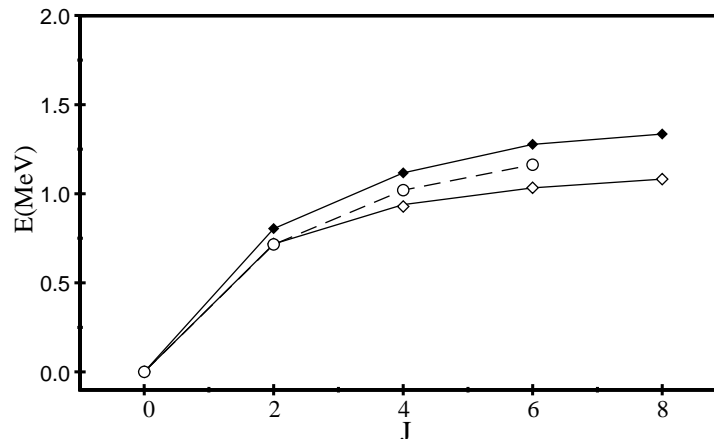


FIG. 1: Energies of the low-lying states in ^{136}Sn and ^{212}Pb . The theoretical results are represented by open diamonds (^{212}Pb) and open circles (^{136}Sn) while the experimental data for ^{212}Pb by black diamonds.

The theoretical framework of our realistic shell-model calculations is described in detail in Ref. [8] while the results for ^{132}Sn neighbors are discussed in the works cited above. Here, we would only like to report some of our predictions

for neutron-rich Sn isotopes, whose spectroscopic properties are still unknown. In Fig. 1 we report our results for ^{136}Sn together the calculated and experimental [9] energies of the lowest states in ^{212}Pb . We see that the calculated curve for ^{136}Sn shows the same behavior as that relative to its counterpart ^{212}Pb , which is just what we have found for the two-valence nucleon systems. Note that the calculated levels for ^{212}Pb reproduce quite well the experimental ones.

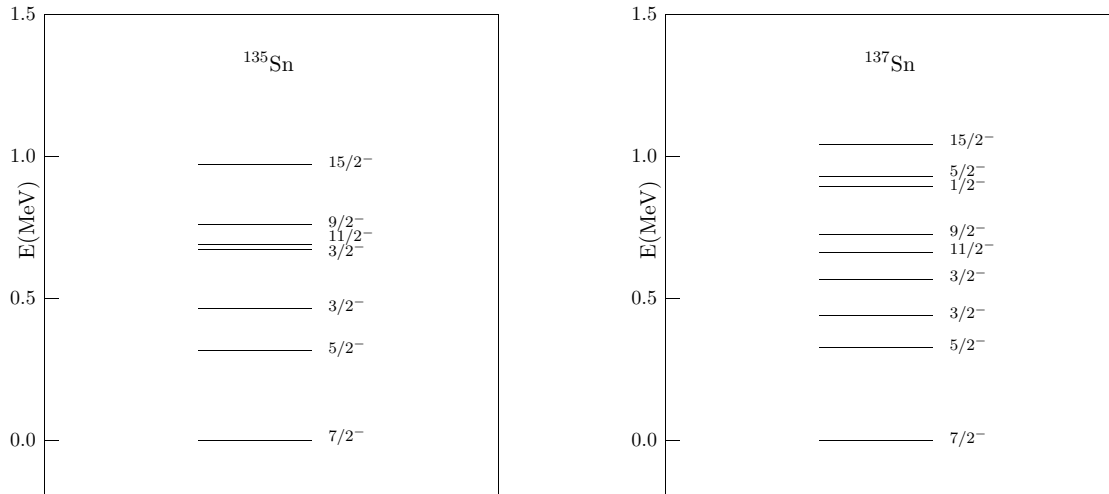


FIG. 2: Calculated spectra of ^{135}Sn and ^{137}Sn

The calculated spectra of the two odd nuclei ^{135}Sn and ^{137}Sn are shown in Fig. 2 while in Table I we report the binding energies (with respect to ^{132}Sn) for the four isotopes $^{134-137}\text{Sn}$. The only measured energy [10], relative to ^{134}Sn , compares very well with the calculated one. It is worth mentioning that this experimental value has been obtained in a recent measurement at ISOLDE, which has revealed a 0.5 MeV deviation from the previous accepted value.

TABLE I: Binding energies (in MeV) for Sn isotopes

Nucleus	^{134}Sn	^{135}Sn	^{136}Sn	^{137}Sn
Calc	5.99	8.30	11.86	14.18
Expt	5.91			

-
- [1] L. Coraggio, A. Covello, A. Gargano, and N. Itaco, Phys. Rev. C **72**, 057302 (2005).
[2] L. Coraggio, A. Covello, A. Gargano, and N. Itaco, Phys. Rev. C, **73**, 031302(R) (2006).
[3] A. Covello, L. Coraggio, A. Gargano, and N. Itaco, Eur. Phys. J. ST **150**, 93 (2007).
[4] G. S. Simpson, J. C. Angelique, J. Genevey, J. A. Pinston, A. Covello, A. Gargano, U. Köster, R. Orlandi, and A. Scherillo, Phys. Rev. C **76**, 041303(R) (2007).
[5] R. Machleidt, Phys. Rev. C, **63**, 024001 (2001).
[6] L. Coraggio, A. Covello, A. Gargano, and N. Itaco, Phys. Rev. C **80**, 021305 (2009).
[7] A. Covello, L. Coraggio, A. Gargano, and N. Itaco, Acta Phys. Pol. B **40**, 401 (2009).
[8] L. Coraggio, A. Covello, A. Gargano, N. Itaco, and T. T. S. Kuo, Prog. Part. Nucl. Phys. **62**, 135 (2009).
[9] Data extracted using the NNDC On-line Data Service from the ENSDF database, version of January 29, 2010.
[10] M. Dworschak *et al.*, Phys. Rev. Lett. **100**, 072501 (2008).

Current Status of Nuclear Structure Studies in the ^{132}Sn Region

G. S. Simpson

LPSC, Université Joseph Fourier Grenoble 1,
CNRS/IN2P3, Institut National Polytechnique de Grenoble,
F-38026 Grenoble Cedex, France

The nucleus ^{132}Sn is one of only two doubly magic, neutron-rich, medium-heavy nuclei currently accessible for nuclear-structure studies, the other being ^{78}Ni . The regions around these two nuclei are of prime importance for testing the interactions used in shell-model calculations and searching for any deviations from these predictions far from stability. Of these two nuclei, the region around ^{132}Sn has been more intensely studied, due to its proximity to the peak of the heavy fragment mass distribution in fission. This has allowed a wealth of detailed information to be gathered on the nuclei of this region with $Z \geq 50$ and $N \leq 82$. Data on nuclei here with proton holes however are much more scarce.

Information on excited states of nuclei close to ^{132}Sn , with $Z \geq 50$ and $N \leq 82$, has been obtained from β -decay, isomer, deep-inelastic and prompt-fission spectroscopy over the last few decades. Generally, modern shell-model predictions for nuclei with $Z \geq 50$ and $N \leq 82$ agree well with the experimental data, as summarized in a recent review article [1] on isomeric states of this region.

State-of-the-art shell-model calculations are also able to correctly reproduce the level orders and transition rates for nuclei near ^{132}Sn with $Z \geq 50$ and $N \geq 82$, where experimental data exist. The measured decay scheme of the nucleus ^{136}Sb [2] has been successfully reproduced by calculations performed by the Napoli Group [2]. This is the most neutron-rich nucleus with particles outside ^{132}Sn where any spectroscopic information exists. No evidence for any changes in shell structure or interactions were found. These realistic, effective, two-body interactions were made from a nucleon-nucleon interaction derived from the CD-Bonn potential, with no use of any adjustable parameter.

Spectroscopy data on nuclei with both proton and neutron holes, relative to ^{132}Sn are rare. Some β - and isomer-decay studies have been performed on the indium and cadmium nuclei of this region with $N \leq 82$ [3, 4]. Shell-model calculations are able to reproduce well the observed decays schemes close to the $N = 82$

shell closure, however the agreement becomes worse when moving further away. These problems may arise due to some collectivity being present in these nuclei or a difference between hole-hole and particle-particle (or particle-hole) interactions. A simple examination of the energies of lowest lying levels of these nuclei would appear to hint at the presence of some collectivity, due to the similarity of the $2^+ \rightarrow 0^+$ and $4^+ \rightarrow 2^+$ transitions energies. Shell-model calculations produce 2^+ energies some 200 or 300 keV too high, however this is a general feature of calculations of this region and the problem exists also for nuclei with $Z \geq 50$ and $N \leq 82$. Coulomb excitation measurements are necessary on these nuclei to search for any collective effects. More spectroscopy data are also needed to further test the shell-model predictions and to improve the interactions. EURISOL will be able to deliver such beams of the required In, Cd, Ag, and Pd nuclei using the fragmentation of a ^{132}Sn beam.

Excited states of nuclei with $Z \leq 50$ and $N > 82$, close to ^{132}Sn are currently unknown. Spectroscopy information here will again allow shell-model predictions to be tested. EURISOL will be able to provide beams of these species using fragmentation reactions of beams such as ^{144}Xe or ^{144}Cs . Such reactions possibly provide the best mechanism to populate and study the nuclei of this region.

References

- [1] J.A. Pinston and J. Genevey, *J. Phys. G* **30** (2004) R57.
- [2] G.S. Simpson *et al.*, *Phys. Rev. C* **76** (2007) 041303.
- [3] A. Scherillo *et al.*, *Phys. Rev. C* **70** (2004) 054318.
- [4] L. Caceres *et al.*, *Phys. Rev. C* **79** (2009) 011301.

Neutron transfer measurements around the doubly-magic ^{132}Sn

S. D. Pain^{*,**}, K. L. Jones[‡], R. L. Kozub[§], D. W. Bardayan^{**}, J. C. Blackmon^{**}, K. Y. Chae[‡], K. A. Chipps[¶], J. A. Cizewski[†], R. Hatarik[†], M. S. Johnson^{||}, R. Kapler[‡], C. Matei^{||}, B. H. Moazen[‡], C. D. Nesaraja^{**}, P. O'Malley[†], M. S. Smith^{**} and J. S. Thomas[†]

^{*}*Nuclear Physics Research Group, University of the West of Scotland, Paisley, PA1 1AG, Scotland*

[†]*Department of Physics and Astronomy, Rutgers University, New Brunswick, NJ 08903, USA*

^{**}*Physics Division, Oak Ridge National Laboratory, Oak Ridge, TN 37831, USA*

[‡]*Department of Physics and Astronomy, University of Tennessee, Knoxville, TN 37996, USA*

[§]*Department of Physics, Tennessee Technological University, Cookeville, TN 38505 USA*

[¶]*Physics Department, Colorado School of Mines, Golden, CO 80403, USA*

^{||}*Oak Ridge Associated Universities, Oak Ridge, TN 37830 USA*

Abstract. Calculations of r-process nucleosynthesis rely significantly on nuclear structure models as input, which are not well tested in the neutron-rich regime, due to the paucity of experimental data on the majority of these nuclei. The measurement of (d,p) reactions on unstable nuclei in inverse kinematics can yield information on the development of single-neutron structure away from stability in close proximity to suggested r-process paths. The Oak Ridge Rutgers University Barrel Array (ORRUBA) has been developed for the measurement of such reactions. An early partial implementation of ORRUBA has been utilized to measure the $^{132}\text{Sn}(d,p)^{133}\text{Sn}$, the $^{130}\text{Sn}(d,p)^{131}\text{Sn}$ and $^{134}\text{Te}(d,p)^{135}\text{Te}$ reactions for the first time.

Keywords: Transfer reactions, neutron-rich nuclei, r-process, silicon detectors

PACS: 25.45.Hi, 25.60.-t, 27.60.+j, 29.40.Wk

INTRODUCTION

Neutron-induced reactions on unstable neutron-rich nuclei involved in the r-process, especially near closed neutron shells, are important in determining the reaction flow as the environment cools, and therefore influence the final elemental abundances [1]. Due to the short lifetimes of the nuclei involved, direct measurements of neutron-capture cross sections are impractical. However, the energies, spins and spectroscopic information of single-particle states near to shell closures provide an important constraint on nuclear-structure models, and are directly relevant to direct neutron-capture cross sections. Transfer reactions have long been an important tool for the study of single-particle structure. Traditionally, they have been employed using light ion beams incident on stable (or very long lived) targets; a technique that cannot be applied to nuclei far from stability. However, the availability of high quality radioactive heavy ion beams is now enabling the study of such reactions on much shorter lived nuclei in inverse kinematics. In particular, the (d,p) reaction preferentially populates levels with low orbital angular momentum and with significant single-particle structure, which are of astrophysical interest [2], and can be performed in inverse kinematics on deuterated plastic targets

[3]. This technique is allowing the first measurements of the single-particle structure of a limited set of these nuclei to be studied [4, 5]. Furthermore, the majority of nuclei involved in the r-process are beyond the reach of present facilities. Their masses (or, equivalently, neutron separation energies) are calculated globally and included in r-process codes. The measurement of single-particle structure of unstable nuclei provides an important benchmark of nuclear structure models away from stability, facilitating an improvement of effective interactions, and an improvement in the calculation of global masses.

The strongly inverse kinematics, and the relatively weak intensities currently obtainable with radioactive beams, require a large solid-angular coverage $\theta_{lab} = 90^\circ$ for ejectile detection, with high resolution detection in energy and angle, over a large dynamic range. Additionally, particle identification is required in the forward hemisphere. The Oak Ridge Rutgers University Barrel Array (ORRUBA) [7] is a new array of silicon detectors, developed to meet the requirements of performing transfer reactions in inverse kinematics. The array consists of two rings of silicon detectors, designed to operate typically with one ring forward and one backward of $\theta_{lab} = 90^\circ$. The forward-angle ring consists of detector telescopes comprised of $65\mu\text{m}$ thick non-resistive silicon strip detectors for ΔE measurement, and position-sensitive $1000\mu\text{m}$ thick resistive strip detectors as stopping detectors. The backward angle ring is comprised of a single layer of resistive strip detectors. The array gives approximately 80% coverage in azimuthal angle over the polar angular range $\sim 45^\circ$ to $\sim 135^\circ$.

MEASUREMENTS OF (d, p) AROUND A \sim 132

The recent measurements of (d,p) reactions at the Holifield Radioactive Ion Beam Facility (HRIBF) at ORNL have focused on the single-neutron structure around the doubly-magic ^{132}Sn nucleus. An important metric of nuclear magicity is the distribution of the spectroscopic strength of single-particle states in nuclei with one nucleon beyond the shell closure. Three measurements of (d,p) reactions have been performed in inverse kinematics: $^{130}\text{Sn}(d,p)^{131}\text{Sn}$, $^{132}\text{Sn}(d,p)^{133}\text{Sn}$ [6] and $^{134}\text{Te}(d,p)^{135}\text{Te}$. All three measurements, performed at ~ 4.8 MeV/nucleon on thin CD_2 targets, utilized a partial implementation of the ORRUBA and SIDAR detector arrays.

The ^{133}Sn Q value spectrum spectrum (Figure 1) shows the population of four states below the neutron separation energy at ~ 2.4 MeV. The angular distributions for these states are shown in the right-hand panel of figure 1. The distributions for the ground state and first excited state are clearly distinguished as $\ell = 3$ and $\ell = 1$ transfer respectively. Both states yield spectroscopic factors compatible with unity ($S = 0.866 \pm 0.16$ for the ground state and $S = 0.92 \pm 0.18$ for the 0.854 MeV state), confirming their structure as states with very pure $^{132}\text{Sn} \otimes \nu(f_{7/2})$ and $^{132}\text{Sn} \otimes \nu(p_{3/2})$ configurations. The low proton energies from the 1.363 MeV and 2.005 MeV states prohibited significant angular distributions from being extracted. However, angle-integrated cross sections were used to determine spectroscopic factors for these two levels. The state at 1.363 MeV is a strong candidate for the $3p_{1/2}$ single-particle state previously missing in ^{133}Sn , matching with the theoretically expected ordering of the single-particle levels, and the observation of the 2.005 MeV state through β -decay. The spectroscopic factors for these states, assum-

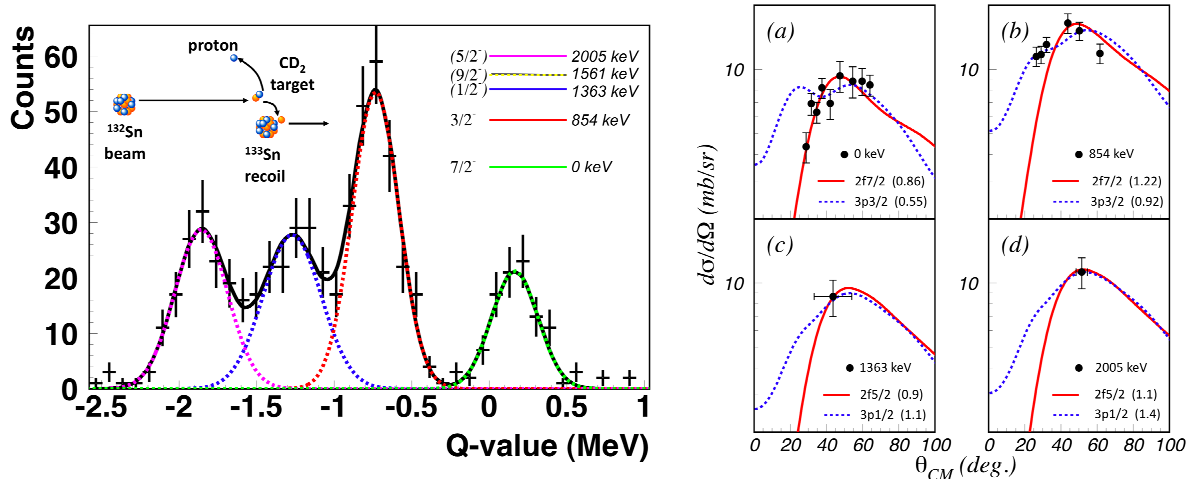


FIGURE 1. (Left panel) Excitation energy spectrum [6] for ^{133}Sn , showing yield to the ground state and three excited states located at 0.854 MeV, 1.363(31) MeV and 2.005 MeV. This work reports the first observation of the 1.363(31) MeV state. (Right panel) Angular distributions [6] for $^{132}\text{Sn}(d,p)^{133}\text{Sn}$ for **a**, the Ground state; **b**, the 854-keV state; **c**, the 1,363-keV state; **d**, the 2,005-keV state.

ing $^{132}\text{Sn} \otimes v(p_{1/2})$ and $^{132}\text{Sn} \otimes v(f_{5/2})$ configurations respectively, were determined to be 1.1 ± 0.3 and 1.1 ± 0.2 .

States in ^{131}Sn have been studied through the $^{130}\text{Sn}(d,p)^{131}\text{Sn}$ reaction. Previously, Yrast cascades in ^{131}Sn involving states with $J = 11/2$ have been studied by Bhattacharyya *et al.* [8], and some of the low-lying hole states have been assigned tentatively from β -decay experiments [9]. Since there are nominally two neutron holes in the ($N = 80$) ^{130}Sn core, one or more low-lying, low angular momentum hole states of ^{131}Sn may be observed in a (d,p) experiment, depending on the complexity of the ^{130}Sn ground-state wave function. From shell model considerations, one expects the strongest states to be $\ell = 1$ and $\ell = 3$ transfers coupled to the ^{130}Sn ground state, populating negative-parity 1p-2h states. The $\ell = 1$, $3p_{3/2}$ and $3p_{1/2}$ single-particle states are of particular importance for DC in the r-process, as this typically involves the capture of an s-wave neutron followed by an $E1$ γ -ray transition. However, no single-particle information for any of these states in ^{131}Sn has been reported previously. In this measurement, four strong single-particle states were observed at similar Q values and with similar intensities as those populated in the $^{132}\text{Sn}(d,p)^{133}\text{Sn}$ reaction. No population of lower-lying hole states was observed.

The excitation energy spectrum obtained preliminarily from the $^{134}\text{Te}(d,p)^{135}\text{Te}$ measurement (Figure 2) shows the population of a number of states up to ~ 4 MeV. The ground- and first-excited states are well resolved, and yield preliminary angular distributions which are compatible with $5/2^-$ and $3/2^-$ assignments. That more than four states are strongly populated, in contrast to the cases of the $^{132}\text{Sn}(d,p)^{132}\text{Sn}$ and $^{130}\text{Sn}(d,p)^{131}\text{Sn}$ experiments, is indicative that the single-particle strength is comparatively fragmented in this nucleus. This may potentially provide some p -strength at higher excitation energies, closer to the neutron separation energy, which would crucially affect

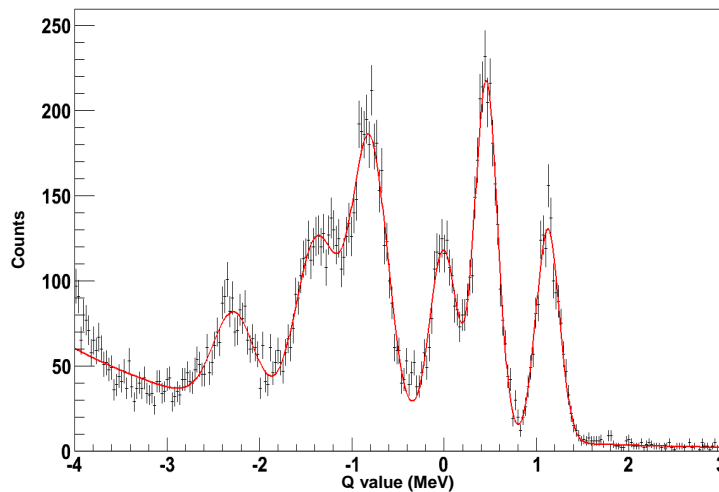


FIGURE 2. Preliminary Q value spectrum from the $^{134}\text{Te}(d,p)^{135}\text{Te}$ measurement.

the magnitude of the direct-capture cross section at astrophysical energies. Further analysis is currently underway to extract yields and angular distributions for the states populated, providing spectroscopic information imperative to direct-capture calculations.

ACKNOWLEDGMENTS

This work was supported by the US Department of Energy under contract numbers DEFG02-96ER40955 (Tennessee Technological University (TTU)), DE-FG52-03NA00143 (Rutgers, ORAU), DE-AC05-00OR22725 (ORNL), DE-FG02-96ER40990 (TTU), DE-FG03-93ER40789 (Colorado School of Mines), DE-FG02-96ER40983 (University of Tennessee), DE-FG52-08NA28552 (MSU), DE-AC02-06CH11357 (MSU), the National Science Foundation under contract numbers NSF-PHY0354870 and NSF-PHY0757678 (Rutgers) and NSF-PHY-0555893 (MSU), and the UK Science and Technology Funding Council under contract number PP/F000715/1.

REFERENCES

1. R. Surman and J Engel, *Phys. Rev. C* **64**, 035801 (2001).
2. S. Chiba *et al.*, *Phys. Rev. C* **77**, 015809 (2008).
3. K. L. Jones *et al.*, *Phys. Rev. C* **067602**, 2066 (2004).
4. J. S. Thomas *et al.*, *Phys. Rev. C* **71**, 021302(R) (2005).
5. J. S. Thomas *et al.*, *Phys. Rev. C* **76**, 044302 (2007).
6. K. L. Jones *et al.*, *Nature* **465**, 454 (2010).
7. S.D. Pain *et al.*, *Nucl. Inst. Methods Phys. Res. B* **261**, 1122 (2007).
8. P. Bhattacharyya *et al.*, *Phys. Rev. Lett.* **87**, 062502 (2001).
9. Yu. V. Sergeenkov *et al.*, *Nuclear Data Sheets* **72**, 487 (1994).

Study of neutron-rich nuclei with PRISMA-CLARA. Future perspectives with EURISOL

Calin Ur

INFN, Sez. di Padova

Binary reactions such as multi-nucleon transfer and deep-inelastic collisions have proven since long to be an efficient tool to populate neutron-rich nuclei at relatively high angular momentum [1]. The use in recent years of large acceptance magnetic spectrometers coupled with high efficiency γ -ray arrays allowed the identification and study of more and more exotic neutron-rich nuclei. The PRISMA-CLARA complex [2] was operated at the National Laboratories of Legnaro and benefited of the most neutron-rich stable beams available in nature delivered by the Tandem-PIAVE-ALPI accelerators complex.

One of the main physics topics addressed with the PRISMA-CLARA complex concerned the evolution of the nuclear shell gaps when adding more neutrons to the nuclei. The properties of the exotic neutron-rich nuclei far from beta-stability are expected to differ substantially from those of the nuclei close to the valley of beta-stability. The relative energies of single particle orbitals evolve as a function of the neutron number leading to modifications of the well established magic numbers. This is of fundamental importance for nuclear structure models, such as the shell model, as it impacts on the definition of the effective interactions. The location of the shell gaps for neutron-rich nuclei with neutron numbers between 50 and 126 is of high interest in the nuclear astrophysics for the description of the rapid neutron capture processes (r-processes). It was recently inferred that such evolution of the shell structure is related to the action of the tensor part of the nucleon-nucleon interaction [3]. The tensor-force is responsible of the strong attraction between a proton and a neutron in spin-flip partner orbits. A recent generalization predicts that also for orbitals with non-identical orbital angular momenta a similar behavior has to be observed: an attraction is expected for orbitals with anti-parallel spin configuration whereas orbitals with parallel spin configuration should repel each other [4].

By using the most neutron-rich 'stable' Se beam (^{82}Se) the question whether there is a quenching of the $N=50$ shell gap in the region of ^{78}Ni was addressed with PRISMA-CLARA [5]. A wide range of nuclei were populated through multi-nucleon transfer and deep-inelastic processes. The data provided were enough to assign the γ -rays to the produced nuclei based on the coincidence with their mass and atomic charge reconstructed in PRISMA but were not sufficient for γ - γ coincidences and angular distributions of the γ -rays. For this reason a complementary measurement was performed with the same reaction but employing a thick target, that completely stopped the recoiling nuclei, placed in the center of the the high efficiency γ -ray array GASP. This method of complementary measurements for the study of the neutron-rich nuclei has become a common practice. The data from the GASP measurement allowed for the building of the level schemes based on γ - γ coincidence relationships and for the determination of the γ -rays multipolarity based on their angular distributions. The evolution of the structure in the neutron-rich Cu ($Z=29$) isotopes, ^{71}Cu , ^{73}Cu and ^{75}Cu , offer an interesting example of the tensor-force effect on the migration of the nuclear single-particle orbitals with the neutron number.

The deduced level schemes indicate a reduction of the $5/2^-$ level energies with increasing neutron number. The $5/2^-$ state correspond to the occupation of the $1f_{5/2}$ single-particle orbital while the $3/2^-$ state is associated with the occupation of the $2p_{3/2}$ single-particle orbital. The monopole effect of the tensor force shifts systematically the single-particle levels as protons and neutrons fill certain orbits, the proton-neutron part of the force being the dominant. For the $Z=29$ isotopes due to the strong attraction between particles filling the $1f_{5/2}$ and the $1g_{9/2}$ orbits and the repulsion between the particles filling the $2p_{3/2}$ and the $1g_{9/2}$ orbits one predicts an inversion of the relative position of the $1f_{5/2}$ - $2p_{3/2}$ effective single-particle states with respect to the usual order for $N \leq 40$ where the $2p_{3/2}$ state is the lowest in excitation energy (see Ref. [6] for discussion).

The experimental data allowed for the construction of the high-spin level schemes of the $N=50$ isotones ^{81}Ga , ^{82}Ge and ^{83}As . In these nuclei low-lying excitations involve mainly proton configurations whereas, with increasing spin and excitation energy the breaking of the $N=50$ core becomes more important. The knowledge of the excitation energy of such medium- and high-spin states can then be used for extracting the shell gap through the comparison with shell-model calculations. Data were compared with shell model calculations where $0p-0h$ and $2p-2h$ excitations were allowed. The value of the $N=50$ shell gap was used as a parameter in the calculations. The best agreement between the calculated and experimentally determined excitation energy of the states was obtained for an energy gap at $N=50$ of 4.7 MeV [7]. This result can be considered as a strong indication that, when moving away from the stability line down to $Z=32$, the gap at $N=50$ remains constant and no weakening of the $N=50$ shell is apparent.

For the study of neutron-rich nuclei with $N=60$ a new approach was used consisting in transfer reactions and Coulomb-induced fission of ^{238}U with ^{136}Xe beam [8]. This reaction produced many neutron-rich nuclei in the region of Zn-Pd isotopes. The properties of the heavy Kr isotopes (with $A \geq 96$) are important for nuclear astrophysics as they were proposed as waiting-point nuclei in certain scenarios of the rapid neutron capture process (r -process) [9]. The first excited state in ^{96}Kr ($Z=36$, $N=60$) was identified at an excitation energy of 241 keV allowing for the extension of the empirical systematics of the evolution of collectivity in the neutron-rich Kr isotopes. This enables a better comparison with other isotopic chains, of the behavior at the deformation changing $N=60$ region. A sharp transition (or sudden onset of deformation) at this point takes place in the isotopic chains from Rb ($Z=37$) to Zr ($Z=40$), with the maximum variation in the Y chain ($Z=39$) [30]. In Mo ($Z=42$), the region $N=50-60$ shows a gradual change of the deformation. In the Kr chain ($Z=36$), symmetrically placed to Mo with respect to the center ($Z=39$) of this region, the present data indicate that there may still be a relatively important change of deformation between $N=58$ and $N=60$, less drastic, however, than the corresponding transition in the isotonic Sr and Zr chains. For a solid confirmation, and a more detailed comparison with different theoretical model predictions, measurements of the $B(E2)$ transition probability in both ^{94}Kr and ^{96}Kr are highly desirable.

Binary reactions will remain the main technique to reach exotic nuclei in the neutron-rich region also with the future use of radioactive beams and the experience gained with the use of the PRISMA-CLARA complex offers an important know-how for the detection, identification, spectroscopy of such nuclei and for the development of specific spectroscopic techniques and methods. The new radioactive beams will give access to regions of nuclei nowadays out of reach with stable beams. An example is the use of a radioactive ^{92}Kr beam

on a ^{238}U target at an energy of 600 MeV. According to the GRAZING calculations [10] multi-nucleon transfer and deep-inelastic processes following the reaction will populate with relatively high cross-sections neutron-rich Se, Kr, Rb, Sr nuclei presently completely unknown.

References

- [1] R. Broda, J. Phys. G: Nucl. Part. Phys. 32 (2006) R151.
- [2] A. Gadea *et al.*, Acta Phys. Pol. B38 (2007) 1311.
- [3] T. Otsuka *et al.*, Phys. Rev. Lett. 87 (2001) 082502.
- [4] T. Otsuka *et al.*, Phys. Rev. Lett. 95 (2005) 232502.
- [5] E. Sahin *et al.*, Legnaro Annual Report 2007, INFN-LNL-222(2008), p.21, and to be published
- [6] K.T. Flanagan *et al.*, Phys. Rev. Lett. 103 (2009) 142501 and references therein.
- [7] G. de Angelis *et al.*, to be published.
- [8] N. Marginean *et al.*, Phys. Rev. C 80 (2009) 021301.
- [9] U.C. Bergmann *et al.*, Nucl. Phys. A714 (2003) 21.
- [10] G. Pollarolo, private communication.

Studies of dissipative heavy ion collisions and probes of the symmetry energy

M.Colonna¹⁾, V.Baran²⁾, M. Di Toro^{1,3)}, C.Rizzo^{1,3)}

1) LNS-INFN, I-95123 Catania, Italy

2) NIPNE-HH, Bucharest and Bucharest University, Romania

3) Physics and Astronomy Dept. University of Catania, Italy

The future availability of radioactive beams will allow us to investigate the properties of nuclei far from the valley of stability. Apart from the information that one can get on spectroscopic properties, radioactive beams will also provide tools to investigate reaction mechanisms involving such exotic systems.

Dissipative collisions, including fusion, binary and three-body breakings, offer a unique opportunity to study phenomena occurring in nuclear matter under extreme conditions with respect to shape, intrinsic excitation energy, spin, N/Z ratio (isospin). For dissipative collisions at low energy (around 10 MeV/u), interaction times are quite long and therefore a large coupling among various mean-field modes is expected, leading to a co-existence of reaction mechanisms. The collision dynamics is expected to be sensitive to the details of the nuclear interaction below normal density. Hence dynamical processes involving exotic beams allow one to address the study of the nuclear interaction in terms of energy density functionals and, in particular, to constrain the isovector terms and the so-called symmetry energy E_{sym} .

This has important implications in the astrophysical context and also for the understanding of the structure of exotic systems. In fact, energy density functionals are probably the only possible framework to describe medium-heavy nuclei. The strategy that we follow consists in implementing different effective interactions into transport codes employed to simulate the collision dynamics. Then results can be compared to experimental data for specific reactions mechanisms and related observables.

Interesting effects are already seen when studying the competition between (incomplete) fusion and deep inelastic (binary processes) for neutron rich systems in semi-peripheral reactions. Transport calculations of the Stochastic Mean Field (SMF) type are the appropriate tool to shape the evolution of the system in terms of the relevant degrees of freedom [Bar05]. The break-up probability is deduced from the observation of non-vanishing (and correlated) quadrupole moments in coordinate and momentum space.

Exploratory simulations have been carried out for the neutron-rich system $^{132}\text{Sn}+^{64}\text{Ni}$ at 10 MeV/u, showing a larger fusion cross section (a 10% effect) when using a soft (flat around normal density) parameterization of the symmetry energy, with respect to a stiff (rapidly increasing with density) behavior. This can be ascribed to the larger value of the derivative of the symmetry energy around normal density in the asystiff case, leading to a stronger repulsion between the neutron-rich reaction partners, that inhibits fusion. A larger incomplete fusion cross section should be accompanied by the emission of few neutrons, ruled by the strength of the symmetry energy in the low density and neutron-rich surface of the composite system. The use of very neutron-rich (exotic) systems would be extremely useful for this analysis.

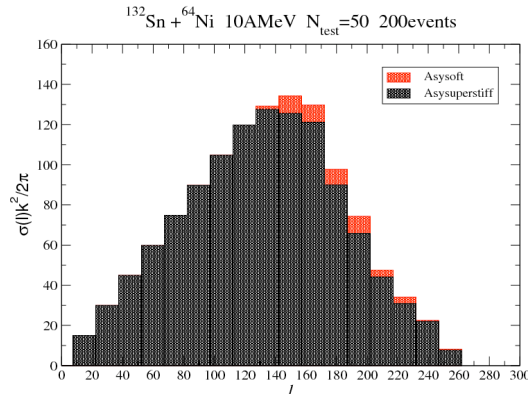


Fig.1

Fusion probability, as a function of angular momentum, as obtained for the reaction $^{132}\text{Sn}+^{64}\text{Ni}$ at 10 MeV/u, using the asy-stiff (black histogram) or the asy-soft (red) parameterizations.

Beams with exotic isospin contents can also induce changes in the classical two-body dissipation mechanisms of typical deep inelastic collisions. In particular, the properties of the direct fragment emission from the neck low density region between projectile and target can provide important probes of the symmetry energy. This emission originates from a combined Coulomb and angular momentum (deformation) effect. Some instabilities can show up, like in fission decays [Col95], leading to three-body breakings, where a cluster is emitted from the neck region [Dav79, Def05].

The development of surface (neck-like) instabilities, contributing to ternary breakings can certainly provide access to the isovector part of the nuclear interaction through a detailed comparison with transport model predictions. SMF simulations [Bar05] of $^{132}\text{Sn}+^{64}\text{Ni}$ collisions at $E/A=10$ MeV/u and impact parameters $b=6, 7, 8$ fm show a sensitivity of the neck dynamics to the detailed density dependence of the symmetry energy [Dit06], indicating a large probability for ternary break-up in the case of the asy-stiff interaction, as it can be evidenced by looking at quadrupole or octupole moments (i.e. to the deformation) of PLF and/or TLF.

The charge equilibration mechanism, probed by entrance channels with large N/Z asymmetries, like $^{124}\text{Sn}(N/Z=1.48) + ^{112}\text{Sn}(N/Z=1.24)$, can also provide relevant information on the low density behavior of the symmetry energy [Tsa09], once compared with transport model simulations. The amount of neutrons and protons exchanged depends on the N/Z asymmetry of the colliding nuclei and on the density behavior of the symmetry energy. For reactions at intermediate energies (30-50 MeV/u), it has been shown that the degree of isospin equilibration is correlated to the dissipation reached in the collision, that can be expressed in terms of the total kinetic energy loss (relative to the total energy available in the center of mass). Hence, using the latter as a sorting variable, the degree of isospin equilibration should only depend on the strength of the symmetry energy, that drives the isospin diffusion through the low-density interface between the two reaction partners [Riz08]. This is nicely confirmed by SMF simulations, see Fig.2.

As the beam energy is lowered below 20 MeV/u interaction times are longer and one can expect to achieve more easily isospin equilibration between projectile and target. This should allow one to investigate more in detail dissipative events, corresponding to

high value of the kinetic energy loss, where isospin diffusion is rather sensitive to the symmetry energy, see Fig.2. Moreover, one can also test the possible appearance of new equilibration mechanisms when using very N/Z asymmetric beams, such as ^{132}Sn (N/Z=1.64).

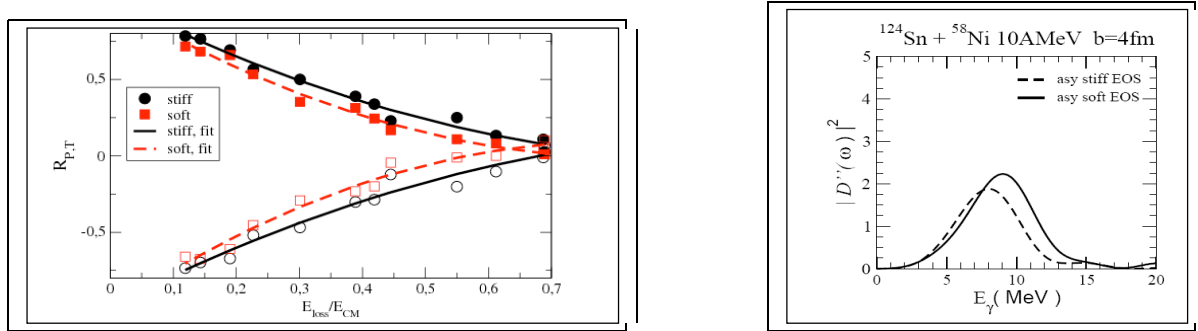


Fig. 2

(Left) Isospin transport ratios, R , as a function of the kinetic energy loss (renormalized to the total energy available in the center of mass) for $^{124}\text{Sn} + ^{112}\text{Sn}$ collisions, at 35 and 50 MeV/u. Full isospin equilibration corresponds to $R = 0$. Black line and points: asy-soft; Red line and points: asy-stiff. (Right) Strength of the pre-equilibrium dipole emission, as obtained for the systems $^{132}\text{Sn} + ^{64}\text{Ni}$ at 10 MeV/u and impact parameter $b = 4$ fm. Full line: asy-soft; Dashed line: asy-stiff.

For more central collisions the isospin equilibration mechanism can be studied via the direct measurement of the prompt dynamical dipole emission, nucleus-nucleus collective bremsstrahlung radiation during the charge equilibration path [Sim00,Bar05,Pap05]. Experimental features of such dipole radiation are the angular anisotropy, with centroid at energies well below the expected GDR emission from the residues. The energy range around 10 MeV/u seems to optimize the effect [Mar08]. These features can be investigated performing SMF simulations. Fig.2 (right) shows an amplified pre-equilibrium dipole emission in the very asymmetric system ^{132}Sn (N/Z=1.64) + ^{58}Ni (N/Z=1.07), that should lead to an easier experimental detection and analysis of this component. In this case, calculations also show a good sensitivity to the symmetry energy (see Fig.2), with higher frequency and yield in the asy-soft case, corresponding to the larger value of the symmetry energy at low density [Bar09].

References

- [Bar05] V.Baran et al., Phys.Rep. 410, 335 (2005) and references therein
- [Bar09] V.Baran et al., Phys. Rev. C79, 021603 (2009)
- [Col95] M.Colonna et al., Nucl. Phys. A589, 160 (1995)
- [Dav79] K.T.R.Davies et al., Phys. Rev. C20, 1372 (1979)

- [Def05] E. De Filippo et al., Phys. Rev. C71, 044602 (2005)
[Dit06] M.Di Toro et al., Nucl. Phys. A787, 585c (2007)
[Mar08] B.Martin et al., Phys. Lett. B664, 47 (2008)
[Pap05] M. Papa et al., Phys. Rev. C72, 064608 (2005) and Refs. therein
[Riz08] J.Rizzo et al., Nucl. Phys. A806, 79 (2008)
[Sim00] C.Simenel et al., Phys. Rev. Lett. 86, 2971 (2000)
[Tsa09] M.B.Tsang et al., Phys. Rev. Lett. 102, 122701 (2009)

High-precision measurement of the ${}^8\text{Li} + {}^4\text{He} \rightarrow {}^{11}\text{B} + n$ reaction cross section at astrophysical energies by means of the EXCYT radioactive ion beam facility.

M. La Cognata^{a,b}, A. Del Zoppo^{a,*}, P. Figuera^a, A. Musumarra^{a,b}, R. Alba^a, S. Cherubini^{a,b}, N. Colonna^c, L. Cosentino^a, V. Crucillà^{a,b}, A. Di Pietro^a, M. Gulino^{a,b}, L. Lamia^a, M.G. Pellegriti^{a,d}, R.G. Pizzone^a, S.M.R. Puglia^{a,b}, G.G. Rapisarda^{a,b}, C. Rolfs^{c,1}, S. Romano^{a,b}, M.L. Sergi^{a,b}, C. Spitaleri^{a,b}, S. Tudisco^a, A. Tumino^{a,f}

^aINFN-Laboratori Nazionali del Sud, Via S. Sofia 62, I95123 Catania, Italy

^bDipartimento di Metodologie Fisiche e Chimiche per l'Ingegneria, Università di Catania, I95123 Catania, Italy

^cInstitut für Physik mit Ionenstrahlen, Ruhr-Universität Bochum, Bochum, Germany

^dDipartimento di Fisica e Astronomia, Università di Catania, I95123

^eINFN-Sezione di Bari, Via Orabona 4, I70126 Bari, Italy

^fUniversità Kore, Enna, Italy

*Corresponding Author: DELZOPPO@lns.infn.it

¹Supported in part by Deutsche Forschungsgemeinschaft.

The ${}^8\text{Li} + {}^4\text{He} \rightarrow {}^{11}\text{B} + n$ reaction bears great importance in the primordial Universe and in other relevant nucleosynthesis sites, in particular core-collapse supernovae and neutron-star mergers. Within the frame of the inhomogeneous big-bang model, still representing a viable possibility for the early universe (Lara et al. 2006; Malaney & Fowler 1988; Kajino & Boyd 1990; Rauscher et al. 2007), this reaction could have allowed to overcome the $A = 8$ mass gap. This would provide a possible explanation for the experimental observation of a non-negligible abundance of heavy elements in the oldest astrophysical objects (Matsuura et al. 2005, and references therein). The magnitude of the cross section is the key parameter to model the elemental yield. The ${}^8\text{Li} + {}^4\text{He} \rightarrow {}^{11}\text{B} + n$ reaction also plays an important role in the context of the r-process nucleosynthesis (Sasaqui et al. 2006; Terasawa et al. 2001). Currently, the most popular scenario is neutrino-driven winds from Type II SNe. Anyway, it could be associated with neutron-star mergers or gamma-ray bursts, in which the required neutron fluxes can be realized as well. Therefore, it is of critical importance to constrain the parameter space for the r-process to single out the most likely environment where r-process nucleosynthesis is taking place. In this framework, the ${}^8\text{Li} + {}^4\text{He} \rightarrow {}^{11}\text{B} + n$ reaction is critical as Sasaqui et al. (2006) found that it would lead to a more efficient production of seed nuclei, such as ${}^{78}\text{Ni}$, so that a larger neutron/seed ratio would be required for a successful r-process. This, in turn, allows one to constrain the entropy per baryon and the astrophysical site for production of r-process nuclei.

For these reasons, the ${}^8\text{Li} + {}^4\text{He} \rightarrow {}^{11}\text{B} + n$ inclusive cross section has been measured at INFN-LNS Catania by using the ${}^8\text{Li}$ exotic beam produced by the EXCYT ISOL radioactive-ion-beam facility. A detailed discussion can be found in La Cognata et al. (2008,2009) and in Del Zoppo et al. (2007). Here we summarize the main results. The ${}^8\text{Li}$ radioactive beam emerging from a two micro-channel plate telescope impinged onto a 4 cm diameter and 15 cm long cylindrical gas cell filled with ${}^4\text{He}$ at the pressure of 150 mbar. The gas target was connected to the beam line through a $\sim 5 \mu\text{m}$ Ni entrance window that acted as a beam energy degrader. A 3.15 MeV ${}^8\text{Li}$ beam energy was obtained at the target centre by adjusting the energy of the ${}^8\text{Li}$ ions to about 11 MeV. The mean energy in the centre of mass of the ${}^8\text{Li} + {}^4\text{He} \rightarrow {}^{11}\text{B} + n$ reaction was $E_{\text{cm}} = 1.05$ MeV, with the variance square root 0.16 MeV. The beam energy upper tail in the gas cell was well below the threshold of the ${}^8\text{Li} + {}^4\text{He} \rightarrow {}^7\text{Li} + {}^4\text{He} + n$ reaction. In these conditions the ${}^{11}\text{B} + n$ was the only open neutron production channel of the ${}^8\text{Li} + {}^4\text{He}$ reaction in this measurement. Neutrons were detected in a 4π thresholdless moderation counter (Del Zoppo et al. 2007), which did not provide information on the neutron energy. To separate neutrons from the ${}^8\text{Li} + {}^4\text{He} \rightarrow {}^{11}\text{B} + n$ reaction and background neutrons the capture time distribution has been recorded. Indeed, a gate set on the ${}^8\text{Li}$ events in the TOF spectrum started a time-to-amplitude (TAC) converter and the stop signals of the TAC were provided by the neutron detector. Neutrons from the ${}^8\text{Li} + {}^4\text{He} \rightarrow {}^{11}\text{B} + n$ reaction, moderated and absorbed in

the detector, exhibit a die-away curve that can be approximated with a sum of two exponentials ($\tau_{\text{fast}}=68 \mu\text{s}$, $\tau_{\text{slow}}=169 \mu\text{s}$), while background neutrons yield an uncorrelated flat contribution. Therefore, a fitting of the time-correlation spectrum provided the total number of time-correlated events that is converted to cross section taking into account the target thickness, the collected projectiles and the detector efficiency.

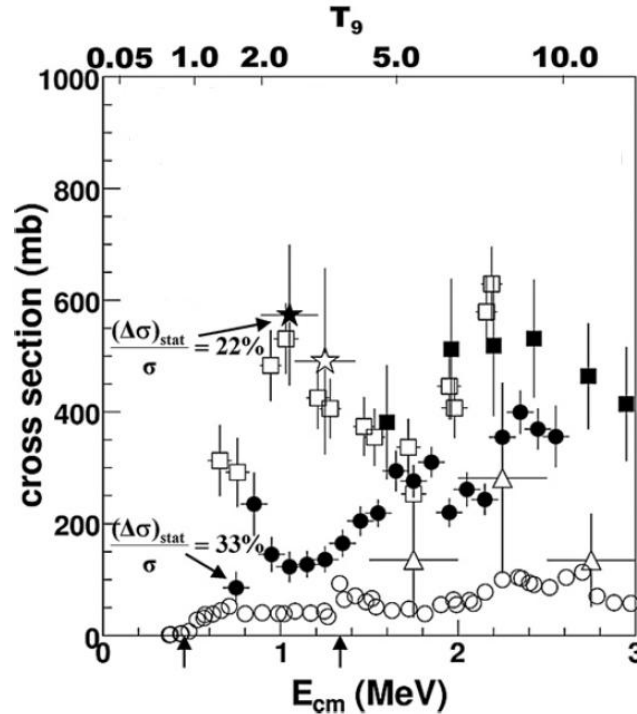


Figure 1 Summary of the available cross sections for the ${}^8\text{Li}+{}^4\text{He}\rightarrow{}^{11}\text{B}+n$ reaction. Open circles (Paradellis et al. 1990), open triangles (Mizoi et al. 2000), open squares (Gu et al. 1995), solid squares (Boyd et al. 1992), solid circles (Ishiyama et al. 2006), open star (Cherubini et al. 2004) and solid star (La Cognata et al. 2008). The arrows set the limits of the Gamow window for $T=10^9$ K.

The resulting cross section is given in Figure 1 (solid star: La Cognata et al. 2008) together with the result from a previous time-correlation experiment (Cherubini et al. 2004), the data from ${}^{11}\text{B}$ inclusive experiments (Gu et al. 1995; Boyd et al. 1992), from ${}^{11}\text{B}$ -n exclusive measurements (Mizoi et al. 2000; Ishiyama et al. 2006) and the lower limit set by the indirect estimate by Paradellis et al. (1990). In spite of its importance, a remarkable disagreement between inclusive measurements of the ${}^8\text{Li} + {}^4\text{He}\rightarrow{}^{11}\text{B} + n$ cross section and exclusive ones at center-of-mass energies $E_{\text{cm}} < 2$ MeV shows up. In detail, neutron inclusive (La Cognata et al. 2008; Cherubini et al. 2004) and ${}^{11}\text{B}$ inclusive measurements (Gu et al. 1995; Boyd et al. 1992) give comparable values of the reaction cross section, in contrast with the exclusive approach (Mizoi et al. 2000; Ishiyama et al. 2006), giving cross section values smaller by a factor 4 with respect to the inclusive ones right at the energy of astrophysical interest, $E_{\text{cm}} \sim 1$ MeV. The origin of such discrepancy has been traced back to, on one hand, the selective feeding of the highest excited ${}^{11}\text{B}$ levels and, on the other, the threshold effect preventing the detection of low-energy neutrons in exclusive measurements (La Cognata et al. 2009), making us confident that present-day inclusive measurements provide the most reliable estimate of the cross section (La Cognata et al. 2009). This result confirms the exotic cluster structure recently discovered in ${}^{11}\text{B}$ (Kawabata et al. 2007) and ${}^{12}\text{B}$ (Soic et al. 2003) and may significantly alter the constraints on models of the r-process astrophysical site (Sasaqui et al. 2006).

References

- Boyd, R. N., et al. 1992, Phys. Rev. Lett., 68, 1283
 Cherubini, S., et al. 2004, Eur. Phys. J. A, 20, 355

Del Zoppo, A., et al., 2007 Nucl. Instrum. Methods A, 581, 783
Gu, X., et al. 1995, Phys. Lett. B, 343, 31
Ishiyama, H., et al. 2006, Phys. Lett. B, 640, 82
Kajino, T., & Boyd, R. 1990, ApJ, 359, 267
Kawabata, T., et al. 2007, Phys. Lett. B, 646, 6
La Cognata, M., et al. 2008, Phys. Lett. B, 664, 157
La Cognata, M., et al. 2009, ApJ, 706, L251
Lara, J. F., et al. 2006, Phys. Rev. D, 73, 083501
Malaney, R. A., & Fowler, W. A. 1988, ApJ, 333, 14
Matsuura, S., et al. 2005, Phys. Rev. D, 72, 123505
Mizoi, Y., et al. 2000, Phys. Rev. C, 62, 065801
Paradellis, T., et al. 1990, Z. Phys. A, 337, 211
Rauscher, T., et al. 2007, Phys. Rev. D, 75, 068301
Sasaqui, T., et al. 2006, ApJ, 645, 1345
Soic, N., et al. 2003, Europhys. Lett., 63, 524
Terasawa, M., et al. 2001, ApJ, 562, 470

NUCLEAR ASTROPHYSICS AT LABORATORI NAZIONALI DEL SUD

Silvio Cherubini for the ASFIN collaboration

Nuclear astrophysics at INFN Laboratori Nazionali del Sud in Catania dates back to the beginning of 1990s, when the experiment ASFIN (ASTroFisica Nucleare, nuclear astrophysics in Italian) was proposed to and approved by the INFN “Commissione 3”.

As it is well known, measurements of nuclear reaction cross sections between charged particles of interest for astrophysics are severely hindered by the presence of the coulomb barrier between the colliding nuclei. In order to overcome this problem, and others originating from this, many indirect methods for measuring this kind of cross sections have been suggested.

Our group developed a method, called the Trojan Horse Method, based on the properties of quasi free reactions with three bodies in the exit channel. The idea is that a reaction of astrophysical interest $x+b \rightarrow c+d$ (I) can be studied using a well suited three-body reaction $A+b \rightarrow c+d+s$ (II) where the nucleus A has a strong clusterization into $x+s$. This latter reaction is supposed to proceed via a quasi-free mechanism and hence s can be considered a simple spectator to the process. If this is the case then the cross section of reaction (I) can be easily related to that of (II) by means of various approximations that can be as simple as PWIA. The method has been widely discussed in a number of papers, see e.g. (1) and references therein.

The main astrophysical problems studied using the THM were that of the LiBeB abundances and some of the key reactions for AGB stars and for the Nova phenomenon. Also, the role of the electron screening in the determination of the cross sections of many of these reactions was also studied.

In Figure 1 the results of a series of measurements of cross sections related to the LiBeB abundances are reported in the form of astrophysical factors. These works are reported in (2) and (3).

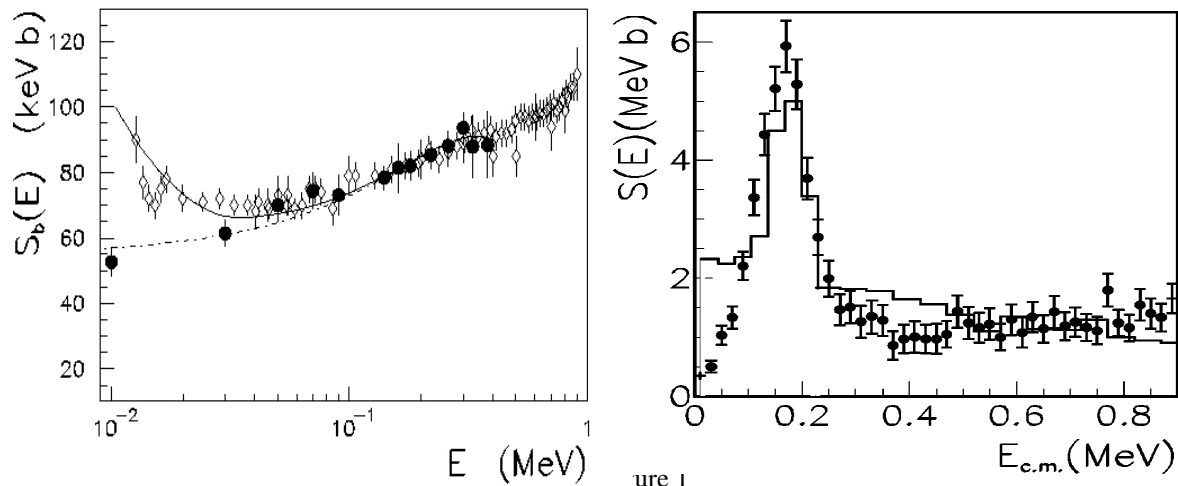


Figure 1

The panel on the left shows the results obtained for the reaction ${}^7\text{Li}+p \rightarrow \alpha+\alpha$ using the THM (2).

The empty diamonds are direct data and the black dots are THM data. The solid line is a fit to the direct data, the dashed one to the THM data. The direct data are affected by the electron screening effect. The panel on the right shows the results for the measurements of the cross section of the reaction ${}^{11}\text{B}+p \rightarrow {}^8\text{Be} + \alpha_0$ using THM. Points are THM data, the histogram represents direct data. See (3) for further explanations.

AGB stars are the sites for the synthesis of elements beyond iron along the stability valley (s-processes). The ^{19}F abundances are used to fix AGB star model parameters as they are extremely sensitive to the dredge-up mechanisms. The ratio of the abundances of the isotopes ^{18}O , ^{17}O , ^{15}N and ^{13}C to the most abundant ones ^{16}O , ^{14}N and ^{12}C also sensitive probes. The observed abundances are though inconsistent with models (e.g. $^{14}\text{N}/^{15}\text{N}$ too small). In order to contribute to the understanding of these problems we measured various cross sections responsible for the production and destruction of these isotopes. In Figure 2 the results for the reaction $^{15}\text{N}+p\rightarrow^{12}\text{C}+\alpha$ is shown as an example of these studies, reported in (4).

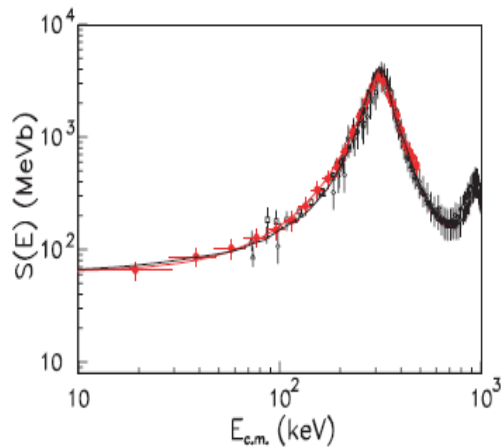


Figure 2

This panel shows the astrophysical factor for the $^{15}\text{N}+p\rightarrow^{12}\text{C}+\alpha$ reaction at energies corresponding to those of the AGB star scenario (4). The red dots represent THM data, the black triangles are direct data. The line is a fit to THM data.

The ASFIN group also made experiment using direct methods. In particular one of these experiments, performed at LNS, aimed at the measurement of the $^8\text{Li}+\alpha\rightarrow^{11}\text{B}+n$ reaction at energies relevant for the Big Bang scenarios. This experiment was performed by producing a radioactive ^8Li beam in flight. A particular detection technique was dictated by the low intensity of the beam (10^3 pps) and the long response time (1 ms) of the neutron detector used in the experiment. The results of this experiment are reported in (5). The measurement of this cross section was also the first experiment performed with the new RIB facility EXCYT at LNS. The results of this experiment are reported in (6)

References

- 1) C. Spitaleri et al., Phys. Rev. C 63, 055801 (2001)
- 2) R.G. Pizzone et al., Astronomy & Astrophysics 398, 423427 (2003)
- 3) C. Spitaleri et al., Phys. Rev. C 73, 049905 (2006) and references therein
- 4) M. La Cognata et al., Phys. Rev. C 76, 065804 (2007)
- 5) S. Cherubini et al., EPJ A 20, 355-358 (2004)
- 6) M. La Cognata et al., Phys. Lett. B 664, 157161 (2008)

The LNS Facilities

Luciano Calabretta

INFN Laboratori Nazionali del Sud, Via S. Sofia 62, 95123 Catania, Italy

A briefly description of the accelerators, of the Radioactive Ion Beam (RIB) facilities and of the main experimental equipment in operation at Laboratori Nazionale del Sud (LNS) is presented. The layout of the INFN-LNS with its main facilities and experimental equipment is shown in figure 1. The main accelerators of the LNS are the Superconducting Cyclotron and the electrostatic Tandem. Both the accelerators are used to deliver ion beams mainly for nuclear physics experiment, about 70% of available beam time, while the residual 30% is devoted for applied physics and medical treatment of eye melanoma.

EXCYT A FIRST GENERATION RIB AT LNS

The commissioning of the EXCYT facility started in the first months of 2005 [1]. The production of the radioactive ions was performed by injecting a $^{13}\text{C}^{4+}$ primary beam at energy of 45 AMeV on a graphite target up to a beam power of 150 W. The maximum production yield of ^8Li , measured at the entrance of the first stage of isobaric separator, was $9 \cdot 10^6$ pps.

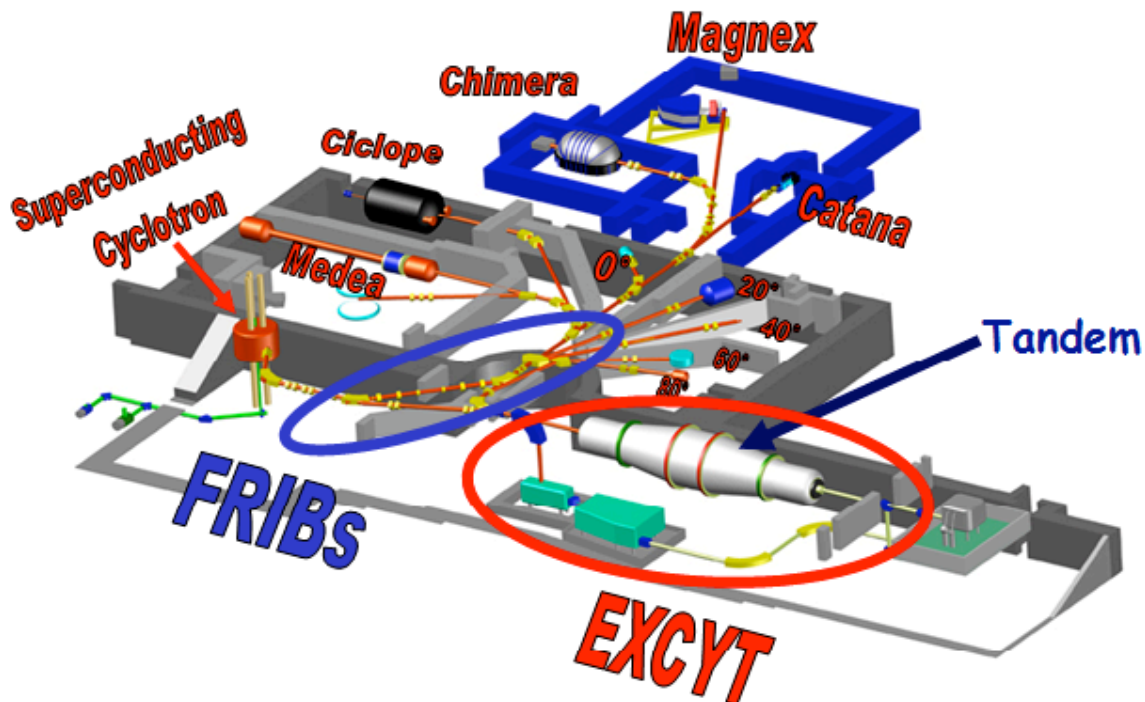


FIGURE 1. Layout of the LNS. The EXCYT and FRIBs facilities are indicated.

The yields of ${}^9\text{Li}$ and ${}^{21}\text{Na}$ measured with a lower beam power, about 82 W, in not optimized conditions and at the entrance of the isobaric separator were about $3.5 \cdot 10^5$ pps. The atoms produced by nuclear reactions in the target will effuse through a transfer tube to the ionizer, where an ISOLDE-type ion source ionizes them. The source presently used is a positive surface ionization type sources PIS. Efficiency measurements indicate an ionization rate around 70% for Lithium beam.

The selection of our target material has been done following the criteria of high porosity, small grain size, high thermal conductivity, high chemical purity, high melting point and low vapour pressure [2]. Despite, at the operating temperature of 2600°K, many diffusion mechanisms are active inside the target, lithium atoms will mainly diffuse through interstices in graphite. Once the particle reaches the grain boundary it can diffuse in a neighbour grain or effuse in the target porosity. Moreover, at this temperature, after the effusion process through the porosity, the probability of re-diffusion inside a grain is quite high. In particular, the simulations suggest that only the ${}^8\text{Li}$ particles produced within the first hundreds of microns are able to reach the target surface before their decay, ${}^8\text{Li}$ atoms produced deeper will decay during their path inside the target and will never be collected [3]. These considerations led the decision to modify the target design by employing ten, uniformly spaced, 1 mm thick, graphite disks, see figure 2a. The experimental test shows an increased yield of a factor 3.6. This value is lower than the expected factor 6 achieved by the simulation. The lower value is probably due to a non ideal temperature distribution inside the new target design. Anyway, this value is very promising for the future when the beam power will be increased up to 500 W.

The acceleration with the Tandem is feasible only for negative ions. Therefore, we use a charge exchange cell (CEC), consisting of a cell containing Cesium vapors at a variable temperature, allow to converts the positive Li^+ beam into a negative charged Li^- beam. The CEC efficiency strongly depends on the energy of the Li^+ extracted from the Target Ions Source (TIS): the lower the lithium energy the higher the CEC efficiency. The maximum efficiency in this case lies at about 5 keV. The beam optics elements have been originally designed to operate at typical extraction energy of 15-20 keV. Strong efforts were dedicated to improve the beam transmission at the lowest suitable voltage extraction. This value was fixed at 8-10 keV as a good compromise between a good transmission and CEC efficiency. On-line measurements confirm the expectations: the measured CEC efficiency for ${}^8\text{Li}$ at 10 keV is 3.4%, very close to the expected value of 3.6%.

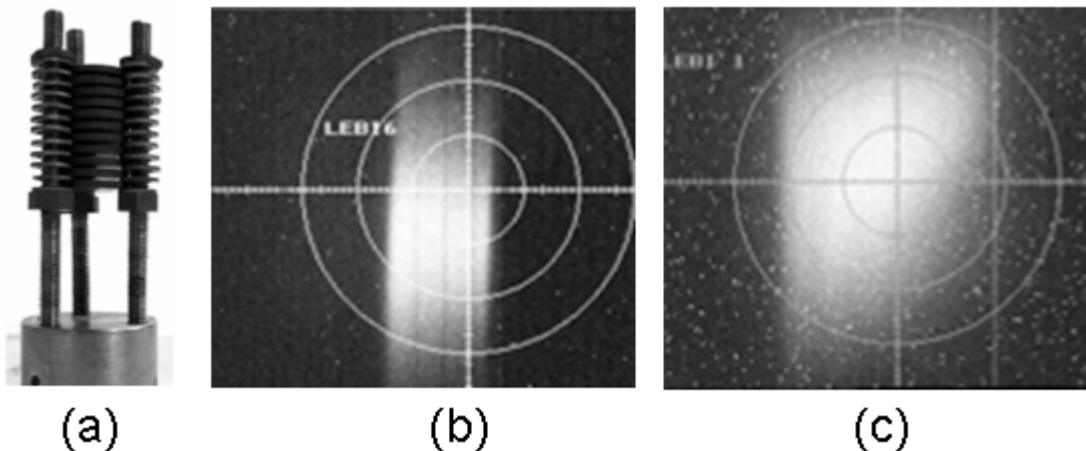


FIGURE 2. The new multilayer target (a). Beam profiles acquired with LEBI for a stable (b) and a radioactive beam (c). The intensities are below 1. pA.

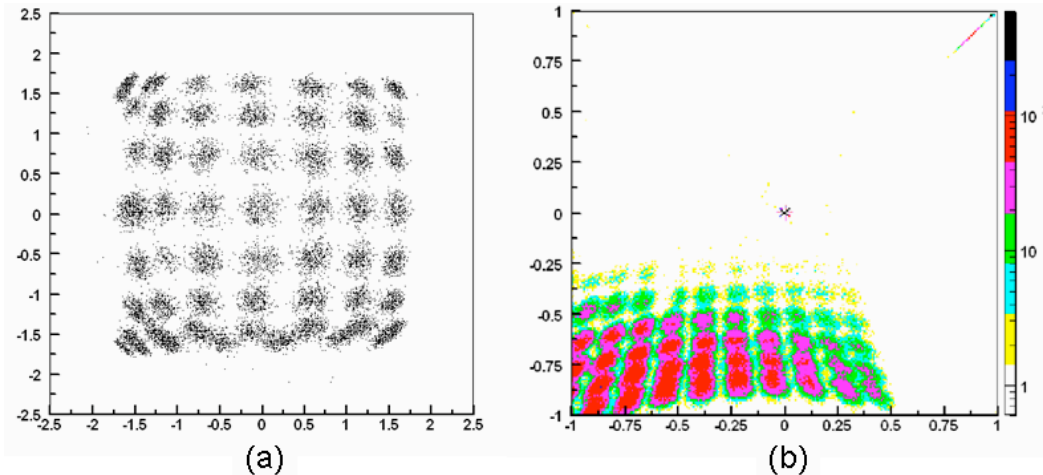


FIGURE 3. Mask profiles acquired with alpha particles (a) and ^8Li beam (b), using the silicon PSD. The scale axes are different for the two pictures.

Diagnosics

The beam diagnostics installed along the beam pipeline before the Tandem is the so called LEBI (Low Energy Beam Imager/Identifier) devices, which allow us to visualize the 2D shape of radioactive and stable beams, to measure the beam intensity and to perform the nuclear identification [4]. The LEBI sensitivity is so high to allow us to work with very low intensity beams (down to 10^3 pps). The LEBI high sensitivity scintillating screen consists of a Cesium Iodide doped with thallium, CsI(Tl). In front of this screen a very thin ($6\ \mu\text{m}$) aluminized mylar tape is placed. The tape is mounted in front of the CsI(Tl) crystal and cover just the lower half part of the screen. The LEBI is of course out of the beam line, when it is inserted to look at the beam it has two positions to intercept the beam. Whether stable beam has to be monitored, the LEBI is moved to stop the beam in the position “in-down”, so the beam strike on the screen directly, while for radioactive beam the LEBI is moved in the position “in-up”, to stop the beam just on the aluminized mylar tape, in order to avoid the contamination of the CsI(Tl) screen. In this case, the light spot is produced by the radioactive decay of the radionuclides impinging into the tape. Profiles for a stable and unstable ^8Li beam are shown in figure 2b and 2c.

A position sensitive silicon detector (PSD $50 \times 50\ \text{mm}^2$) has been adopted as the new beam profile monitor to look at beams accelerated by the Tandem. The signals produced by the detector are read at the four vertexes and used to reconstruct the impact position of the ion. This configuration allows identifying the charge and mass of each particle. In figure 3, the reconstructed positions of alpha and beam particles crossing a mask with several holes, are shown. Installation of these new detectors along the main beam line of the LNS is in progress.

FRIBS: IN-FLIGHT PRODUCTION OF RIB

Despite several laboratories have already installed RIBs facilities and new projects for large-scale advanced facilities have been developed, up to now, only few facilities produce RIBs whit energies in the range from 20 to 50 MeV/amu. This circumstance has motivated the development of the FRIBs (in Flight Radioactive Ions Beams) project at the LNS in Catania

[5]. In order to separate, the nuclei of interest from the primary beam and from contaminating fragments produced in the target, the fragmentation products are analyzed through the cyclotron extraction line that acts as fragment separator. However, the optic of the beam line allows only a rough selection. Therefore, mixtures of radioactive ions are transmitted. Consequently, it will be never possible to determine whether the detected reaction residues result from the collision with the target nucleus of one or another ion of the RIBs mixture. To select one radioactive ion beam or at least to reduce significantly the neighbors' contaminants the degrader technique is often used. Unfortunately, in our case the moderate energy and the optic of our beam line do not allow a significant cleaning effect.

In this context the leading idea of our project was to identify on a event-by-event basis (tagging technique) the separated ions with respect to the mass and atomic number (Z, A). A combined measurement of time-of-flight and energy loss allows us to identify each projectile. From the knowledge of the mass, charge and energy of each ion it is possible to explore nuclear reactions in secondary target for each of the tagged fragmentation products.

RIBs production yield was measured at the final focus of the FRIBs line by a ΔE - E telescope consisting of a Si detector 300 μm thick and $3 \times 3 \text{ cm}^2$ active area measuring the energy loss and of a plastic scintillator (0.5 mm thick and $2.5 \times 2.5 \text{ cm}^2$ active area) measuring the residual energy. Intermediate and light mass RIBs were produced by the fragmentation of ^{12}C , ^{20}Ne , ^{40}Ar and ^{58}Ni projectiles on Be and Al targets at energy between 62 and 40 A MeV and at low intensity primary beam (100 p nA) to avoid pile-up in the telescope. The production target of Be 500 μm thick was used for all the studied primary beams except for the ^{58}Ni projectile for which was used the Al 100 μm thick one. The target element and its thickness have been chosen in order to optimize the production of RIBs [6]. However, despite the Bp of FRIBs was set to select respectively the ^{18}Ne , ^{39}Cl and ^{55}Co ions a lot of other contaminant were also detected. The elemental production at the final focus of the FRIBs, measured by the ΔE - E technique, is shown in Fig. 4. The four different primary beams allow us to produce a lot of neutron and proton rich nuclei, and the measured yields were in good agreement with the LISE simulations. RIBs rate up to 10^5 ions/sec were estimated, by scaling the primary beam current up to 500 enA [6].

The tagging technique has been successfully applied in some experiment and in particular to the study of di-proton decays [7].

The encouraging results achieved and the interest of many national and international scientists convinced the INFN management to fund the project to upgrade the FRIBs line. The upgrading project plans to increase the solid angle and the momentum acceptance of the FRIBs line of a factor 20 and 2 respectively. Moreover, to achieve a similar increase also on the RIB delivered to the experimental room LS-20° and CHIMERA it is mandatory to minimize the beam emittance delivered by the FRIBs line. If the beam delivered by the cyclotron will be focused on a beam spot smaller than 2 mm on the production target it will be possible to minimize the beam emittance at values acceptable also for the beam lines LS-20° and CHIMERA. A further improvements in the FRIBs project will consists to replace the present 16×16 Si-Strip detector of active area $5 \times 5 \text{ cm}^2$, by a 24×24 Si strip $2.4 \times 2.4 \text{ cm}^2$ in order to increase the detector granularity, allowing the tagging detector to sustain a larger RIBs rate. All the analog electronics will be also digitized in order to store all timing information. Since we experienced some identification difficulties by using the RF signal for time of flight measurements, set up of specific start detectors at the appropriate distance from the Si-strip is

also planned. A thin (25 μm thick) plastic foil, read out by four photomultiplier for light RIBs and a PPAC detector for the heaviest ones are the best candidates.

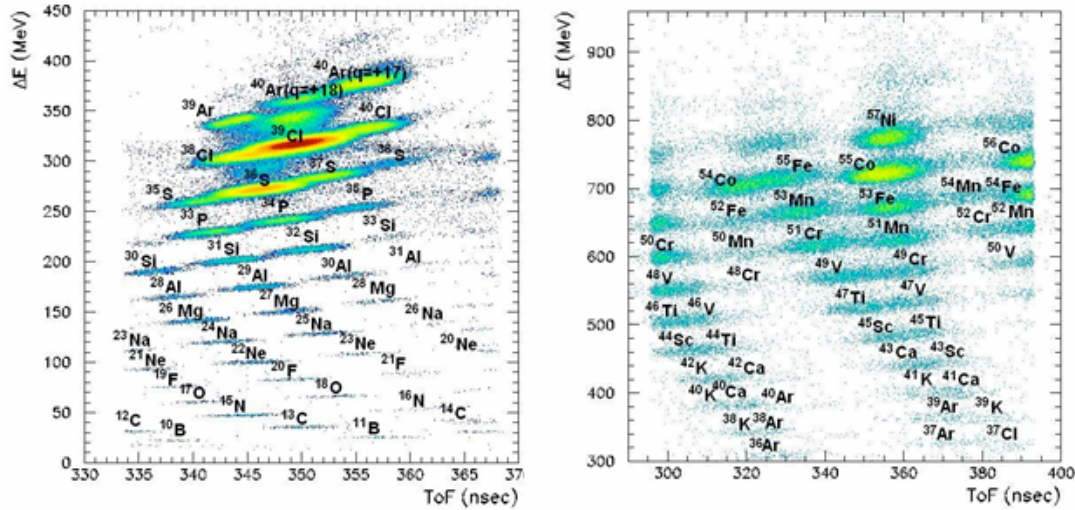


Figure 4: (a) Energy-loss versus time-of-flight plot for the ^{40}Ar fragmentation; (b) energy-loss versus time-of-flight plot for ^{58}Ni fragmentation.

THE MAIN EXPERIMENTAL EQUIPMENTS

MAGNEX is a general purpose spectrometer to be used both in inclusive measurements and in coincidence with other detectors. The second and higher-order optical aberrations are partially compensated for by the shape of the dipole entrance and exit field boundaries (hardware correction), and partially by means of trajectory reconstruction (software correction). A set of surface coils mounted on the dipole pole faces provides tuneable quadrupolar and sextupolar fields used for the compensation of the kinematic effect up to 2nd order. MAGNEX is designed to correct kinematic factors from 0.0 up to 50 mrad.

The MAGNEX focal plane detector (FPD) is a gas-filled detector with a "wall" of stopping silicon detectors at the back. The silicon detectors have active areas of approximately 7 cm (vertical) by 5 cm (horizontal) and are arranged in columns of three, each column being turned to face the mean angle of particles at the focal plane. The position and angle measurement is done via two sets of drift sections which are separated by an energy-loss section. The FPD can be filled with different gases and with a pressure in the range 5÷60 mbar. The small gas pressure, together with the absence of intermediate foils gives a very low energy threshold of about 0.5 MeV/A. The full identification of Z and A is obtained for ions up to the calcium region. The FPD may be also adapted to detect particles produced by the nuclear reactions induced by high energy light ions delivered from cyclotron, see ref.[8] and references therein.

CHIMERA detector consists of 1192 detection cells, arranged in cylindrical geometry around the beam axis, in 35 ring. The forward 18 rings are assembled in 9 wheels covering the polar angles between 1° and 30° and placed at a distance from the target going from 350 to 100 cm. The remaining 17 rings, covering the angular range 30-176 degrees, are assembled in such a way to form a sphere 40 cm in radius. The overall detection solid angle is about 94% of 4π . Each detection cell consists of a double telescope. The first stage is made of a 300 micron thick

silicon detector, while the second one is a thick CsI(Tl) crystal coupled to a photodiode for the light readout. More news available on ref.[9]

MEDEA a multi element detector consists of a ball, built up with 180 barium fluoride crystals, that covers the angular range between 30° and 170°, and a forward phoswich detector wall covering the angles between 10° and 30°. To reduce the threshold on the charged particle detection the whole system is under vacuum inside a large scattering chamber, ref.[10]. **MACISTE** detector has been designed to complete, at forward angles, the MEDEA detector. It works as a wall detector, placed downstream about 16 m from the target. A superconducting solenoid, **SOLE**, has been placed at the exit of the MEDEA and conveys the emitted particles to **MACISTE**. The detector consists of four telescopes with a useful area of 30 x 40 cm². Each one consists in turn, of a drift chamber for ΔE measurements, a wire chamber for position and time of flight measurement and a large plastic scintillator, for energy measurement, ref. [11].

MULTIDISCIPLINARY ACTIVITIES

CATANA is the first Italian protontherapy center for the ocular melanoma treatment. It is in operation since 2002. The treatments are performed using the proton beam delivered by the superconducting cyclotron at energy of 62 MeV, see ref. [12].

The **LNS-Irradiation Facility** site has been validated with an ESA audit on November 2009, exploiting a collaboration with **MAPRAD**, a private company. Two different setups allow studying Single Event Effects (SEL, SEU, SEFI etc.) with 20 MeV/amu heavy ions and Displacement Damage with 62 MeV protons. Both setups, located in a suitable hall along the 0-degree beam line, are placed in air just outside a thin cap on the beam pipe. They implement a motorized stepper with four degrees of freedom and position repeatability accuracy of 1 μ m.

LANDIS is a facility for application in the cultural heritage field, more news on ref. [13]. It is equipped with:

- Portable systems able to deliver alfa particle, x-rays or both;
- A laboratory to manipulate alpha emitters radionuclide nuclei;
- Material analysis based on proton beam delivered by the LNS accelerators.

1. G. Cuttone et al., *Nucl. Instr. & Methods B* 261, (2007) 1040.
1. M. Re et al., Proc. of the Particle Accelerator Conference 2005, Knoxville (USA), (2005) 898.
2. D. Rifuggiato et al., LNS activity report 2008, (2009) 149-152.
3. L. Cosentino, S. Cappello, P. Finocchiaro, *Nucl. Instr. & Methods A* 479 (2002) 243.
4. G. Raciti et al., *Nucl. Instr. & Methods B* 266 (2008) pp. 4632-4636.
6. E. Rapisarda et al., *Eur. Phys. Jour. ST* 150 (2007) pp. 169.
7. G. Raciti, et al., *Phys. Rev. Lett.* 100, 192503 (2008) pp1-4.
8. F. Cappuzzello et al. *NIM A* (2010) DOI information: 10.1016/j.nima.2010.05.027
9. A. Pagano et al., *Nucl. Phys. A* 681(2001)331-338
10. E. Migneco, et Al., *Nucl. Instr. & Meth. A* 314(1992)31-55
11. G. Bellia et al., *IEEE Transactions on Nuclear Science* 43(1996)1737-1740
12. <http://lnsweb.lns.infn.it/CATANA/CATANA/default.htm>
13. http://www.lns.infn.it/index.php?option=com_content&view=article&id=302&catid=129&Itemid=117